



Universiteit  
Leiden  
The Netherlands

## Miniaturized metabolomics methods for enabling the study of biomass-restricted samples

He, B.

### Citation

He, B. (2025, May 1). *Miniaturized metabolomics methods for enabling the study of biomass-restricted samples*. Retrieved from <https://hdl.handle.net/1887/4239100>

Version: Publisher's Version

License: [Licence agreement concerning inclusion of doctoral thesis in the Institutional Repository of the University of Leiden](#)

Downloaded from: <https://hdl.handle.net/1887/4239100>

**Note:** To cite this publication please use the final published version (if applicable).

# **Miniaturized metabolomics methods for enabling the study of biomass-restricted samples**

Bingshu He 何秉淑

The publication of the thesis was financially supported by:  
Leiden University Libraries

Cover design: Bingshu He

Thesis layout: Bingshu He

Printing: PrintSupport4U

© Copyright, Bingshu He, 2025

ISBN: 978-94-93289-77-2

All rights reserved. No part of this book may be reproduced in any form or by any means without permission of the author.

# **Miniaturized metabolomics methods for enabling the study of biomass-restricted samples**

## **Proefschrift**

ter verkrijging van

de graad van doctor aan de Universiteit Leiden,

op gezag van rector magnificus prof.dr.ir. H. Bijl,

volgens besluit van het college voor promoties

te verdedigen op donderdag 01 mei 2025

klokke 16:00 uur

door

**Bingshu He 何秉淑**

geboren te Chifeng, China

in 1993

## **Promotores**

Prof. dr. T. Hankemeier

Dr. R. Ramautar

## **Co-promotor**

Dr. A. C. Harms

## **Promotiecommissie**

Prof. dr. H. Irth (Chair)

Prof.dr. E.C.M. de Lange (Secretary)

Prof. dr. M. van der Stelt

Dr. E. Dominguez-Vega

*Leiden University Medical Center, the Netherlands*

Prof. dr. D. Y. Chen

*The University of British Columbia, Canada*

Dr. R.J. Vreeken

*Maastricht University, the Netherlands*

The research described in this thesis was performed at Metabolomics and Analytics Center (MAC) of the Leiden Academic Centre for Drug Research (LACDR), Leiden University (Leiden, The Netherlands). The research was financially supported as indicated in each chapter.

见微知著

*From the minute to the profound*



# Contents

<b>Chapter I</b>	General introduction and scope	<b>1</b>
<b>Chapter II</b>	Analytical techniques for biomass-restricted metabolomics: an overview of the state-of-the-art <i>Microchemical Journal (2021)</i>	<b>13</b>
<b>Chapter III</b>	Quantification of endocannabinoids in human cerebrospinal fluid using a novel micro-flow liquid chromatography-mass spectrometry method <i>Analytica Chimica Acta (2022)</i>	<b>41</b>
<b>Chapter IV</b>	A micro-flow liquid chromatography-mass spectrometry method for the quantification of oxylipins in volume-limited human plasma <i>ELECTROPHORESIS (2024)</i>	<b>65</b>
<b>Chapter V</b>	Capillary Electrophoresis-Mass Spectrometry for Creatinine Analysis in Residual Clinical Plasma Samples and Comparison with Gold Standard Assay <i>ELECTROPHORESIS (2024)</i>	<b>97</b>
<b>Chapter VI</b>	Conclusions and perspectives	<b>113</b>
<b>Appendix</b>	Summary	<b>124</b>
	Nederlandse samenvatting	<b>127</b>
	Curriculum vitae	<b>130</b>
	List of publications	<b>131</b>
	Acknowledgements	<b>132</b>





# Chapter I

---

## General introduction and scope

Clinical and pharmaceutical studies face a persistent obstacle with biomass-restricted samples, which impede the comprehensive deciphering of biological progresses and disease mechanisms. Traditional analytical methods often fall short when confronted with these challenges, necessitating the development of alternative approaches. Micro-flow LC-MS methods offer a compelling solution by enabling the analysis of minute sample volumes with high sensitivity and good precision. Biomass-restricted samples in this thesis refers to biospecimens with low concentrations or limited amount for analytical measurements.

In clinical studies, we seek a non-invasive sampling method that causes minimal pain or trauma to the patients. The development of micro-sampling methods including fine needle aspiration biopsy (tissue), fine microextraction techniques, dried blood spots(blood), microdialysis (cerebrospinal fluids), and so on, have achieved the goal for minimal sample amount (e. g. blood sampling volume  $<50\ \mu\text{L}$ ) [1]. However, the biomass requirements for biochemical and analytical analysis methods are normally larger than this to reach reliable quantification limits. Not to mention the common circumstance when multiple aliquots need to be made for comprehensive investigation with various analytical methods [2, 3]. Similarly, analyses with experimental animals are challenging as well, since the model animals have less blood/CSF/tissue, while pharmaceutical studies require sampling over multiple time points.

### **Development of miniaturized analytical methods for Metabolomics studies**

Metabolomics studies typically employ analytical techniques to investigate changes in metabolites resulting from factors such as disease, diet, and exposure to specific environments. Liquid chromatography-mass spectrometry (LC-MS) and capillary electrophoresis-mass spectrometry (CE-MS) are commonly utilized due to their ability to analyze a wide range of compounds based on their physical chemical properties [4]. Although the analytical workflows using these techniques have been well-developed and contribute a lot to metabolomics, clinical and pharmaceutical studies [5-7], for some research when biomass-restricted samples are involved, the sensitivity of conventional methods can be an issue. To address this, miniaturized metabolomics has emerged as a promising approach. The common matrices for metabolomics studies include blood, urine,

feces, cerebrospinal fluids, and tissues. Miniaturized metabolomics methods are required for matrices such as body fluids from infants, small animal models, or other biospecimens obtained with micro-sampling devices. Advances in miniaturized workflows are crucial for enhancing our understanding of various diseases and pathological processes in biomass-restricted samples.

By operating at micro- to nano-liter flow rates, miniaturized LC-MS and CE-MS methods minimize sample dilution within the ionization source, thereby enhancing ionization efficiency. These techniques require only minute sample volumes to achieve equivalent or better limits of detection while maintaining broad coverage of metabolites [8]. Additionally, the reduced sample volume reduces source contamination and matrix effects [9]. The adoption of miniaturized techniques offers financial benefits and improves the welfare of experimental subjects. Reduced consumption of organic solvents for mobile phase and sample extraction significantly lowers costs. Furthermore, it mitigates the risk of researchers' exposure to toxic organic solvents like chloroform and acetonitrile (classified as class 2 solvents for toxicity in FDA guidance). In an era increasingly concerned with the welfare of patients, clinical study volunteers, and laboratory animals, minimizing sample volume translates to less harm inflicted on study subjects.

Miniaturized analytical techniques show promise for revolutionizing future clinical diagnostics and personalized medicine by offering minimally invasive procedures and the ability to detect important disease biomarkers even at lower concentrations. However, concerns about their robustness occasionally arise due to issues such as column clogging, tubing leaks, and spray emitter malfunctions. These challenges can be mitigated by implementing cleaner sample preparation methods and ensuring correct tubing connections within the system. The development of a miniaturized analytical method requires understanding the contributions from sampling, sample preparation, and LC/CE-MS instrumentation to sensitivity and robustness. By combining microsampling, miniaturized sample preparation method, and micro flow-LC-MS, CE-MS methods, the miniaturized workflow will be an optimal choice for studies with biomass-restricted samples, ultimately advancing our understanding of disease mechanisms and aiding in the discovery of novel biomarkers.

## **Biomass-restricted studies**

### **-Pediatric studies**

Pediatric studies involve the examination of medical conditions, treatments, and interventions specifically tailored to children, from birth through adolescence. These studies encompass a wide range of disciplines, including pediatric oncology, neonatology, developmental biology, pharmacology, psychology, and public health [10-12]. The difference of how children react to disease or treatment can be differ among various age stages [13]. In order to address the unique physiological, developmental, and psychological needs of children, as well as help with the diagnosis and treatment in this vulnerable population, analysis using pediatric samples is necessary.

Blood is one of the most frequently analyzed matrices in pediatric studies. It provides valuable information about the child's overall health, including levels of various biomarkers, hormones, nutrients, and medications. The volume of blood that can be safely obtained from children, especially infants and newborns, is limited since they possess lower total blood volume (TBV) [14]. In a newborn, the total volume of blood is estimated at 80–90 mL/kg body weight. According to the European regulatory guidelines, trial-related blood loss should not exceed 3% of the total blood volume during a period of 4 weeks and should not exceed 1% at any single time [15]. A study including 141 children from six months to 12 years old also suggested repeated sampling totaling up to 3% of blood volume is safe [16]. According to the WHO, the average birth weight of a full-term male baby is 3.3 kilograms (kg). The average birth weight of a full-term female is 3.2 kg. This means there is a total volume of around 276.3 mL blood per full-term baby, the volume that could be sampled a single time is not more than 2.8 mL (1% TBV), and not more than 8.3 mL for repeated sampling (3% TBV). The volume will be only less if preterm and children with health issues are taken into account. However, in extreme circumstance, medical intervention is required in preterm infants, and they could lose almost one-third of their total blood volume in the first month of life due to multiple blood draws for laboratory investigations, and procedures [17, 18], which leads to extra trauma to the patients. Blood samples can be obtained via heel puncture or fingerstick, which is painful for the vulnerable infants and newborns.

Microsampling techniques, which allow minimally invasive sampling using microneedles, can ease the pain from blood sampling as well as reduce excessive blood loss. However, the smaller sample volume obtained may pose challenges for conventional analytical measurements.

Given the volume limitations inherent in pediatric samples, to ease the pain from the sampling procedure as well as lower risks from too much blood loss, analytical methods with higher sensitivity for trace volume samples is urgently required.

### **-Animal studies**

Experimental animals can serve as models for studying complex biological processes and disease mechanisms that often cannot be adequately replicated in vitro or in silico. By studying diseases and treatments in animals, researchers gain valuable insights into the underlying mechanisms of disease pathology, drug metabolism, and pharmacokinetics [19-22].

During pharmaceutical development, before the candidate drug can be tested in clinical studies on humans for treatment purpose, it must undergo rigorous preclinical testing in animal models to assess its safety and efficacy, including potential side effects, toxicities, allowing researchers to refine dosing regimens and prioritize drug candidates for further development. For PK/TK purposes, multiple sampling over 24 hours is required. Apart from pharmaceutical studies, to gain a comprehensive understanding of certain health-related conditions, samples from animal models are commonly analyzed by multiple platforms including metabolomics, proteomics and transcriptomics. However, the sample amount acquired from some small animal models is inadequate for all of those analysis.

Take mouse as an example, a mouse with body weight of 25 g has a total blood volume around 1.8 mL, a single sampling above 15% TBV ( $>270\ \mu\text{L}$ ) and multiple sampling more than 20% TBV ( $>360\ \mu\text{L}$ ) are not recommended since hypovolemic shock may occur [23] and affect the following sampling timepoints. For metabolomics studies, the interference of such acute stress caused by sampling could also cause changes in the metabolite profile and deliver unreliable data [24]. Moreover, excessive sampling is against animal welfare and the 3R (replacement, reduction, refinement) principle [25]. While multiple blood sampling

from tail vein is normally applied on experimental mice/rats in pharmaceutical study, the biomass of blood sample could be limited per collection point.

The zebrafish and zebrafish larvae exhibit a correlation between neuroanatomical and physiological features that is comparable to what has been observed in mammals. This similarity enables the creation of dependable and pertinent experimental models for researching neurological disorders [26, 27]. As an ideal alternative experimental model to mammals, the analysis of zebrafish or zebrafish larvae using LC/CE-MS usually requires pooling several samples, resulting in a loss of data on the heterogeneity between animals [28].

While animal research remains essential for advancing medical science, efforts to refine experimental techniques, minimize suffering for better experimental animal welfare, and explore alternative models are ongoing. As an example, a pharmacokinetic study of insulin in rat plasma combined microsampling and micro flow-LC-MS analysis, which proved the advantage of miniaturized analytical workflow over conventional method. A 47-fold sensitivity increasement enabled the analysis of volume-limited samples [29].

#### **- Miniaturized method development for concentration-limited compounds**

Miniaturized analytical methods offer a significant advantage in sensitivity enhancement, enabling the detection and quantification of compounds including drugs and metabolites in trace level concentrations [30-32]. Upon analyzing concentration-limited samples, the method development strategy is the same as conventional methods. For hydrophobic compounds like lipids, the micro flow-RPLC-MS method provides benefits such as high-resolution separation, sensitivity, and robustness. However, RPLC is not the ideal separation method for polar compounds such as amino acids and their derivatives. In contrast, hydrophilic interaction liquid chromatography (HILIC) is a valuable tool for analyzing polar compounds, although miniaturizing it is comparatively challenging compared to RPLC. The inclusion of salts in HILIC mobile phases decreases retention and improves peak shape, but also leads to ionization suppression and the risk of clogging in micro-LC column and spray emitter. Conversely, capillary electrophoresis (CE), which is sometimes overlooked, allows for the measurement of polar compounds by separating them

based on size and charge within an electric field. The advancement of sheathless CE-MS avoids dilution in ionization source and highly improves its sensitivity. The low-nano liter injection volume makes it ideally suited for miniaturized sample analysis [33].

Proper sample preparation methods are crucial for concentration-limited analytes in miniaturized metabolomics workflow. To avoid clogging systems and improve the detection sensitivity, a clean and efficient sample preparation procedure is required. In theory, a consistent extraction recovery through different concentration levels is good enough for bioanalysis. However, for concentration-limited compounds, sample loss such as due to adsorption on wall of sample vials could be fatal to the quantification. Online sample preparation techniques such as solid-phase microextraction coupled with miniaturized systems could help overcome the sample loss during sample transfer as well as increase throughput [34]. On the other hand, up-concentration strategy by evaporation or electro-extraction is commonly used for sensitivity improvement. While miniaturized LC-MS or CE-MS systems are easier to be clogged by matrix samples, extra attention should be paid on sample clean up.

## Scope and outline of the thesis

Quantification of trace level compounds is always challenging to conventional analytical techniques. The demand of using limited volume samples further emphasizes that more sensitive and robust analytical methods are urgently required. As a concentration-sensitive detector at the flow rates used in this thesis, MS exhibits the same sensitivity when samples with identical concentrations are sprayed into the MS via the electrospray interface. In this thesis, the hypothesis is that by using micro/nano flow rates, we can significantly reduce sample dilution in the MS ionization source when working with biomass-restricted samples and a rugged source design is needed for clinical applications. In addition, when further decreasing the flow rate as with sheathless CE-MS, the MS detector becomes mass sensitive as the ionization becomes more efficient, and the detection limits become more favorable for biomass-limited samples.



In order to verify this hypothesis, we investigate how miniaturized analytical methods can enhance the sensitivity for biomass-restricted samples in metabolomics studies. This will be achieved by selecting and optimizing analytical techniques based on the properties of matrices and targeted compounds. Micro-flow LC-MS and sheathless CE-MS methods are established respectively for the analysis of lipids and amino acids, and these methods are applied on various biomass-restricted biospecimens to prove their applicability in biological and clinical studies.

To address the biomass mismatch challenge during quantitative analysis, and increase the sensitivity of analytical methods, this thesis discusses the development of miniaturized analytical methods using micro-flow LC-MS and CE-MS and investigates their potential for clinical studies with biomass-restricted samples. An overview structure of the thesis and the aim of each chapter is shown in **Figure 1**.

A robust system with stable ionization spray and high ionization efficiency is the key for method development and application on biological studies. At the start of the thesis, the focus is on performance evaluation of current commercial instrumentation for miniaturized analysis, including LC, MS, and ionization sources designed for low flow rates. An overview of the state-of-art analytical techniques for biomass-restricted analysis is presented in **chapter 2**, giving a critical overview of current microscale analytical techniques for the analysis of small-volume biological samples with a metabolomics approach. Technological developments are highlighted and relevant applications are discussed. However, the robustness of miniaturized techniques needs to be further improved for their application in clinical studies.

After comparing the currently available micro-flow LC-MS techniques, investigation of their practical performance is done in **Chapter 3&4**. The aim of **Chapter 3** is to develop a new micro-LC-MS approach for the selective and sensitive determination of endocannabinoids and its analogues in human cerebrospinal fluid (CSF). Such a method is needed in order to study the role of the endocannabinoid system in various brain disorders, as current LC-MS approaches are not sensitive enough or lack the analytical performance for this purpose. In particular, a modified micro-ESI spray needle is used in this study (Shimadzu Mikros), which enhances the analytical performance and durability of our

method for the quantitative determination of endocannabinoids in human CSF samples. The developed workflow is successfully used for the determination of endocannabinoids in 288 human CSF samples, thereby clearly showing the utility of this approach for endocannabinoids profiling in biomass-restricted clinical samples.

Low flow LC-MS in negative mode is often not robust due to ionization discharge. In addition to the quantification of concentration limited compounds, the applicability of micro-LC-MS in volume-limited plasma under negative mode is discussed in **chapter 4**, where a sensitive method dedicated to the study of oxylipins in 5  $\mu$ L human plasma is developed. The method is validated and compared to a published conventional UHPLC-MS method, particularly in terms of sensitivity enrichment. The same triple quad MS is used for both methods to ensure a fair comparison. In order to demonstrate its applicability, the method is applied to 40 human plasma samples from a healthy aging study.

The coverage of compounds is important for metabolomics study in biomarker discovery. As reverse-phase LC-MS is utilized in the previous chapters for hydrophobic compounds. The potential of a miniaturized analytical method for polar compounds in volume-limited samples is discussed in **chapter 5**. We focus on developing and assessing the utility of a sheathless CE-MS-based analytical workflow for the determination of creatinine in residual plasma samples with the aim to assess whether this approach is suited for the reliable quantitative determination of endogenous metabolites in small-volume samples. The latter is a requirement before actually testing the analytical workflow on neonatal samples, which will be the logical next step/follow-up work. In this study, we demonstrate that with a starting amount of only 5 microliter of human plasma, we can quantitate creatinine in a reliable way, and compare this with a gold standard assay for creatinine analysis, which requires 100 microliter in clinical labs. Apart from creatinine, we can analyze many other metabolites with sheathless CE-MS in the residual plasma sample, in contrast to the limited scope of the gold standard assay, opening up the possibility to study the role of metabolites and metabolite profiles in neonatal healthcare.

Finally, **chapter 6** offers a general conclusion of the studies described in this thesis. Perspectives and recommendations on further improvement and applications of the proposed miniaturized analytical methods are also discussed.

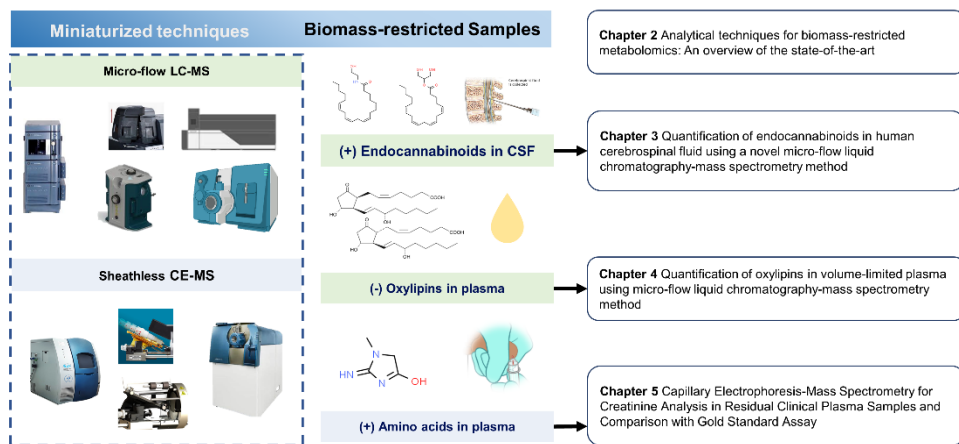


**Figure 1.** Overview structure of the thesis and the aim of each chapter.

## References

- [1] K.J. Williams, J. Lutman, C. McCaughey, S.K. Fischer, Assessment of low volume sampling technologies: utility in nonclinical and clinical studies, *Bioanalysis*, 13 (2021) 679-691.
- [2] Q. Xuan, Y. Ouyang, Y. Wang, L. Wu, H. Li, Y. Luo, X. Zhao, D. Feng, W. Qin, C. Hu, L. Zhou, X. Liu, H. Zou, C. Cai, J. Wu, W. Jia, G. Xu, Multiplatform Metabolomics Reveals Novel Serum Metabolite Biomarkers in Diabetic Retinopathy Subjects, *Advanced Science*, 7 (2020) 2001714.
- [3] M. Fernández-García, M. Ares-Arroyo, E. Wedel, N. Montero, C. Barbas, M.F. Rey-Stolle, B. González-Zorn, A. García, Multiplatform Metabolomics Characterization Reveals Novel Metabolites and Phospholipid Compositional Rules of *Haemophilus influenzae* Rd KW20, *Int J Mol Sci*, 24 (2023) 11150.
- [4] B.C. Muthubharathi, T. Gowripriya, K. Balamurugan, Metabolomics: small molecules that matter more, *Molecular Omics*, 17 (2021) 210-229.
- [5] C.-J. Chen, D.-Y. Lee, J. Yu, Y.-N. Lin, T.-M. Lin, Recent advances in LC-MS-based metabolomics for clinical biomarker discovery, *Mass Spectrometry Reviews*, 42 (2023) 2349-2378.
- [6] M. Beccaria, D. Cabooter, Current developments in LC-MS for pharmaceutical analysis, *Analyst*, 145 (2020) 1129-1157.
- [7] W. Zhang, R. Ramautar, CE-MS for metabolomics: Developments and applications in the period 2018–2020, *ELECTROPHORESIS*, 42 (2021) 381-401.
- [8] G.A. Valaskovic, L. Utley, M.S. Lee, J.-T. Wu, Ultra-low flow nanospray for the normalization of conventional liquid chromatography/mass spectrometry through equimolar response: standard-free quantitative estimation of metabolite levels in drug discovery, *Rapid Communications in Mass Spectrometry*, 20 (2006) 1087-1096.
- [9] S.R. Needham, Microspray and Microflow Liquid Chromatography: The Way Forward for LC–MS Bioanalysis, *Bioanalysis*, 9 (2017) 1935-1937.
- [10] B. Hutzen, S.N. Paudel, M. Naeimi Kararoudi, K.A. Cassady, D.A. Lee, T.P. Cripe, Immunotherapies for pediatric cancer: current landscape and future perspectives, *Cancer and Metastasis Reviews*, 38 (2019) 573-594.
- [11] R. Dasgupta, D. Billmire, J.H. Aldrink, R.L. Meyers, What is new in pediatric surgical oncology?, *Current Opinion in Pediatrics*, 29 (2017) 3-11.
- [12] A.A. Vinks, J.S. Barrett, Model-Informed Pediatric Drug Development: Application of Pharmacometrics to Define the Right Dose for Children, *The Journal of Clinical Pharmacology*, 61 (2021) S52-S59.
- [13] H.K. Batchelor, J.F. Marriott, Paediatric pharmacokinetics: key considerations, *British Journal of Clinical Pharmacology*, 79 (2015) 395-404.
- [14] S.R. Howie, Blood sample volumes in child health research: review of safe limits, *Bulletin of the World Health Organization*, 89 (2011) 46-53.

- [15] E. Lopriore, The total volume of blood in an extremely preterm neonate is about the size of a double espresso, *Acta Paediatrica*, 112 (2023) 2458-2459.
- [16] C. Peplow, R. Assfalg, A. Beyerlein, J. Hasford, E. Bonifacio, A.-G. Ziegler, Blood draws up to 3% of blood volume in clinical trials are safe in children, *Acta Paediatrica*, 108 (2019) 940-944.
- [17] C.E. Counsilman, L.E. Heeger, R. Tan, V. Bekker, J.J. Zwaginga, A.B. te Pas, E. Lopriore, Iatrogenic blood loss in extreme preterm infants due to frequent laboratory tests and procedures, *The Journal of Maternal-Fetal & Neonatal Medicine*, 34 (2021) 2660-2665.
- [18] A. Aboalqez, P. Deindl, C.U. Ebenebe, D. Singer, M.E. Blohm, Iatrogenic Blood Loss in Very Low Birth Weight Infants and Transfusion of Packed Red Blood Cells in a Tertiary Care Neonatal Intensive Care Unit, *Children*, 8 (2021) 847.
- [19] I.J. Marques, E. Lupi, N. Mercader, Model systems for regeneration: zebrafish, *Development*, 146 (2019).
- [20] H. Hou, E. Nudleman, Robert N. Weinreb, Animal Models of Proliferative Vitreoretinopathy and Their Use in Pharmaceutical Investigations, *Ophthalmic Research*, 60 (2018) 195-204.
- [21] J. Song, Y.-K. Kim, Animal models for the study of depressive disorder, *CNS Neuroscience & Therapeutics*, 27 (2021) 633-642.
- [22] N.B. Robinson, K. Krieger, F.M. Khan, W. Huffman, M. Chang, A. Naik, R. Yongle, I. Hameed, K. Krieger, L.N. Girardi, M. Gaudino, The current state of animal models in research: A review, *International Journal of Surgery*, 72 (2019) 9-13.
- [23] K.-H. Diehl, R. Hull, D. Morton, R. Pfister, Y. Rabemampianina, D. Smith, J.-M. Vidal, C.V.D. Vorstenbosch, A good practice guide to the administration of substances and removal of blood, including routes and volumes, *Journal of Applied Toxicology*, 21 (2001) 15-23.
- [24] W.D. Lee, L. Liang, J. AbuSalim, C.S.R. Jankowski, L.Z. Samarah, M.D. Neinast, J.D. Rabinowitz, Impact of acute stress on murine metabolomics and metabolic flux, *Proceedings of the National Academy of Sciences*, 120 (2023) e2301215120.
- [25] E. Harstad, R. Andaya, J. Couch, X. Ding, X. Liang, B.M. Liederer, K. Messick, T. Nguyen, M. Schweiger, J. Tarrant, S. Zhong, B. Dean, Balancing Blood Sample Volume with 3Rs: Implementation and Best Practices for Small Molecule Toxicokinetic Assessments in Rats, *ILAR Journal*, 57 (2017) 157-165.
- [26] J.G.S. Rosa, C. Lima, M. Lopes-Ferreira, Zebrafish Larvae Behavior Models as a Tool for Drug Screenings and Pre-Clinical Trials: A Review, *Int J Mol Sci*, 23 (2022) 6647.
- [27] B. Bauer, A. Mally, D. Liedtke, Zebrafish Embryos and Larvae as Alternative Animal Models for Toxicity Testing, *Int J Mol Sci*, 22 (2021) 13417.
- [28] A. Bartoszek, A. Trzpił, A. Kozub, E. Fornal, Optimization of the Zebrafish Larvae Pentylentetrazol-Induced Seizure Model for the Study of Caffeine and Topiramate Interactions, *Int J Mol Sci*, 24 (2023) 12723.
- [29] G.B. Troché, T. Søbørg, T.B. Bødvarsdottir, M. Bjelke, N.J. Nielsen, Comparison of pharmacokinetic study profiles of insulin in rat plasma through conventional sampling and microsampling by micro-LC-MS/MS, *Bioanalysis*, 15 (2023) 283-294.
- [30] X. Yi, E.K.Y. Leung, R. Bridgman, S. Koo, K.-T.J. Yeo, High-Sensitivity Micro LC-MS/MS Assay for Serum Estradiol without Derivatization, *The Journal of Applied Laboratory Medicine*, 1 (2016) 14-24.
- [31] V. Fitz, Y. El Abiead, D. Berger, G. Koellensperger, Systematic Investigation of LC Miniaturization to Increase Sensitivity in Wide-Target LC-MS-Based Trace Bioanalysis of Small Molecules, *Frontiers in Molecular Biosciences*, 9 (2022).
- [32] M. Zhang, B. An, Y. Qu, S. Shen, W. Fu, Y.-J. Chen, X. Wang, R. Young, J.M. Canty, Jr., J.P. Balthasar, K. Murphy, D. Bhattacharyya, J. Josephs, L. Ferrari, S. Zhou, S. Bansal, F. Vazvaei, J. Qu, Sensitive, High-Throughput, and Robust Trapping-Micro-LC-MS Strategy for the Quantification of Biomarkers and Antibody Biotherapeutics, *Analytical Chemistry*, 90 (2018) 1870-1880.
- [33] E. Sánchez-López, G.S.M. Kammeijer, A.L. Crego, M.L. Marina, R. Ramautar, D.J.M. Peters, O.A. Mayboroda, Sheathless CE-MS based metabolic profiling of kidney tissue section samples from a mouse model of Polycystic Kidney Disease, *Scientific Reports*, 9 (2019) 806.
- [34] J.C. Cruz, I.D.d. Souza, F.M. Lanças, M.E.C. Queiroz, Current advances and applications of online sample preparation techniques for miniaturized liquid chromatography systems, *Journal of Chromatography A*, 1668 (2022) 46292



# Chapter II

---

## **Analytical techniques for biomass-restricted metabolomics: an overview of the state-of-the-art**

### **Based on:**

Bingshu He, Wei Zhang, Faiza Guled, Amy Harms, Rawi Ramautar, Thomas Hankemeier

**Analytical techniques for biomass-restricted metabolomics: An overview of the state-of-the-art**

Microchemical Journal 2021; DOI: 10.1016/j.microc.2021.106794

### **Abstract**

Biomedical and clinical questions increasingly deal with biomass-restricted samples. To address these questions with a metabolomics approach, the development of new microscale analytical techniques and workflows is needed. Over the past few years, significant efforts have been made to improve the overall sensitivity of MS-based metabolomics workflows to enable the analysis of biological samples that are low in metabolite concentration or biomass. In this paper, factors that are crucial for the performance of biomass-restricted metabolomics studies are discussed, including sampling and sample preparation methods, separation techniques and ionization sources. Overviews of MS-based miniaturized metabolomics studies reported over the past five years are given in tables, with information provided on sample type, sample preparation volume, injection volume, separation techniques and MS analyzers. Finally, some general conclusions and perspectives are given.

## 1. Introduction

Metabolomics has become an important tool in biological and clinical research and is particularly promising for biomarker discovery studies. Currently, reversed-phase liquid chromatography-mass spectrometry (RPLC-MS), gas chromatography-mass spectrometry (GC-MS) and nuclear magnetic resonance spectroscopy (NMR) are used as the main analytical tools in metabolomics, providing the performance needed for the analysis of hundreds to thousands of samples [1, 2]. However, these well-established analytical tools require a relatively large amount of sample for work-up and injection or detection (especially in case of NMR), thereby limiting their applicability to those biological and clinical problems that inherently deal with (very) low metabolite concentrations or biomass. For instance, one of the most crucial endocannabinoids, anandamide, possesses a concentration in the range from 0.5 to 2.7 pM in human cerebrospinal fluid (CSF) [3], and prohormone thyroxine and 3,3',5-triiodothyronine are present in concentrations from 1.4 to 2.3 pg/mL in biological samples [4]. The development of miniaturized RPLC-MS methods was required in order to determine these trace-level compounds [5, 6]. Besides addressing issues with low metabolite concentrations, another analytical challenge is the study of biological and clinical questions intrinsically dealing with low amounts of starting material, such as exosomes, primary cells, single cell analysis [7], zebra fish, and samples from 3D microfluidic cell culture systems (**Figure 1**). Improved or new analytical techniques are therefore needed to enable the study of these questions with metabolomics.

Over the last few years, considerable efforts have been dedicated to improving the overall sensitivity of MS-based metabolomics workflows to enable the analysis of samples that are limited in metabolite concentration or biomass. **Figure 2** shows a typical analytical workflow used for metabolomics. In this work, specific attention will be given to the developments in sampling, sample preparation and separation-based MS approaches for biomass-restricted metabolomics studies. General factors dictating the sensitivity of MS-based approaches are shortly considered including the development of miniaturized ionization sources. An overview of recently developed micro- and nanoscale separation techniques coupled to MS and their applications to biomass-restricted metabolomics studies is provided in table format. Selected examples will be highlighted to illustrate the utility of miniaturized methods for biomass-restricted metabolomics with emphasis given on some



analytical performance metrics. Finally, some general conclusions and perspectives are provided.

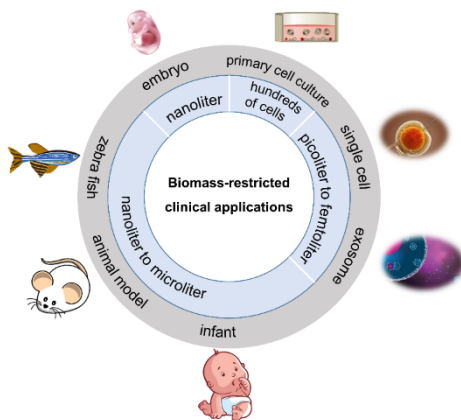


**Figure 1.** An illustration of biomass-restricted applications requiring microscale separation techniques for performing metabolomics studies. \*Blood and sweat samples are only considered in case of infants.

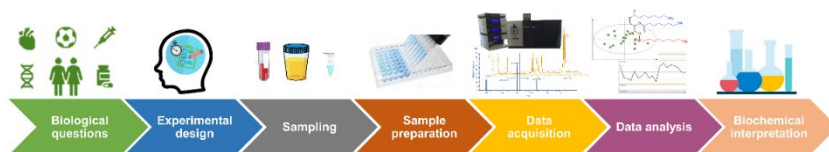


**Figure 2.** Typical analytical workflow used for metabolomics studies.

## 2 Sampling and sample preparation strategies for biomass-restricted metabolomics

The volume-mismatch between the volume-limited biological samples and the minimum volume requirements for sampling and/or sample preparation could be considered as one of the main analytical challenges for biomass-restricted metabolomics studies. The commonly used animal models in biological and biomedical studies, such as mouse, guinea pig and zebra fish, have restrictions in terms of the amount of body fluid or tissue available for experimental work, resulting in samples which are rather hard to analyze with conventional analytical methods and workflows employed in metabolomics. Thus, sampling and sample

preparation methods for these kinds of samples should be scaled-down enough to minimize sample loss and provide as much sample as possible for the follow-up analysis.

## 2.1 Developments in sampling strategies

In order to obtain samples from volume-limited experimental subjects, recent advancements in sampling methods endeavor to acquire microliter to nanoliter volumes with micromanipulation techniques. One of the promising sampling techniques for limited sample volume is microdialysis sampling, which was designed to continuously obtain samples from extracellular regions of living tissues. Since the collected samples can be analyzed by any appropriate analytical technique [8], microdialysis sampling has been used in studies on brain diseases including Alzheimer's disease, Parkinson's disease, Huntington's disease, traumatic brain injury and epilepsy [9, 10]. However, due to the relatively large size of probe, the first applications of microdialysis sampling suffered from poor spatial resolution. To overcome this weakness, a low-flow push–pull strategy was proposed. By using this strategy, there is less tissue damage than normal microdialysis, as artificial CSF would be pushed into the same sampling position with low flow rate (50 nL/min). This low-flow push-pull perfusion design contributed to a higher spatial resolution and provided more information from intact tissues than previous methods for neurochemical monitoring [11]. For application to other tissues, Weisenberger *et al.* developed an online microdialysis-capillary electrophoresis method for the *in vivo* monitoring of amino acids from adipose tissue. This microdialysis probe was constructed with two fused silica capillaries inserted into a hollow fiber and gave a sampling region of 3 mm. Laser-induced fluorescence (LIF) detection was used in this method together with CE, after derivatization with 20 mM 4-fluoro-7-nitrobenzofurazan /250  $\mu$ M hydrochloric acid in 50% methanol. As a result, 12 amines were detected with only 22 seconds per analysis in inguinal adipose tissue. This method has been successfully assessed by administering an insulin stimulation via tail vein injection to record dynamic, *in vivo* changes in amino acid metabolism with good reproducibility[12]. Schoors *et al.* developed a sensitive method by coupling the microdialysis sampling probe with ultra-high pressure liquid chromatography-electrochemical detection (UHPLC-ECD). A 1 mm I.D. column was used for the simultaneous determination of monoamines, dopamine, noradrenaline and serotonin with lower limit of quantification (LLOQ) of 100-150 pM in material-limited samples, such as

rat hippocampus, prefrontal cortex and striatum [13]. The direct connection with sensitive analytical techniques such as LC-MS, immunoassay, and capillary electrophoresis with laser-induced fluorescence (CE-LIF)[10] is conducive to higher temporal and spatial resolution.

Apart from its application in microdialysis, the pull-push strategy was also used on a dual-probe microfluidic chip developed by Huang *et al.*. Instead of artificial matrix, extraction solvents or ionization buffer were pushed for the sample extraction in dried spot samples and liquid-phase samples, providing better conditions for ambient MS ionization. The sampling procedure of dried spots takes about 10 seconds for each spot with 500 nL/min flow rate, and sample volume was 100 nL for liquid-phase sampling. While they used reserpine solution to validate these two methods, the detection limit with dried spot sampling device was 0.4 pg with RSDs ranges from 8.9-31.5% in all tested concentrations. As for liquid-phase sampling, the sampling volume was 100 nL, limit of detection was 41 nM for reserpine, the peak area RSD of 63 reserpine droplets was 15.6%. By integrating the micro-sampling probe, electrospray emitter probe and online mixer (for derivatization) on one glass microchip, this technique was applied on an analysis for *in situ* evaluation of residual pesticide on apples and also an evaluation of nanoliter-scale Ugi-type reactions for 8 compounds [14]. This study demonstrated the versatility of the micro sampling method and its promising utility in sampling nanoliter samples.

When it comes to single cells, direct infusion mass spectrometry analysis with integrated micro sampling probes is preferable since the nanoliter (or even lower) level sample amount would impose a tremendous challenge on sample preparation and/or transfer. Moreover, the biochemical heterogeneity of each cell could be preserved as much as possible by using this approach [15]. Pipette-based micromanipulation and chip-based sampling strategies were normally used prior to MS analysis [16]. In this context, Liu *et al.* recently designed a “T-probe” for the sampling of intracellular samples in single mammalian cells followed by direct infusion nanoESI analysis (see **Figure 3**). Cytoplasm was sampled through the sampling capillary and injected directly through the nanoESI emitter into an LTQ Orbitrap XL MS together with sampling solvents. Four standard compounds including two lipids, one anticancer drug and a peptide were selected to validate this method, the limit of detection ranges from 0.1 to 10 nM. Although the limited sampling volume from one HeLa

cell (1.2 to 4.3 pL) may affect the compound coverage, this method was applied on two cell groups with or without irinotecan treatment, and the multivariate analysis of metabolic profiles showed significant differences between these two groups. Some biomarkers that could be used to evaluate treatment efficacy were identified, indicating the potential utility of this method in pharmaceutical studies [17]. CE-MS is well matched with single cell sampling devices because of its nanoscale injection volume. Onjiko *et al.* developed a sampling system containing a pulled capillary, called a “micropipette”, with a tapered tip (about 20  $\mu\text{m}$  tip inner diameter) to aspirate cytoplasm from cells, coupled to a motorized three-axis micro-manipulator to control the movement of micropipettes with 20 nm resolution. Around 10-15 nL cytoplasm was collected from a single live frog embryo cell and extracted with 4  $\mu\text{L}$  of solvent. The cell extract was deposited in a microvial, together with cell debris and precipitates, and analyzed by CE-MS. Results showed approximately 230 different molecular features were observed, and 70 compounds including spermidine, thiamine, and choline were identified [18]. This method enabled triplicate sampling and analysis from one cell within 5 seconds without influencing cell division from the 8-cell stage embryo to the 16-cell stage. The RSD of 4 to 7 biological replicates was around 22% with only 10 nL injected. In order to look into the *in situ* information from a single cell, it is crucial for the sampling method to preserve the physiological environment of the cell during the metabolomics study, so the results reflect the real metabolic situation in a living organism. Guillaume-Gentil *et al.* used fluidic force microscopy to extract cytoplasmic metabolites from a single HeLa cell under subpicoliter resolution (0.8 to 2.7 pL) without perturbing the biochemical environment or damaging its viability. The picoliter level sample was released as a 95  $\mu\text{m}$  spot on a coated chip for matrix-assisted laser desorption/ionization time-of-flight mass spectrometry (MALDI-TOF MS). The advantage of this fluidic force microscopy was its unique pyramidal geometry probe with small size aperture (400 nm), which could prevent membrane damage while extracting all the soluble intracellular molecules. With the assistance of 9-aminoacridine as MALDI matrix, 20 different metabolites including ribonucleotides, activated sugars, amino acids and glutathione were identified in at least 2 out of 4 cytoplasmic samples [19]. With these single cell sampling methods, heterogeneity could be addressed during the metabolomics analysis, which provided valuable information for the understanding of disease mechanisms and metabolic pathways of other important biological processes.

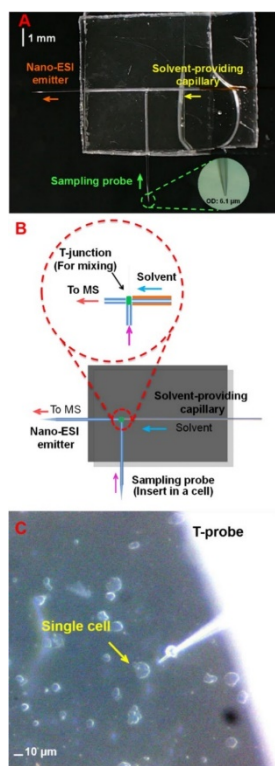


**Figure 3.** Utilizing the T-probe for the single cell MS experiments. (A) Photo of a T-probe. Inset: a zoomed-in photo of the sampling probe tip. (B) Illustration of the working mechanism and fluid flow directions in the T-probe. (C) Photo illustrating the insertion of the T-probe tip into a cell [ref. 17].

As for vulnerable research subjects such as newborns and the elderly, several dried blood spot (DBS) sampling techniques have already been applied for decades in the screening of inborn errors of metabolism and disease diagnosis [20, 21]. Improvements to this technique which minimize discomfort and improve quantitation are found in novel micro/nano-scale minimally invasive sampling methods such as volumetric absorptive microsampling (VAMS) which are now available for clinical and metabolomics research. The volumes sampled by these devices vary from 10 to 30  $\mu\text{L}$  for plasma, urine or oral fluid [20, 22], depending on the tip size.

Generally, sample loss is often observed during the sample transfer in sampling and sample preparation procedures regardless of the adopted strategy. The loss of target compounds can be corrected for through proper use of internal standards in metabolomics analysis. However, corrections will not be possible if the concentration is already below the detection limit. Therefore, it is crucial to find strategies to avoid sample loss during extraction and increase the sensitivity of analytical methods as much as possible.

Although it is possible to collect samples with limited volume, it is still challenging to perform efficient sample preparation in especially sub-microliter samples without dilution. Choices have to be made whether it is more important to provide enough volume for following analysis or if concentrating targeted compounds to reach the detection limits is required. Pooling several volume-limited samples together is normally used to provide enough starting material, but this is not an ideal option in metabolomics studies since it only provides an average read-out instead of reflecting individual differences due to diseases or drug response. In order to determine the internal drug exposure in the blood of zebrafish larvae, Van Wijk et al. developed a sampling method with pulled glass capillary needles under microscope. In this method, around 1 nL of blood could be obtained from zebrafish larvae. However, in order to reach measurable levels of paracetamol and its main metabolites, 15-35 samples were pooled together for sample preparation for analysis using a UHPLC-MS method where they were quantified with sub-picomole levels [23]. The same pooled strategy was also commonly used in many other zebrafish studies [24, 25] due to the minimal material for the required sensitivity. Unfortunately, the metabolic heterogeneity of different organisms is overlooked in this way.

## **2.2 Developments in sample preparation strategies**

After choosing a suitable sampling method, development of sample preparation strategies for especially volume limited samples is the next important step for biomass restricted sample analysis. Sample transfers between tubes or vials should be avoided as much as possible for an ideal miniaturized sample preparation procedure to prevent unnecessary sample loss. Microvials or nanovials are recommended during sample preparation for better sampling of small volumes [18]. Protein precipitation, LLE and SPE methods are still the most used sample preparation procedures in bioanalysis, including metabolomics [26, 27].

Protein precipitation and LLE strategies can be used for many volume-limited applications. By using volatile liquids in these two strategies, relatively large amounts of organic solvents can be evaporated and then the sample can be reconstituted in only a small amount of solvent compatible with the follow-up separation technique. Obviously, when the starting amount is lower than the reconstitution volume, there would still be a dilution effect with these steps. The extent to which compounds can be enriched with an evaporation step is

sometimes limited by solubility, and for good quantification, methods should avoid supersaturation of abundant components, while still concentrating the low abundance compounds.

Ideally, human and animal studies would be able to collect real-time metabolomics data. In animal studies where samples are collected post mortem or when biopsies are taken in clinical setting, there is a risk that the metabolome may degrade between collection and sample preparation and analysis. One potential solution to this issue could be *in vivo* solid phase micro extraction (SPME) which is gaining more interest in metabolomics. In SPME, a thin probe is often coated with a C18 sorbent in union with polyacrylonitrile to increase biocompatibility. This probe is then inserted directly into tissue of a (sedated) organism to sample the metabolome in a minimized invasive manner, as no tissue is removed. The total sample “mass” is just the metabolites adsorbed to the C18 SPME material. Collecting sample in this manner is non-depleting and thus collects sample in real time during normal cellular metabolism while causing minimal metabolomics disruption [28]. *In vivo* SPME has proven to be effective for the analysis of a wide range of metabolites including low abundance steroids and lipids. These studies demonstrate particularly good recoveries for non-polar analytes as a result of the non-polar nature of the C18 phase being used as a sorbent [29]. Vasiljevic et al. introduced a solid-phase microextraction (SPME) minitip featuring a tip apex (1 mm) coated with polyacrylonitrile (PAN) and N-vinylpyrrolidone-co-divinylbenzene (also known as HLB) particles for the extraction of compounds from several sample-limited matrix types. In one application, this minitip was used in the quantification of several drugs of abuse in 1  $\mu$ L human blood with LODs from 0.1-2.5 ng/mL. After static extraction, the blood sample was desorbed in 3  $\mu$ L MeOH: ACN: FA (80:20:0.1) and transferred to a nanoESI sprayer. The minitip was also used for untargeted metabolomic profiling of single caviar eggs. The study of 4 different types of caviar eggs (6 replicates per type) with LC-HRMS showed the SPME minitip method was able to distinguish samples based on metabolomics profiles. 149 significant metabolites including eicosapentaenoic acid, L-tryptophan, and retinoic acid were detected. Although the repeatability of SPME minitip method was still not satisfying (20-30 RSD%) due to the deviations during the coating procedure, it is indeed promising as an integrated method of sampling and sample preparation for volume limited samples [30]. By combining SPME

with a miniaturized probe, another study developed a promising technique for the *in vivo* sampling and sample preparation of neurotransmitters from macaque brain. After thorough optimization of probe shape, desorption solvent and extracting phase, the SPME probe was coated with in-house synthesized HLB particles with a total diameter less than 200  $\mu\text{m}$ . Validation of this method was carried out by using brain surrogate matrix, LOQ from 25 ng/mL to 20  $\mu\text{g/mL}$  were reached with a 20% RSD value. When the method was applied on a macaque brain, 3 brain areas (prefrontal cortex area, premotor cortex area, and caudate nucleus head) were sampled simultaneously in consecutive triplicates, each extraction procedure in brain took 20 minutes. Several compounds including dopamine, serotonin, glutamate and taurine were quantified after extraction. Meanwhile, untargeted analysis revealed the possibility of detecting a wide polarity range of endogenous metabolites in brain sample using a SPME-based miniaturized *in vivo* sampling method (**Figure 4**) [31].

Other than its use for sampling endogenous metabolites, a SPME method was also reported for the quantification of doxorubicin in pig lung tissue. The quantification abilities of SPME in intact lung tissue, *ex vivo* SPME homogenized samples and solid-liquid extraction showed no significant difference. The LOD for doxorubicin was 2.5  $\mu\text{g/g}$  in tissue. Therefore, without extra sample preparation steps or significant invasive injury to the organism, *in vivo* SPME could be a future solution as a rapid quantitative method for monitoring and adjusting drug dosages during chemotherapy [32].

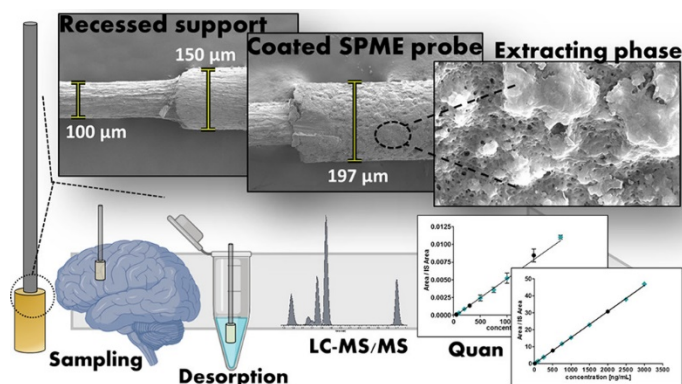


**Figure 4.** Solid Phase Microextraction-Based Miniaturized Probe and Protocol for Extraction of Neurotransmitters from Brains *in Vivo* [ref. 31]



### 3 MS-based separation techniques for biomass-restricted metabolomics

For miniaturized metabolomics studies with biomass-restricted samples, after effective microsampling and sample preparation procedures, proper chromatographic or electrophoretic separation methods and sensitive electrospray mass spectrometry (ESI-MS) are crucial aspects that determine the overall sensitivity of MS-based analytical methods.

When a sample is analyzed by LC-MS, the flow rate controls the amount of sample that reaches the ion source per unit time. In fact, sensitivity loss is likely to happen when there's limited current and the charge on each sample droplet is lower than the concentration of metabolites and causes insufficient ionization, hence the signals of compounds with lower proton affinity or surface activity could lose the competition for charge to compounds with a fixed charge or with higher proton affinity. With micro or nano flow rates, smaller droplets with higher surface-to-volume ratio will reduce ion suppression, thus not only increasing the detection sensitivity, but also broadening the coverage of metabolites [33, 34]. To describe the influence of flow rate on sensitivity, n-octyl-glucopyranoside ( $c = 10^{-6}$  mol/L) and turanose ( $c = 10^{-5}$  mol/L) in methanol/water (30:70) was injected under ESI condition. The result showed that at the flow rates of a few nanoliter per minutes, the ion suppression effects have totally disappeared while at flow rate above 50 nL/min the suppression increased to about a factor of five [35]. A higher sensitivity for fructose 6-phosphoric acid was also observed from nano-flow injection analysis (nano-FIA), indicating nano-flow rates give better analytical sensitivity than higher flow rates. In addition, the wider peak width from nano-flow allows a large number of analytes to be detected and identified under nano-flow. In this study, the peak areas of 22 metabolites were 7.6 to 66 times higher with nano-FIA compared to the conventional flow [36].

In a miniaturized analysis, the typical inner diameters of columns are decreased to below 1 mm for micro-LC, and to 75  $\mu$ m for nano-LC. Tubings and connectors in LC system are also narrowed down to avoid too much dead volume, reduce analysis time and increase sensitivity for the analysis of biomass-restricted samples (**Table 1**) [37-39]. However, the tradeoff here is that smaller inner diameters generate higher back pressure and therefore require more complex instrumentation. Recently developed microPillar Array columns ( $\mu$ PAC) could offer a solution to this problem. Their highly ordered pillars containing an

outer porous shell grafted with C18 groups could limit backpressure while enhancing chromatographic performance [40].

**Table 1.** Analytical characteristics of standard and micro- to nanoscale analytical separation techniques [37-39]

	HPLC-MS	micro-LC-MS	nano-LC-MS	CE-MS
<b>flow rate</b>	0.5 – 1 mL/min	500 – 4000 nL/min	up to 500 nL/min	20 – 100 nL/min
<b>column i.d.</b>	1 – 4.6 mm	75 $\mu$ m – 1 mm	up to 75 $\mu$ m	-
<b>injection volume</b>	above 5 $\mu$ L	up to 2 $\mu$ L	up to 1 $\mu$ L	up to 20 nL
<b>sensitivity</b>	nM to $\mu$ M level	pM level	fM level	Low nM range
<b>application</b>	Less limited volume / high concentration	Limited volume / low concentration		

Downscaling of the LC method improves sensitivity and increases the coverage of analyzed compounds. A nanoscale ion-pair reversed-phase HPLC-MS method was developed to analyze highly polar metabolites in the low femtomolar down to hundreds of attomolar range in solvent as well as in cell extracts. Compared to previous HPLC-MS study, the sample amount required per injection was 1000 times lower with nano flow rate, indicating very low LODs could be reached with small matrix sample volume [41]. By adding the metal chelating agent ethylenediaminetetraacetic acid (EDTA) to the sample solution, Myint *et al.* managed to improve peak shapes of multiply charged anionic compounds with nano-LC/MS. The method was applied on cell extracts, mouse brain tissues, human plasma and CSF with detection limits of 0.19 to 2.81 pM [42]. Furthermore, the trap-and-elute strategy which was first developed for proteomics studies also became a classic strategy in metabolomics study, which further improves the sensitivity of miniaturized LC methods [43].

Apart from LC systems, CE-MS is also highly suited for biomass-restricted metabolomics because of its low sample injection volume. A sheath liquid interface is most commonly used for electrical contact in CE-MS. However, the addition of the sheath liquid flow dilutes the sample, decreasing sensitivity. In contrast, sheathless interfaces couple the CE to the MS without dilution for higher sensitivity. An example using a standard sheath liquid CE-MS method, Zhang *et al.* analyzed limited mouse plasma samples (10  $\mu$ L) and detected 44 polar components [44]. Through the application of field amplified sample injection (FASI), Liao *et al.* obtained enhanced detection sensitivity for cationic metabolites and identified

some important metabolites in single neurons from *A. californica* [45]. Examples using a sheathless CE-MS interface demonstrating better sensitivity are shown in the work of Zhang *et al.* which adopted transient-isotachopheresis (tITP) as the preconcentration technique when analyzing the sample derived from an extract of 500 HepG2 cells with a sheathless CE-MS method, and uncovered more than 24 cationic metabolites by injecting merely the content of 0.25 cell [46]. With the use of a thin-walled tapered emitter in CESI-MS, Kawai *et al.* obtained satisfying repeatability of migration time (1.5%) and peak areas (6.8%) after fifty consecutive analyses on 20 amino acids [47]. By further incorporating a dual preconcentration strategy, the authors acquired LOD improvement of up to 800 folds compared with normal sheathless CE-MS. The metabolic profiling of single HeLa cells by this approach led to the quantitation of 20 and detection of 40 metabolites (**Figure 5**). The versatility of CE-MS in interfaces [48, 49], injection modes [50, 51], and preconcentration strategies [52] renders CE-MS a promising tool for the analysis of biomass-restricted samples.

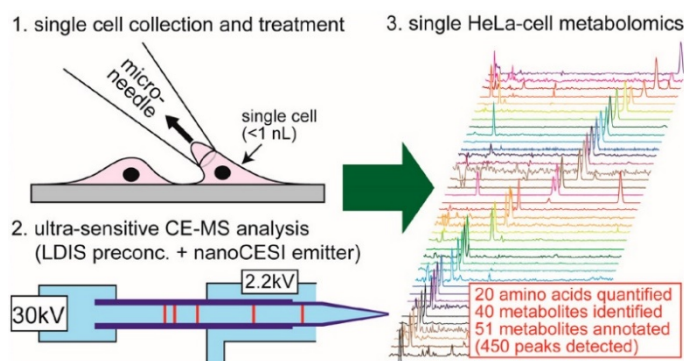


**Figure 5.** Brief procedure of single HeLa-cell metabolomics by capillary electrophoresis–mass spectrometry with a thin-walled tapered emitter and large-volume dual sample preconcentration [ref. 44].

Lower flow rates require better ionization environments from electrospray ion sources. Recent developments on ion sources include providing more stable structures for continuous spray, incorporating the column oven directly into the ion source to reduce band broadening, avoiding possible leakage and minimizing dead volume, and by optimizing the tip inner diameter of spray needles for smaller droplets to improve ionization and transfer

efficiency [53]. Improved spray emitters were designed and are commercially available for micro/nano-ESI-MS, such as the PicoTip™ emitter from New Objective and the stainless steel NanoTip emitter from Thermo Fisher. Instead of using single nozzle emitter, a chip-based multi-nozzle emitter (M3 emitter) was produced by NewOmics. By combining multiple emitters on one chip, this emitter splits the sample flow into multiple smaller streams to generate even and smaller droplets, which enhances the ionization efficiency. All these spray emitters are provided with various inner diameter for both micro and nano flow rate, they have proven to be robust and sensitive in several studies [54-56]. Furthermore, the angle between the spray needle and ionization interface was adjusted to gain more sensitivity (**Table 2**). Some of the commercially available ion sources performed well in both proteomics and metabolomics studies. Taki *et al.* performed a robust analysis on 17 highly polar metabolites using nano-flow injection analysis (nano-FIA) with a CaptiveSpray Ionization (CSI) source, which was initially designed for protein analyses, and presented results in good repeatability for small molecular compounds with 1000 nL/min flow rate [36].

**Table 2.** Current commercially available micro- or nanospray ion sources

Ion source name	Flow rate	Emitter i.d.	remarks
Thermo fisher Nanospray Flex	50-500 nL/min	1-30 $\mu\text{m}$	Provides stable electrospray
Agilent Nanospray	100-900 nL/min	-	Offers three choices of spray orientation
Waters NanoLockSpray Exact Mass	up to 1 $\mu\text{L/min}$	-	Enables valid exact mass measurement and improves mass accuracy
Sciex OptiFlow Turbo V	micro: 1-200 $\mu\text{L/min}$ nano: 100-1000 nL/min	20 $\mu\text{m}$ , 25 $\mu\text{m}$ , 50 $\mu\text{m}$	Switch between nanoflow and microflow in minutes
Waters ionKey/MS	1-50 $\mu\text{L/min}$	150 $\mu\text{m}$ /300 $\mu\text{m}$ iKey Separation Device	Integrates microflow directly into the source Provides an increased level of sensitivity, ease-of-use
Shimadzu Nexera Mikros	1-500 $\mu\text{L/min}$	20 $\mu\text{m}$	Connected with UF-link column oven to avoid dead volume.
Sciex Nanospray III	30-1000 nL/min	5-30 $\mu\text{m}$	Possessed an X-Y-Z positioning unit that can be used to position the emitter tip relative to the curtain plate.
Bruker CaptiveSpray	nano-flow	-	A vortex gas that sweeps around the emitter spray tip for better desolvation. The direct connection to the inlet capillary making the source truly Plug-and-Play.

Decades have been passed since the introduction of miniaturized techniques, various of improvements regarding to micro/nano flow LC and comparable columns, nanospray ionization sources and spray emitters have been achieved. Current MS-based separation techniques for biomass-restricted metabolomics are able to analyze trace level compounds, as well as nanoliter level liquid sample or even single cell matrix. Although these techniques have only been used in academic studies so far, by coupling with efficient sampling and sample preparation methods, they are promising to contribute to future pharmaceutical and clinical research.

## 4 Applications

With the advantages of high sensitivity and high throughput, analytical techniques for biomass-restricted samples have been applied in relevant metabolomics studies, such as food quality tests, biomedical and clinical studies. A selection of recent studies of recent micro/nano-LC-based metabolomics studies is given in **Table 3**, which provides information about the type of samples and compounds analyzed, volumes for sample preparation and injection, separation techniques and MS analyzers employed. **Table 4** shows some metabolomics studies using CE-MS during 2019 to April 2021, more applications from previous years can be found in reference [38, 57]. Representative application examples with both analytical techniques in metabolomics are discussed.

Lipids have been shown to be important in understanding many diseases including Alzheimer's disease, kidney diseases and cardiovascular diseases [58-60]. Several lipidomics studies were carried out with miniaturized methods for the identification and quantification of important lipids. The total ion chromatograms of yeast lipidomics profiles with good separation and response are shown in **Figure 6**. The coverage and sensitivity of lipids measured utilizing a nanoLC-MS method clearly increased over those obtained using standard flow rates with 447 lipids from the core phospholipid lipid classes (PA, PE, PC, PS, PG, and PI) identified. The stability of retention time and repeatability of some targeted compounds were evaluated with 25 replicate measurements from one extract. Results showed the average retention time standard deviation was  $5.2 \pm 2.3$  s, and RSDs of most compounds peak area were below 15% [33]. Another lipidomics study on rabbits with non-alcoholic fatty liver disease managed to quantify approximately 300 lipids within 20 min using nanoflow UPLC-MS/MS, revealing that non-alcoholic disease was highly associated

with high-cholesterol diet and high-cholesterol diet combined with inflammation [61]. Byeon *et al.* performed comprehensive lipid profiling in plasma and urine samples from Fabry disease patients with nanoflow LC-MS/MS and 129 plasma lipids and 111 urinary lipids were identified. The results showed currently used enzyme replacement therapy influenced lipids in plasma more than those in urine [62].

As a group of crucial hormones involves in inflammation, immune functions and gender development, steroid hormones are of low abundance in biological matrices. Márta *et al.* established a sensitive and robust microflow UHPLC-MS/MS method for the simultaneous determination of 13 different steroid molecules in human plasma, the LODs ranged from 0.008 to 0.178 ng/mL with a repeatability less than 8% RSD for all the compounds [63]. A metabolite profiling of fecal extracts using nanoflow UHPLC-nanospray ESI-MS method revealed the presence of trace levels of eicosanoid and sex steroid signaling compounds in the presence of other compounds with high abundance like major bile acid metabolites. Furthermore, researchers applied this method to feces from colorectal cancer patients, and the results indicated that signaling metabolites as well as other key metabolic pathways are potentially related to this disease [64]. Concentration restricted lipids could be detected and quantified in many studies with miniaturized analytical methods, which shows the advantage of down-scaling analysis for better sensitivity for diseases diagnose and treatments in the future.

Among volume-restricted samples, microfluidic cell culture such as organ-on-chip has become a research focus in recent years. High sensitivity of miniaturized analytical techniques laid the foundation for the analysis of small number cells and promoted the development of related studies. By using nano-LC-MS/MS, Luo *et al.* developed a method based on high-performance chemical isotope labeling for the analysis of 100, 1000 and 10000 cells, resulting in acquiring over two thousand peak pairs of metabolites in the amine/phenol submetabolome, and more than half of them could be identified [65]. For targeted metabolomics, Junaid *et al.* were able to detect several signaling lipids in conditioned cell medium sample from blood vessels-on-a-chip upon exposure of to TNF $\alpha$  with less than 1  $\mu$ L injection [66]. CE-MS has proven to be a key microscale method for biomass-restricted samples, and nanomole level of LOD could be reached with only a few nanoliters injection volume [46]. Zhang *et al.* developed a highly sensitive and efficient

sheathless CE-MS method for the profiling of nucleotides, which are difficult to analyze with conventional analytical techniques, including adenosine triphosphate, adenosine diphosphate and adenosine monophosphate in 50 000 down to 500 HepG2 cells, with the LODs in matrix ranging from 0.1 to 0.9 nM [67]. A sample limited tissue example is from Sánchez-López *et al.* who performed an interesting study by analyzing 20 µm-thick kidney sections from a mouse model of polycystic kidney disease using CE-MS. Injections were performed from a modified vial containing only 2 microliter sample. The profiling covered more than 100 metabolic features with acceptable repeatability and could distinguish the experimental groups, which highlighted the use of biomass-restricted samples for metabolomics studies [68].

Meanwhile, non-invasive sampling methods yielding only a few microliter samples are expected to become the preferred strategy for clinical studies and applications. Rainville *et al.* successfully employed an integrated capillary scale (300 µm i.d.) ceramic microfluidic LC-MS/MS method for the quantitative analysis of pharmaceutical compounds in low volume human plasma and dried blood spot samples. In addition, this method showed 11-38 folds increase in sensitivity for different drugs compared to conventional LC-MS/MS methods [69].

Details of several miniaturized metabolomics applications can be found in **Table 3** [3, 4, 7, 17, 33, 34, 36, 61-65, 69-74] and **Table 4** [44, 46, 67, 68, 75-84]. Low flow rates ranging from 200 nL/min to 50 µL/min were used to achieve high sensitivity and increase coverage of metabolome. For samples that are low in metabolite abundance but are not of limited volume, the trap-and-elute strategy was often used. In general, highly sensitive LC-MS with micro- or nano-flow and CE-MS methods were developed and applied for the analysis of biomass-restricted samples such as low number cells, dry blood spots, tissue sections and many other matrices.

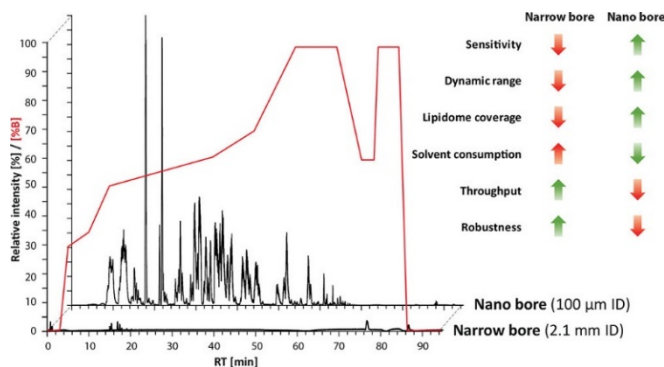


**Figure 6.** Total ion chromatograms from a yeast lipidomics study using two columns with 100 µm and 2.1 mm inner diameters (red line: LC gradients) [ref. 33].

## 5 Conclusions and perspectives

To deal with the desired sensitivity and coverage of analytical metabolomics technologies for biomass-restricted samples in biomedical and clinical studies, some developments have been realized in MS-based metabolomics workflows. Even more importantly, over the past 5 years, optimizations of separations and ionization techniques, and hardware including columns, LC pumps and ionization sources have been made in micro and nano flow methods, yielding higher sensitivity for biomass-restricted samples not only for metabolomics but also other fields. Delicate parts such as micro- or nano-volume connectors, unions and tubings in miniaturized LC-MS systems have been designed for lower dead volume and improved the system robustness. We are convinced that the advances in analytical technologies and metabolomics will allow to further increase sensitivity and robustness for ultrasample samples by further optimization of sampling and sample preparation procedures. Sampling methods for volume limited samples are required to avoid sample loss and preserve the biological heterogeneity in each sample as much as possible, and several strategies have been reported for this. After that, efficient sample preparation methods suitable for volume and especially concentration limited samples are also essential to gain higher sensitivity during analysis. While protein precipitation, liquid-liquid extraction and solid phase extraction are classic strategies for metabolomics sample preparation, current tools such as vials and sample transfer methods have to be further optimized for biomass-restricted samples. In summary, where development of sensitive



LC/CE-MS techniques has been advanced for over recent years, the development of sample handling for small samples has progressed less for small molecules. Therefore, future developments should put more emphasis on miniaturized sampling and sample preparation methods in order to further increase the sensitivity and strengthen the robustness of miniaturized analytical methods.

### **Acknowledgements**

Bingshu He would like to acknowledge the China Scholarship Council (CSC, No.201906390032). Dr. Rawi Ramautar would like to acknowledge the financial support of the Vidi grant scheme of the Netherlands Organization of Scientific Research (NWO Vidi 723.016.003).

**Table 3.** Overview of applications using miniaturized analytical techniques from January 2015 to April 2021 (micro/nano-LC-MS)

Compounds	Sample matrix	Sample prep volume	Injection volume	Separation technique	Column <sup>a</sup>	flowrate	LOD <sup>b</sup>	MS analyzer	Ref.
endocannabinoids	human CSF	600 µL CSF/ethanol mixture (200 µL/400 µL)	8 µL	Agilent 1100/1200 series nano-LC system	Agilent Polaris-HR-Clip 3C18 (75 µm × 15 cm, 3 µm)	2 µL/min	0.28-146.9 pM	Agilent 6400 triple quadrupole MS system	[3]
thyroid hormones 3,3',5-triiodothyronine (T3) prohormone thyroxine (T4)	egg yolk	50-150 mg	5 µL	Thermo Easy-nLC1000	trapping column C18 (100 µm × 2 cm, 5 µm) separation column C18 (75 µm × 15 cm, 5 µm)	300 nL/min	T3 5.9 aM T4 3.5 aM	Thermo TSQ Vantage MS	[4]
profiling	single HeLa cells	n.s.	0.1 µL	Thermo UltiMate 3000 RSLCnano system	nanodLC column (100 µm × 18 cm, 3 µm)	600 nL/min	0.02-38 fmol	Shimadzu LCMS-8060	[7]
irinotecan, leucine encephalin, PC (18:1/6:0), TG (16:0/18:1/16:0)	single cell extraction	-	n.s.	T-probe	-	200 nL/min	0.1-10 nM	Thermo LTQ Orbitrap XL MS	[17]
17 highly polar metabolites	rodent serum/plasma samples	45 µL	2 µL	ParadigmMS4 pump system	-	1000 nL/min	0.11-2.2 µg/mL	Sciex TripleTOF 5600 Captivespray ion source	[36]
lipids	yeast extraction	500 µL of yeast suspension (≈6.7x10 <sup>8</sup> cells)	1 µL	Thermo UltiMate 3000 system	Ascentis Express C18 (100 µm × 30 cm, 2.7 µm)	600 nL/min	n.s.	Thermo QExactive Plus MS	[33]
polyphenols and related compounds	red wine	n.s.	n.s.	Sciex Eksigent MicroLC 200 Plus UHPLC System	Kinetex C18 (100 µm × 5 cm, 2.6 µm)	50 µL/min	n.s.	SCIEX TripleTOF 5600	[34]
lipids	rabbit hepatic tissue	10 mg	n.s.	Waters nanoACQUITY UHPLC System	C18 (75 µm × 7 cm, 3 µm)	400 nL/min	n.s.	Thermo LTQ Velos ion trap MS	[61]
lipids	human plasma and urine	50 µL plasma 2 mL urine	4 µL	Agilent model 1200 capillary UPLC	C18 (75 µm × 6 cm, 3 µm)	300 nL/min	n.s.	Thermo LTQ Velos ion trap MS	[62]
steroid hormones	human plasma	90 µL	n.s.	Sciex Eksigent MicroLC 200 Plus UHPLC System	trap column ProntoSIL 120 C18H (0.5 × 10 mm, 5 µm) separation column HALO Fused-Core Phenyl Hexyl (0.5 × 50 mm, 2.7 µm)	40 µL/min	0.01-1 ng/mL	Sciex QTRAP 6500 with Turbo V Source	[63]
amine/phenol submetabolome	breast cancer cell extraction	100 cells 1000 cells 10000 cells	n.s.	micro LC: Thermo UltiMate 3000 UHPLC nano LC: Waters NanoAcquity UPLC	micro : Eclipse Plus C18 (2.1 mm × 10 cm, 1.8 µm) nano : Acclaim PepMap 100 trap column (75 µm × 2 cm, 3 µm) and Acclaim PepMap RSLC C18 (75 µm × 15 cm, 2 µm)	n.s.	n.s.	micro: Bruker Maxis II QTOF nano: Bruker Impact HD Q-TOF Captivespray ion source	[65]
small molecular drugs	dried blood spot and plasma	15 µL blood for dried blood spot 50 µL plasma	0.1-2 µL	Waters nanoACQUITY UPLC system	capillary scale LC on the ceramic BEH C18 (0.3 × 100 mm, 1.7 µm)	12 µL/min	n.s.	Waters Xevo TQS MS	[69]
profiling	human faeces	10 g	0.5 µL	Waters nanoAcquity UHPLC	Waters nanoAcquity HSS-T3 (100 µm × 10 cm, 1.8 µm)	700 nL/min	-	Waters Xevo G2 TOF MS	[64]

Compounds	Sample matrix	Sample prep volume	Injection volume	Separation technique	Column <sup>a</sup>	flowrate	LOD <sup>b</sup>	MS analyzer	Ref.
endocannabinoids	serum	50 $\mu$ L	10 $\mu$ L	Waters M-class UPLC	iKey with a post-column addition (PCA) channel (Peptide BEH C18 150 $\mu$ m $\times$ 5 cm, 1.7 $\mu$ m)	2 $\mu$ L/min	0.36–4.02 pg/mL	Waters Xevo TQ-S tandem MS	[70]
profiling	cell extraction	n.s.	2 $\mu$ L	Eksigent nanoLC system	Self-packed columns (15 cm in length): 5 $\mu$ m Magic C18-AQ beads (New Objective), PicoFrit column (360 $\mu$ m OD $\times$ 100 $\mu$ m ID, 15 $\mu$ m Tip ID)	positive 400 nL/min negative 500 nL/min	-	Thermo LTQ-Orbitrap hybrid MS	[71]
modified nucleosides in RNA	mammalian cells and tissues	n.s.	n.s.	Thermo EASY-nLC II	precolumn (150 $\mu$ m $\times$ 70 mm, 5 $\mu$ m) separation column Zorbax SB-C18 column (75 $\mu$ m $\times$ 250 mm, 5 $\mu$ m)	300 nL/min	around 10 amol	Thermo LTQ XL linear ion trap MS with nanoelectrospray ion source	[72]
lipids	mouse serum, heart, and kidney tissues	100 $\mu$ L serum 8mg kidney/heart	untargeted analysis: 3 $\mu$ g lipid extract targeted analysis: 2 $\mu$ g lipid extract	untargeted analysis: Thermo Dionex Ultimate 3000 RSLChano System targeted analysis: Waters nanoACQUITY UPLC system	home-made fused silica tubing column (100 $\mu$ m ID, 7 cm length), the end portion (~5 mm) was filled with 3 $\mu$ m of 100 Å Waters® ODS-P-C18 particles, the rest (6.5 cm) was packed with 1.7- $\mu$ m XBridge® BEH.	1 $\mu$ L/min for loading, 300 nL/min for analytical column	0.011 pmol to 0.099 pmol in serum; 0.006 pmol to 0.141 pmol in kidney; 0.010 pmol to 0.119 pmol in heart	untargeted analysis: Thermo LTQ Velos ion trap MS targeted analysis: Thermo TSQ Vantage triple-stage quadrupole MS	[73]
Betalains	rat plasma	250 $\mu$ L	n.s.	Eksigent LC200	Eksigent HALO C18 column (0.5 mm $\times$ 10 cm, 2.7 $\mu$ m)	25 $\mu$ L/min	2.00 to 5.74 nM	Sciex QTRAP 5500	[74]

a) The column sizes are all expressed as I.D.  $\times$  Length, Particle size

b) LOD = limit of detection (S/N = 3); n.s. : not specified in paper.

**Table 4.** Overview of applications of miniaturized analytical techniques from January 2019 to April 2021 (CE-MS)

Compounds	Sample matrix	sample prep volume	BGE	sample pretreatment	MS analyser	LOD*	Ref.
Anionic and cationic metabolites	human urine and plasma	20 µL	1 M formic acid with 15 % acetonitrile (pH 1.8); 50 mM ammonium bicarbonate (pH 8.5)	centrifugation and dilution for urine; Ultrafiltration using 3-kDa filter for plasma	Agilent 6230 TOF-MS	n.s.	[75]
Cationic metabolites	mammalian cells	5000, 2500, 1000, and 500 cells	16 mM ammonium acetate (pH 9.7)	Ultrafiltration using 3-kDa filter	Sciex TripleTOF 6600 MS	0.1 to 0.9 nM	[67]
Cationic metabolites	mouse kidney sections	20 µm-thick kidney sections	10% (v/v) acetic acid (pH 2.3)	extraction in 80:20 MeCN: water (v/v)	Bruker UHR-QqTOF maXis Impact HD MS	n.s.	[68]
Anionic metabolites	cell medium	200 µL	0.8 M formic acid in 10% methanol	centrifugation	Agilent 6224 TOF-MS	n.s.	[76]
Anionic and cationic metabolites	Neonatal dried blood spot and sweats	about 15 µL blood	1 M formic acid, 15% v/v acetonitrile (pH 1.8); 50 mM ammonium bicarbonate (pH 8.5)	ultrafiltration using 3-kDa filter	Agilent 6550/6230 TOF-MS	n.s.	[77]
Cationic metabolites	HepG2 cells	500 and 10,000 cells	10% acetic acid	Ultrafiltration using 5-kDa filter	Sciex TripleTOF 5600+ MS	ranging from 1.4 to 92 nM (except for aspartic acid, 417nM)	[46, 78]
Anionic and cationic metabolites	human serum	50 µL	n.s.	protein precipitation and ultrafiltration using 5-kDa filter	TOF-MS	n.s.	[79]
Cationic metabolites	Macrophages	5 × 10 <sup>6</sup> cells	1 M formic acid in 10% methanol (v/v)	quenching, disruption and centrifugation	Agilent 6224 TOF-MS	n.s.	[80]
Cationic metabolites	human urine	10 µL	500 mM formic acid (PH 1.55)	dilution	Agilent 6410 Triple Quadrupole tandem MS	0.23-5.45 µM	[81]

Compounds	Sample matrix	sample prep volume	BGE	sample pretreatment	MS analyser	LOD <sup>a</sup>	Ref.
Anionic and cationic metabolites	Freeze-dried muscle tissue	2 mg	1 M formic acid with 15 vol % acetonitrile (pH 1.8) 50 mM ammonium bicarbonate (pH 8.5)	modified Bligh-Dyer extraction	Agilent 6230 TOF-MS	n.s.	[82]
Anionic and cationic metabolites	human brain tissues	50 mg	50 mM ammonium acetate (pH 9.0)	Ultrafiltration using 5-kDa filter	Agilent 6210 TOF-MS	n.s.	[83]
Cationic metabolites	extracellular fluid of HK-2 cells	100 µL	1 M formic acid (pH 1.8)	Protein precipitation	Agilent 6530 TOF-MS	n.s.	[84]
Cationic metabolites	seizure mouse plasma	10 µL	water with 10% acetic acid (V/V)	Bligh and Dyer extraction and ultrafiltration using 5-kDa filter	Agilent 6230 TOF-MS	n.s.	[44]

a) LOD = limit of detection ( $S/N = 3$ ); n.s.: not specified in paper.

## References

- [1] N.L. Kuehnbaum, P. Britz-McKibbin, New Advances in Separation Science for Metabolomics: Resolving Chemical Diversity in a Post-Genomic Era, *Chemical Reviews*, 113 (2013) 2437-2468.
- [2] H. Gika, C. Virgiliou, G. Theodoridis, R.S. Plumb, I.D. Wilson, Untargeted LC/MS-based metabolic phenotyping (metabonomics/metabolomics): The state of the art, *Journal of Chromatography B*, 1117 (2019) 136-147.
- [3] V. Kantae, S. Ogino, M. Noga, A.C. Harms, R.M. van Dongen, G.L.J. Onderwater, A.M.J.M. van den Maagdenberg, G.M. Terwindt, M. van der Stelt, M.D. Ferrari, T. Hankemeier, Quantitative profiling of endocannabinoids and related N-acylethanolamines in human CSF using nano LC-MS/MS, *Journal of Lipid Research*, 58 (2017) 615-624.
- [4] S. Ruuskanen, B.-Y. Hsu, A. Heinonen, M. Vainio, V.M. Darras, T. Sarraude, A. Rokka, A new method for measuring thyroid hormones using nano-LC-MS/MS, *Journal of Chromatography B*, 1093-1094 (2018) 24-30.
- [5] A. Chetwynd, A. David, A review of nanoscale LC-ESI for metabolomics and its potential to enhance the metabolome coverage, *Talanta*, 182 (2018).
- [6] M. Cebo, X. Fu, M. Gawaz, M. Chatterjee, M. Lämmerhofer, Micro-UHPLC-MS/MS method for analysis of oxylipins in plasma and platelets, *Journal of Pharmaceutical and Biomedical Analysis*, 189 (2020) 113426.
- [7] K. Nakatani, Y. Izumi, K. Hata, T. Bamba, An analytical system for single-cell metabolomics of typical mammalian cells based on highly sensitive nano-liquid chromatography tandem mass spectrometry, *Mass Spectrometry*, advpub (2020).
- [8] A.G. Zestos, R.T. Kennedy, Microdialysis Coupled with LC-MS/MS for In Vivo Neurochemical Monitoring, *The AAPS Journal*, 19 (2017) 1284-1293.
- [9] A.G. Zestos, H. Luna-Munguia, W.C. Stacey, R.T. Kennedy, Use and Future Prospects of in Vivo Microdialysis for Epilepsy Studies, *ACS Chem Neurosci*, 10 (2019) 1875-1883.
- [10] T. Ngensutivorakul, T.S. White, R.T. Kennedy, Microfabricated Probes for Studying Brain Chemistry: A Review, *ChemPhysChem*, 19 (2018) 1128-1142.
- [11] D.E. Cepeda, L. Hains, D. Li, J. Bull, S.I. Lentz, R.T. Kennedy, Experimental evaluation and computational modeling of tissue damage from low-flow push-pull perfusion sampling in vivo, *Journal of Neuroscience Methods*, 242 (2015) 97-105.
- [12] M.M. Weisenberger, M.T. Bowser, In Vivo Monitoring of Amino Acid Biomarkers from Inguinal Adipose Tissue Using Online Microdialysis-Capillary Electrophoresis, *Analytical Chemistry*, 89 (2017) 1009-1014.
- [13] J. Van Schoors, J. Viaene, Y. Van Wansele, I. Smolders, B. Dejaegher, Y. Vander Heyden, A. Van Eeckhaut, An improved microbore UHPLC method with electrochemical detection for the simultaneous determination of low monoamine levels in in vivo brain microdialysis samples, *Journal of Pharmaceutical and Biomedical Analysis*, 127 (2016) 136-146.
- [14] C.-M. Huang, Y. Zhu, D.-Q. Jin, R.T. Kelly, Q. Fang, Direct Surface and Droplet Microsampling for Electrospray Ionization Mass Spectrometry Analysis with an Integrated Dual-Probe Microfluidic Chip, *Analytical Chemistry*, 89 (2017) 9009-9016.
- [15] T.M.J. Evers, M. Hochane, S.J. Tans, R.M.A. Heeren, S. Semrau, P. Nemes, A. Mashaghi, Deciphering Metabolic Heterogeneity by Single-Cell Analysis, *Analytical Chemistry*, 91 (2019) 13314-13323.
- [16] A. Ali, Y. Abouleila, Y. Shimizu, E. Hiyama, S. Emara, A. Mashaghi, T. Hankemeier, Single-cell metabolomics by mass spectrometry: Advances, challenges, and future applications, *TrAC Trends in Analytical Chemistry*, 120 (2019) 115436.
- [17] R. Liu, N. Pan, Y. Zhu, Z. Yang, T-Probe: An Integrated Microscale Device for Online In Situ Single Cell Analysis and Metabolic Profiling Using Mass Spectrometry, *Analytical Chemistry*, 90 (2018) 11078-11085.
- [18] R.M. Onjiko, E.P. Portero, S.A. Moody, P. Nemes, In Situ Microprobe Single-Cell Capillary Electrophoresis Mass Spectrometry: Metabolic Reorganization in Single Differentiating Cells in the Live Vertebrate (*Xenopus laevis*) Embryo, *Analytical Chemistry*, 89 (2017) 7069-7076.
- [19] O. Guillaume-Gentil, T. Rey, P. Kiefer, A.J. Ibáñez, R. Steinhoff, R. Brönnimann, L. Dörwling-Carter, T. Zambelli, R. Zenobi, J.A. Vorholt, Single-Cell Mass Spectrometry of Metabolites Extracted from Live Cells by Fluidic Force Microscopy, *Analytical Chemistry*, 89 (2017) 5017-5023.
- [20] R. Meesters, Biofluid collection in metabolomics by the application of the novel volumetric absorptive microsampling technology: A mini-review, *Reviews in Separation Sciences*, 1 (2019) 34-46.
- [21] R. Neto, A. Gooley, M.C. Breadmore, E.F. Hilder, F. Lapierre, Precise, accurate and user-independent blood collection system for dried blood spot sample preparation, *Analytical and Bioanalytical Chemistry*, 410 (2018) 3315-3323.
- [22] M. Protti, R. Mandrioli, L. Mercolini, Tutorial: Volumetric absorptive microsampling (VAMS), *Analytica Chimica Acta*, 1046 (2019) 32-47.

- [23] R.C. Van Wijk, E.H.J. Krekels, V. Kantae, A. Ordas, T. Kreling, A.C. Harms, T. Hankemeier, H.P. Spaink, P.H. van der Graaf, Mechanistic and Quantitative Understanding of Pharmacokinetics in Zebrafish Larvae through Nanoscale Blood Sampling and Metabolite Modeling of Paracetamol, *Journal of Pharmacology and Experimental Therapeutics*, 371 (2019) 15-24.
- [24] L.H.J. Richter, J. Herrmann, A. Andreas, Y.M. Park, L. Wagmann, V. Flockerzi, R. Müller, M.R. Meyer, Tools for studying the metabolism of new psychoactive substances for toxicological screening purposes – A comparative study using pooled human liver S9, HepaRG cells, and zebrafish larvae, *Toxicology Letters*, 305 (2019) 73-80.
- [25] Y. Liu, J. Zhang, C. Hu, Validated LC-MS/MS method for simultaneous analysis of 21 cephalosporins in zebrafish for a drug toxicity study, *Analytical Biochemistry*, 558 (2018) 28-34.
- [26] R.-J. Raterink, P.W. Lindenburg, R.J. Vreeken, R. Ramautar, T. Hankemeier, Recent developments in sample-pretreatment techniques for mass spectrometry-based metabolomics, *TrAC Trends in Analytical Chemistry*, 61 (2014) 157-167.
- [27] J. Soares da Silva Burato, D.A. Vargas Medina, A.L. de Toffoli, E. Vasconcelos Soares Maciel, F. Mauro Lanças, Recent advances and trends in miniaturized sample preparation techniques, *Journal of Separation Science*, 43 (2020) 202-225.
- [28] F.S. Mirnaghi, Y. Chen, L.M. Sidisky, J. Pawliszyn, Optimization of the Coating Procedure for a High-Throughput 96-Blade Solid Phase Microextraction System Coupled with LC-MS/MS for Analysis of Complex Samples, *Analytical Chemistry*, 83 (2011) 6018-6025.
- [29] N. Riboni, F. Fornari, F. Bianchi, M. Careri, Recent Advances in In Vivo SPME Sampling, 7 (2020) 6.
- [30] T. Vasiljevic, V. Singh, J. Pawliszyn, Miniaturized SPME tips directly coupled to mass spectrometry for targeted determination and untargeted profiling of small samples, *Talanta*, 199 (2019) 689-697.
- [31] S. Lendor, S.-A. Hassani, E. Boyaci, V. Singh, T. Womelsdorf, J. Pawliszyn, Solid Phase Microextraction-Based Miniaturized Probe and Protocol for Extraction of Neurotransmitters from Brains in Vivo, *Analytical Chemistry*, 91 (2019) 4896-4905.
- [32] A. Roszkowska, M. Tascon, B. Bojko, K. Goryński, P.R. dos Santos, M. Cypel, J. Pawliszyn, Equilibrium ex vivo calibration of homogenized tissue for in vivo SPME quantitation of doxorubicin in lung tissue, *Talanta*, 183 (2018) 304-310.
- [33] N. Danne-Rasche, C. Coman, R. Ahrends, Nano-LC/NSI MS Refines Lipidomics by Enhancing Lipid Coverage, Measurement Sensitivity, and Linear Dynamic Range, *Analytical chemistry*, 90 (2018) 8093-8101.
- [34] Y. Ma, N. Tanaka, A. Vaniya, T. Kind, O. Fiehn, Ultrafast Polyphenol Metabolomics of Red Wines Using MicroLC-MS/MS, *Journal of Agricultural and Food Chemistry*, 64 (2016) 505-512.
- [35] A. Schmidt, M. Karas, T. Dülcks, Effect of different solution flow rates on analyte ion signals in nano-ESI MS, or: when does ESI turn into nano-ESI?, *Journal of the American Society for Mass Spectrometry*, 14 (2003) 492-500.
- [36] K. Taki, S. Noda, Y. Hayashi, H. Tsuchihashi, A. Ishii, K. Zaitzu, A preliminary study of rapid-fire high-throughput metabolite analysis using nano-flow injection/Q-TOFMS, *Analytical and Bioanalytical Chemistry*, (2020).
- [37] W. Zhang, T. Hankemeier, R. Ramautar, Next-generation capillary electrophoresis-mass spectrometry approaches in metabolomics, *Current Opinion in Biotechnology*, 43 (2017) 1-7.
- [38] R. Ramautar, G.W. Somsen, G.J. de Jong, CE-MS for metabolomics: Developments and applications in the period 2014-2016, *Electrophoresis*, 38 (2017) 190-202.
- [39] M. Hilhorst, C. Briscoe, N.v.d. Merbel, Sense and nonsense of miniaturized LC-MS/MS for bioanalysis, *Bioanalysis*, 6 (2014) 3263-3265.
- [40] G. Nys, G. Cobraiville, M. Fillet, Multidimensional performance assessment of micro pillar array column chromatography combined to ion mobility-mass spectrometry for proteome research, *Analytica Chimica Acta*, 1086 (2019) 1-13.
- [41] P. Kiefer, N.L. Delmotte, J.A. Vorholt, Nanoscale Ion-Pair Reversed-Phase HPLC-MS for Sensitive Metabolome Analysis, *Analytical Chemistry*, 83 (2011) 850-855.
- [42] K.T. Myint, T. Uehara, K. Aoshima, Y. Oda, Polar Anionic Metabolome Analysis by Nano-LC/MS with a Metal Chelating Agent, *Analytical Chemistry*, 81 (2009) 7766-7772.
- [43] Z. Wang, L. Bian, C. Mo, M. Kukula, K.A. Schug, M. Brotto, Targeted quantification of lipid mediators in skeletal muscles using restricted access media-based trap-and-elute liquid chromatography-mass spectrometry, *Analytica Chimica Acta*, 984 (2017) 151-161.
- [44] K. Segers, W. Zhang, N. Aourz, J. Bongaerts, S. Declerck, D. Mangelings, T. Hankemeier, D. De Bundel, Y. Vander Heyden, I. Smolders, R. Ramautar, A. Van Eeckhaut, CE-MS metabolic profiling of volume-restricted plasma samples from an acute mouse model for epileptic seizures to discover potentially involved metabolomic features, *Talanta*, 217 (2020) 121107.

- [45] H.-W. Liao, S.S. Rubakhin, M.C. Philip, J.V. Sweedler, Enhanced single-cell metabolomics by capillary electrophoresis electrospray ionization-mass spectrometry with field amplified sample injection, *Analytica Chimica Acta*, 1118 (2020) 36-43.
- [46] W. Zhang, F. Guled, T. Hankemeier, R. Ramautar, Utility of sheathless capillary electrophoresis-mass spectrometry for metabolic profiling of limited sample amounts, *Journal of Chromatography B*, 1105 (2019) 10-14.
- [47] T. Kawai, N. Ota, K. Okada, A. Imasato, Y. Owa, M. Morita, M. Tada, Y. Tanaka, Ultrasensitive Single Cell Metabolomics by Capillary Electrophoresis–Mass Spectrometry with a Thin-Walled Tapered Emitter and Large-Volume Dual Sample Preconcentration, *Analytical Chemistry*, 91 (2019) 10564-10572.
- [48] P. Fang, J.-Z. Pan, Q. Fang, A robust and extendable sheath flow interface with minimal dead volume for coupling CE with ESI-MS, *Talanta*, 180 (2018) 376-382.
- [49] H. Zhang, C. Lou, J. Li, J. Kang, A gold foil covered fused silica capillary tip as a sheathless interface for coupling capillary electrophoresis-mass spectrometry, *Journal of Chromatography A*, 1624 (2020) 461215.
- [50] E. Bermudo, O. Núñez, E. Moyano, L. Puignou, M.T. Galceran, Field amplified sample injection–capillary electrophoresis–tandem mass spectrometry for the analysis of acrylamide in foodstuffs, *Journal of Chromatography A*, 1159 (2007) 225-232.
- [51] M.C. Breadmore, Electrokinetic and hydrodynamic injection: making the right choice for capillary electrophoresis, *Bioanalysis*, 1 (2009) 889-894.
- [52] T. Kawai, Recent Studies on Online Sample Preconcentration Methods in Capillary Electrophoresis Coupled with Mass Spectrometry, *CHROMATOGRAPHY*, 38 (2017) 1-8.
- [53] M. Wilm, M. Mann, Analytical Properties of the Nanoelectrospray Ion Source, *Analytical Chemistry*, 68 (1996) 1-8.
- [54] K.E.V. Burgess, A. Lainson, L. Imrie, D. Fraser-Pitt, R. Yaga, D.G.E. Smith, R. Swart, A.R. Pitt, N.F. Inglis, Performance of five different electrospray ionisation sources in conjunction with rapid monolithic column liquid chromatography and fast MS/MS scanning, *PROTEOMICS*, 9 (2009) 1720-1726.
- [55] Y. Chen, P. Mao, D. Wang, Quantitation of Intact Proteins in Human Plasma Using Top-Down Parallel Reaction Monitoring-MS, *Analytical chemistry*, 90 (2018) 10650-10653.
- [56] P. Mao, R. Gomez-Sjoberg, D. Wang, Multinozzle Emitter Array Chips for Small-Volume Proteomics, *Analytical Chemistry*, 85 (2013) 816-819.
- [57] R. Ramautar, G.W. Somsen, G.J. de Jong, CE-MS for metabolomics: Developments and applications in the period 2016-2018, *Electrophoresis*, 40 (2019) 165-179.
- [58] M.W. Wong, N. Braidy, A. Poljak, R. Pickford, M. Thambisetty, P.S. Sachdev, Dysregulation of lipids in Alzheimer's disease and their role as potential biomarkers, *Alzheimer's & Dementia*, 13 (2017) 810-827.
- [59] B.A. Ference, I. Graham, L. Tokgozoglul, A.L. Catapano, Impact of Lipids on Cardiovascular Health: JACC Health Promotion Series, *Journal of the American College of Cardiology*, 72 (2018) 1141-1156.
- [60] F. Afshinnia, T.M. Rajendiran, S. Wernisch, T. Soni, A. Jadoon, A. Karnovsky, G. Michailidis, S. Pennathur, Lipidomics and Biomarker Discovery in Kidney Disease, *Seminars in Nephrology*, 38 (2018) 127-141.
- [61] S.K. Byeon, J.C. Lee, B.C. Chung, H.S. Seo, M.H. Moon, High-throughput and rapid quantification of lipids by nanoflow UPLC-ESI-MS/MS: application to the hepatic lipids of rabbits with nonalcoholic fatty liver disease, *Analytical and Bioanalytical Chemistry*, 408 (2016) 4975-4985.
- [62] S.K. Byeon, J.Y. Kim, J.-S. Lee, M.H. Moon, Variations in plasma and urinary lipids in response to enzyme replacement therapy for Fabry disease patients by nanoflow UPLC-ESI-MS/MS, *Analytical and Bioanalytical Chemistry*, 408 (2016) 2265-2274.
- [63] Z. Márta, B. Bobály, J. Fekete, B. Magda, T. Imre, K.V. Mészáros, M. Bálint, P.T. Szabó, Simultaneous determination of thirteen different steroid hormones using micro UHPLC-MS/MS with on-line SPE system, *Journal of Pharmaceutical and Biomedical Analysis*, 150 (2018) 258-267.
- [64] A.J. Chetwynd, L.A. Ogilvie, J. Nzakizwanayo, F. Pazdirek, J. Hoch, C. Dedi, D. Gilbert, A. Abdul-Sada, B.V. Jones, E.M. Hill, The potential of nanoflow liquid chromatography-nano electrospray ionisation-mass spectrometry for global profiling the faecal metabolome, *Journal of Chromatography A*, 1600 (2019) 127-136.
- [65] X. Luo, L. Li, Metabolomics of Small Numbers of Cells: Metabolomic Profiling of 100, 1000, and 10000 Human Breast Cancer Cells, *Analytical Chemistry*, 89 (2017) 11664-11671.
- [66] A. Junaid, J. Schoeman, W. Yang, W. Stam, A. Mashaghi, A.J. van Zonneveld, T. Hankemeier, Metabolic response of blood vessels to TNF $\alpha$ , *eLife*, 9 (2020) e54754.
- [67] W. Zhang, F. Guled, T. Hankemeier, R. Ramautar, Profiling nucleotides in low numbers of mammalian cells by sheathless CE–MS in positive ion mode: Circumventing corona discharge, *ELECTROPHORESIS*, 41 (2020) 360-369.
- [68] E. Sánchez-López, G.S.M. Kammeijer, A.L. Crego, M.L. Marina, R. Ramautar, D.J.M. Peters, O.A. Mayboroda, Sheathless CE-MS based metabolic profiling of kidney tissue section samples from a mouse model of Polycystic Kidney Disease, *Scientific reports*, 9 (2019) 806-806.



- [69] P.D. Rainville, J.P. Murphy, M. Tomany, I.D. Wilson, N.W. Smith, C. Evans, J. Kheler, C. Bowen, R.S. Plumb, J.K. Nicholson, An integrated ceramic, micro-fluidic device for the LC/MS/MS analysis of pharmaceuticals in plasma, *Analyst*, 140 (2015) 5546-5556.
- [70] J.S. Kirkwood, C.D. Broeckling, S. Donahue, J.E. Prenni, A novel microflow LC-MS method for the quantitation of endocannabinoids in serum, *Journal of Chromatography B*, 1033-1034 (2016) 271-277.
- [71] J. Deng, G. Zhang, T.A. Neubert, *Metabolomic Analysis of Glioma Cells Using Nanoflow Liquid Chromatography-Tandem Mass Spectrometry*, Springer New York, 2018, pp. 125-134.
- [72] L. Fu, N.J. Amato, P. Wang, S.J. McGowan, L.J. Niedernhofer, Y. Wang, Simultaneous Quantification of Methylated Cytidine and Adenosine in Cellular and Tissue RNA by Nano-Flow Liquid Chromatography-Tandem Mass Spectrometry Coupled with the Stable Isotope-Dilution Method, *Analytical Chemistry*, 87 (2015) 7653-7659.
- [73] J.Y. Eum, J.C. Lee, S.S. Yi, I.Y. Kim, J.K. Seong, M.H. Moon, Aging-related lipidomic changes in mouse serum, kidney, and heart by nanoflow ultrahigh-performance liquid chromatography-tandem mass spectrometry, *Journal of Chromatography A*, 1618 (2020) 460849.
- [74] T. Sawicki, J. Juśkiewicz, W. Wiczowski, Using the SPE and Micro-HPLC-MS/MS Method for the Analysis of Betalains in Rat Plasma after Red Beet Administration, *Molecules*, 22 (2017) 2137.
- [75] J. Wild, M. Shanmuganathan, M. Hayashi, M. Potter, P. Britz-McKibbin, Metabolomics for improved treatment monitoring of phenylketonuria: urinary biomarkers for non-invasive assessment of dietary adherence and nutritional deficiencies, *Analyst*, 144 (2019) 6595-6608.
- [76] A. Villaseñor, D. Aedo-Martín, D. Obeso, I. Erjavec, J. Rodríguez-Coira, I. Buendía, J.A. Ardura, C. Barbas, A.R. Gortazar, Metabolomics reveals citric acid secretion in mechanically-stimulated osteocytes is inhibited by high glucose, *Scientific reports*, 9 (2019) 2295-2295.
- [77] M. Shanmuganathan, P. Britz-McKibbin, New Advances for Newborn Screening of Inborn Errors of Metabolism by Capillary Electrophoresis-Mass Spectrometry (CE-MS), in: T.M. Phillips (Ed.) *Clinical Applications of Capillary Electrophoresis: Methods and Protocols*, Springer New York, New York, NY, 2019, pp. 139-163.
- [78] W. Zhang, T. Hankemeier, R. Ramautar, Capillary Electrophoresis-Mass Spectrometry for Metabolic Profiling of Biomass-Limited Samples, in: T.M. Phillips (Ed.) *Clinical Applications of Capillary Electrophoresis: Methods and Protocols*, Springer New York, New York, NY, 2019, pp. 165-172.
- [79] K. Omori, N. Katakami, Y. Yamamoto, H. Ninomiya, M. Takahara, T.-A. Matsuoka, T. Bamba, E. Fukusaki, I. Shimomura, Identification of Metabolites Associated with Onset of CAD in Diabetic Patients Using CE-MS Analysis: A Pilot Study, *J Atheroscler Thromb*, 26 (2019) 233-245.
- [80] S.M. Muxel, M. Mamani-Huanca, J.I. Aoki, R.A. Zampieri, L.M. Floeter-Winter, Á. López-González, C. Barbas, Metabolomic Profile of BALB/c Macrophages Infected with *Leishmania amazonensis*: Deciphering L-Arginine Metabolism, *Int J Mol Sci*, 20 (2019) 6248.
- [81] J. Piestansky, D. Olesova, J. Galba, K. Marakova, V. Parrak, P. Secnik, P. Secnik, Jr., B. Kovacech, A. Kovac, Z. Zelinkova, P. Mikus, Profiling of Amino Acids in Urine Samples of Patients Suffering from Inflammatory Bowel Disease by Capillary Electrophoresis-Mass Spectrometry, *Molecules*, 24 (2019) 3345.
- [82] M. Saoi, M. Percival, C. Nemr, A. Li, M. Gibala, P. Britz-McKibbin, Characterization of the Human Skeletal Muscle Metabolome for Elucidating the Mechanisms of Bicarbonate Ingestion on Strenuous Interval Exercise, *Analytical Chemistry*, 91 (2019) 4709-4718.
- [83] U.V. Mahajan, V.R. Varma, M.E. Griswold, C.T. Blackshear, Y. An, A.M. Oommen, S. Varma, J.C. Troncoso, O. Pletnikova, R. O'Brien, T.J. Hohman, C. Legido-Quigley, M. Thambisetty, Dysregulation of multiple metabolic networks related to brain transmethylation and polyamine pathways in Alzheimer disease: A targeted metabolomic and transcriptomic study, *PLoS Med*, 17 (2020) e1003012-e1003012.
- [84] S. Bernardo-Bermejo, E. Sánchez-López, M. Castro-Puyana, S. Benito-Martínez, F.J. Lucio-Cazaña, M.L. Marina, A Non-Targeted Capillary Electrophoresis-Mass Spectrometry Strategy to Study Metabolic Differences in an In vitro Model of High-Glucose Induced Changes in Human Proximal Tubular HK-2 Cells, *Molecules*, 25 (2020) 5.

# Chapter III

---

## **Quantification of endocannabinoids in human cerebrospinal fluid using a novel micro-flow liquid chromatography-mass spectrometry method**

### **Based on:**

Bingshu He\*, Xinyu Di\*, Faisa Guled, Aster V.E. Harder, Arn M.J.M. van den Maagdenberg, Gisela M. Terwindt, Elke H.J. Krekels, Isabelle Kohler, Amy Harms, Rawi Ramautar, Thomas Hankemeier,

**Quantification of endocannabinoids in human cerebrospinal fluid using a novel micro-flow liquid chromatography-mass spectrometry method**

Analytica Chimica Acta 2022; DOI: 10.1016/j.aca.2022.339888

\*Authors contributed equally

## **Abstract**

The endocannabinoid system (ECS) is implicated in various brain disorders. Changes in the composition of the cerebrospinal fluid (CSF) may be associated with ECS-related pathologies. Endocannabinoids (eCBs) and their analogues are present at low concentrations in human CSF, which hampered the investigation of the ECS in this body fluid. In this study, we developed a highly sensitive and selective micro-flow liquid chromatography-tandem mass spectrometry (micro-LC-MS/MS) method for the analysis of eCBs and eCB analogues in human CSF. The developed method allowed for the quantitative analysis of 16 eCBs and their analogues in human CSF. Micro-LC-MS/MS analyses were performed at a flow-rate of  $4\ \mu\text{L min}^{-1}$  with a 0.3-mm inner diameter column. A minor modification of a novel spray needle was carried out to improve the robustness of our method. By using an injection volume of  $3\ \mu\text{L}$ , our method reached limits of detection in the range from 0.6 to 1293.4 pM and limits of quantification in range from 2.0 to 4311.3 pM while intra- and interday precisions were below 13.7%. The developed workflow was successfully used for the determination of eCBs in 288 human CSF samples. It is anticipated that the proposed approach will contribute to a deeper understanding of the role of ECS in various brain disorders.

## 1. Introduction

The endocannabinoid system (ECS) is a widely distributed signaling system in the brain, involving cannabinoid receptors 1 and 2 (CB1 and CB2) and their best known endogenous agonists N-arachidonoyl ethanolamine (anandamide, AEA) and 2-arachidonoyl glycerol (2-AG), which are defined as endocannabinoids (eCBs) [1]. Besides AEA and 2-AG, other structural analogues, i.e., other N-acyl ethanolamines (NAEs) and other 2-acylglycerols play important roles in ECS signaling, by enhancing the effects of AEA and 2-AG via increasing receptor affinity or inhibiting hydrolysis, known as the ‘entourage effect’ [2, 3].

Alterations in the ECS have been reported in experimental models of various brain disorders, including Alzheimer’s disease, Parkinson’s disease, and migraine [4-7]. To certain extent, the reported findings were supported by those obtained in clinical studies [8-10]. However, most of the clinical studies used plasma or postmortem tissue samples, which limits the validity of ECS findings. Due to its close connection with brain tissue, cerebrospinal fluid (CSF) represents a more suitable biospecimen. Indeed, CSF reflects the level of metabolites in brain and is thus believed to better capture the brain’s neurochemistry compared to blood. However, eCBs and their analogues in human CSF, especially AEA, are present at concentrations lower than picomolar or even femtomolar range [11-17], highlighting the need for adequate methods to reliably detect and quantify these compounds [18-20]. In studies reporting endogenous concentrations of eCBs and eCB analogues in human CSF [14-17, 20, 21], relatively large volumes of CSF ( $\geq 1$  mL) were needed to reach the required sensitivity.

Using low-flow rate ranges between 1 and 50  $\mu\text{L min}^{-1}$ , micro-flow LC leads to the formation of smaller and more uniform spray droplets during the electrospray ionization process, improving the ionization efficiency significantly. Moreover, with the smaller inner diameter columns that are typically used (75  $\mu\text{m}$  to 1 mm-I.D.), micro-flow LC-MS provides higher sensitivity using lower amounts of sample. Since human CSF samples are difficult to obtain, a more sensitive method to make optimal use of such samples is required. Kantae *et al.* [19] developed a quantitative method based on a chip-based nano-LC-MS system for the analysis of eCBs in CSF. Using only 200  $\mu\text{L}$  of human CSF, the method provided a limit of detection (LOD) from 0.3 to 61.2 pM. Intra- and inter-assay variability

(expressed by the coefficient of variation, CV) varied from 2-23% and 3-21%, respectively. However, due to the small inner diameter of the spray emitter, the LC tubing, and the column, the overall stability of such chips remains a challenging aspect in nano-flow LC-MS, contrary to conventional methods with 2.1-mm columns and milliliter range flow rates [22, 23]. In addition, the chips used in the study of Kantae *et al.* are no longer commercially available, showing the need for an alternative method.

In this study, we developed a sensitive and robust micro-LC-MS/MS method for the simultaneous absolute quantification of eCBs and their analogues in human CSF. To improve robustness, the spray needle in the commercial micro spray ion source was modified to avoid clogging. The overall sensitivity was compared between conventional and micro-flow rates. Parameters were optimized for several flow rates and a final method using 4  $\mu\text{L min}^{-1}$  as flow rate and a 0.3-mm inner diameter column was selected. The method was validated based on the guidance of bioanalytical method validation from EMA (2009) [24] for the quantification of eCBs. The validated method was applied to 288 human CSF samples with acceptable performance metrics, thereby demonstrating the value of this method for future studies focusing on deciphering the involvement of ECS in brain disease.

## **2. Material and methods**

### **2.1 Chemicals and materials**

LC-MS-grade acetonitrile (ACN) and formic acid were purchased from Biosolve B.V. (Valkenswaard, Netherlands). Anhydrous methyl tert-butyl ether (MTBE,  $\geq 99.8\%$ ), ammonium acetate ( $\geq 99.0\%$ ) and ammonium formate ( $\geq 99.9\%$ ) were purchased from Sigma-Aldrich (St. Louis, Missouri, United States). Purified water was obtained from a Milli-Q PF Plus system (Merck Millipore, Burlington, Massachusetts, United States).

The standard reagents  $\alpha$ -linolenoyl ethanolamide ( $\alpha$ -LEA), palmitoleoyl ethanolamide (POEA), pentadecanoyl ethanolamide (PDEA), linoleoyl ethanolamide (LEA), anandamide (AEA), docosahexaenoyl ethanolamide (DHEA), 1-arachidonoylglycerol (1-AG), 2-arachidonoylglycerol (2-AG), 1-linoleoyl glycerol (1-LG), 2-linoleoyl glycerol (2-LG), palmitoyl ethanolamide (PEA), dihomo- $\gamma$ -linolenoyl ethanolamide (DGLEA), docosatetraenoyl ethanolamide (DEA), 1-oleoyl glycerol (1-OG), 2-oleoyl glycerol (2-OG),

stearoyl ethanolamide (SEA), eicosapentaenoyl ethanolamide (EPEA), mead acid ethanolamide (ETAEA), N-oleoylethanolamine (OEA) and deuterated standards N-(2-hydroxyethyl)-1,1,2,2-d<sub>4</sub>)-9Z,12Z-octadecadienamide (LEA-d<sub>4</sub>), N-(2-hydroxyethyl)-1,1',2,2'-d<sub>4</sub>)-4Z,7Z,10Z,13Z,16Z,19Z-docosahexaenamide (DHEA-d<sub>4</sub>), N-(2-hydroxyethyl)-5Z,8Z,11Z,14Z-eicosatetraenamide-5,6,8,9,11,12,14,15-d<sub>8</sub> (AEA-d<sub>8</sub>), 5Z,8Z,11Z,14Z-eicosatetraenoic-5,6,8,9,11,12,14,15-d<sub>8</sub> acid (2-AG-d<sub>8</sub>), N-(2-hydroxyethyl)-hexadecanamide-7,7,8,8-d<sub>4</sub> (PEA-d<sub>4</sub>), N-(2-hydroxyethyl)-octadecanamide-18,18,18-d<sub>3</sub> (SEA-d<sub>3</sub>) and N-(2-hydroxyethyl)-1',1,2,2'-d<sub>4</sub>)-9Z-octadecenamide (OEA-d<sub>4</sub>) were purchased from Cayman Chemical (Ann Arbor, Michigan, United States).

## 2.2 Preparation of standards and internal standards solutions

Pure standards (>98% purity) at different stock concentrations were dissolved in ethanol or ACN. The standard stock solutions were diluted to 1 mM using ACN. Standard solution I, used for direct infusion experiments, included 5 nM of each compound in group A (AEA, DEA, DGLEA, DHEA, ETAEA, LEA, EPEA, PDEA, POEA and  $\alpha$ -LEA), 50 nM of each compound in group B (2-AG, 1-AG, SEA, OEA, and PEA) and 500 nM of each compound in group C (2-LG, 1-LG, 2-OG, 1-OG). Standard solution II was obtained by diluting standard solution I four times with ACN and used for LC-MS method development.

The deuterated internal standard (ISTD) working solution containing 225.3 nM 2-AG-d<sub>8</sub>, 4.5 nM AEA-d<sub>8</sub>, 0.6 nM DHEA-d<sub>4</sub>, 3.0 nM LEA-d<sub>4</sub>, 6.0 nM OEA-d<sub>4</sub>, 0.6 nM PEA-d<sub>4</sub> and 12 nM SEA-d<sub>3</sub> was prepared in ACN. All the standard solutions were stored at -20 °C.

## 2.3 Preparation of calibrant solutions

**Table 1.** Concentrations of eCBs and eCB analogues standards in calibrant solutions.

Compound group	Concentration (pM)									
	C0	C1	C2	C3	C4	C5	C6	C7	C8	C9
A	0	7.3	14.65	29.3	58.6	117.2	468.8	1875	3750	7500
B	0	73.3	146.5	293.0	586.0	1171.9	4687.5	18750	37500	75000
C	0	732.4	1464.9	2929.7	5859.4	11718.8	46875	187500	375000	750000

Each standard stock solution (1 mM) was mixed and diluted in ACN, resulting in nine calibration concentration levels. For each calibration level, 10  $\mu$ L of each solution was

mixed with ISTD working solution to reach the adequate concentration. The concentrations of ISTDs were chosen to be in the middle of the dynamic range, i.e., equivalent to C4 concentration. Final concentrations of all compounds are shown in **Table 1**.

## **2.4 Collection of human CSF samples**

CSF samples were collected via a lumbar puncture (LP) in a randomized fashion between 2008 and 2016 and between 9:00 am and 1:00 pm to minimize diurnal and seasonal variation. The protocol was approved by the ethics committee of Leiden University Medical Center. The LP was performed between the L3/L4, L4/L5 or L5/S1 interspace, whereby 3 mL CSF was sampled directly in a 15-mL polypropylene Falcon tube (Cat. No. 188271; Greiner) that already contained 6 mL of cold ethanol and was placed in an ice bath. Ethanol was used to stabilize the metabolites during long-term storage. After the collection of CSF, the tube was gently shaken and immediately put back on ice. Subsequently, the CSF was divided in aliquots of 1.5 mL in 1.8-mL cryotubes (Art. No. 368632; NUNC Brand). The cryotubes were placed on dry ice within 40 min of sampling and immediately transferred to -80°C. All CSF samples remained at -80°C until analysis.

## **2.5 Sample preparation**

The sample preparation was carried out using 750  $\mu$ L of the mixture of CSF and ethanol (including 500  $\mu$ L ethanol). Samples were evaporated using a SpeedVac (Thermo Fisher, USA) for 90 min to remove ethanol. Next, 1 mL of MTBE, 50  $\mu$ L 0.1 M ammonium acetate solution at pH 4 buffer solution and 10  $\mu$ L ISTD working solution were added to each sample, followed by 10 min of standard vortex and centrifugation. After 5 min, the organic layer was transferred to a 1.5-mL Eppendorf tube and evaporated to dryness. Samples were reconstituted in 20  $\mu$ L of a mixture of water/ACN (1:1, v/v), vortexed for 20 min and centrifuged at 16,000g for 10 min. Finally, 15  $\mu$ L of supernatant was transferred in an autosampler vial and injected into the LC-MS instrument.

## **2.6 Optimization of micro-flow rates and comparison with UHPLC-MS**

During the performance comparison evaluation of different flow rates, direct infusion to mass spectrometer and LC-MS methods were used. Direct infusion MS was performed using a syringe pump connected to SCIEX QTRAP 6500+ mass spectrometer (SCIEX,

Framingham, Massachusetts, United States). A Shimadzu Nexera X2 LC-30AD system (Shimadzu corporation., Kyoto, Japan) and Waters nanoAcquity LC system (Waters, Milford, Massachusetts, United States) were used for high- and micro-flow rates, respectively. Various columns and ionization sources suited for each flow rate were chosen to allow for an adequate comparison (**Table 2**). Moreover, UHPLC-MS/MS and micro-LC-MS/MS parameters in this comparison experiment were also optimized for each flow rate and can be found in **Supplemental Table S1**.

**Table 2.** Experimental conditions used for performance comparison of different flow rates.

	Conventional flow		Micro-flow	
Flow rate	550 $\mu\text{L min}^{-1}$	250 $\mu\text{L min}^{-1}$	100 $\mu\text{L min}^{-1}$ , 50 $\mu\text{L min}^{-1}$	1–4 $\mu\text{L min}^{-1}$
Syringe pump	Harvard Apparatus Model 22			
Syringe (for direct infusion)	Hamilton Gastight #1001			Hamilton Gastight #1750
LC	Shimadzu Nexera X2 LC-30AD			Waters nanoAcquity
Column	Waters BEH C18 (1.7 $\mu\text{m}$ , 2.1 $\times$ 50 mm)		Waters HSS T3 C18 (1.8 $\mu\text{m}$ , 1 $\times$ 100 mm)	Phenomenex C18 (2.6 $\mu\text{m}$ , 0.3 $\times$ 50 mm)
Ionization source (for both direct infusion and LC-MS analysis)	SCIEX Turbo V with a 100- $\mu\text{m}$ I.D. emitter	SCIEX Turbo V with a 100- $\mu\text{m}$ I.D. emitter	SCIEX Turbo V with a 50- $\mu\text{m}$ I.D. emitter	SCIEX nanosprayIII with a 30- $\mu\text{m}$ I.D. emitter

## 2.7 Micro-LC-MS/MS instrumentation and conditions

The micro-LC-MS/MS analyses were performed using a Waters nanoAcquity LC instrument coupled to a Shimadzu LCMS-8060 triple quadrupole mass spectrometer equipped with a micro-ionization source (Shimadzu corporation., Kyoto, Japan) and an optimized spray needle, i.e., 15-cm Metal TaperTip<sup>TM</sup> emitter with 30- $\mu\text{m}$  tip inner diameter (New Objective, Littleton, Massachusetts, United States). The separation was carried out using a Phenomenex C18 column (2.6  $\mu\text{m}$ , 0.3 $\times$ 150 mm) maintained at 45°C. The injection volume was 3  $\mu\text{L}$ . Eluent A was composed of 2 mM ammonium formate with 10 mM formic acid in water, and eluent B was ACN. Using a flow rate of 4  $\mu\text{L min}^{-1}$ , the initial gradient started at 55% eluent B and maintained for 0.5 min, eluent B was increased to 60% from 0.5 to 1.5 min, increased to 70% from 1.5 to 2.0 min, to 85% from 2.0 to 5.5 min, and increased to 95% at 5.6 min, where the gradient was kept until 8.0 min, then decreased to



55% eluent B at 8.1 min. The column was equilibrated for 8 min until the next injection, giving a total analysis time of 16 min. MS data was acquired in positive ionization mode with nebulizing gas flow rate of 0.2 L min<sup>-1</sup>, interface voltage at 2 kV, interface temperature at 58°C, and desolvation line (DL) temperature at 250°C. Selected reaction monitoring (SRM) was used for data acquisition by monitoring the precursor-product ion transitions as indicated in **Supplemental Table S2**. These instruments and conditions were used during method validation and application on CSF samples.

## 2.8 Method validation

**Linearity and limit of detection** Linearity was evaluated by preparing calibration lines (n = 3) on three consecutive days. The calibration ranges are shown in **Table 3**. All calibration lines were fitted to a 1/x<sup>2</sup> weighted linear regression model. The limits of detection (LOD) and limits of quantification (LOQ) were calculated as  $LOD = 3 \times S_a/b$ ,  $LOQ = 10 \times S_a/b$ , where  $S_a$  is the standard deviation of the y-intercept, b is the slope of the calibration curve [25].

**Table 3.** Validation parameters: calibration range, retention time, LODs, and LOQs.

Compound	Calibration ranges (pM)	Retention time (min)	R <sup>2</sup>	LOD (pM)	LOQ (pM)
α-LEA	29.3-7500	10.0	0.9978	3.5	11.8
EPEA	58.6-7500	10.0	0.9980	15.1	50.4
POEA	14.6-7500	10.4	0.9970	2.6	8.7
PDEA	7.3-7500	10.8	0.9978	2.1	7.0
DHEA	58.6-7500	10.8	0.9963	34.4	114.6
AEA	7.3-7500	10.9	0.9982	0.7	2.4
LEA	29.3-7500	11.0	0.9983	14.8	49.3
DGLEA	29.3-7500	11.5	0.9975	2.0	6.5
1-AG/2-AG	146.5-75000	11.6/11.8	0.9965	0.6	2.0
1-LG/2-LG	1464.8-750000	11.7/11.9	0.9957	3.2	10.5
PEA	585.9-75000	11.7	0.9933	1293.4	4311.3
ETAEA	29.3-7500	11.9	0.9966	14.1	46.9
OEA	73.2-75000	12.0	0.9988	5.3	17.8
DEA	7.3-7500	12.1	0.9965	1.3	4.4
1-OG/2-OG	5859.4-750000	12.5/12.7	0.9976	45.7	152.4
SEA	146.5-75000	13.0	0.9963	29.5	98.3

\*R<sup>2</sup>, coefficient of determination.

**Precision** The intra- and interday precisions were evaluated by spiking three different concentrations of ISTD solutions [low-level(C2), medium-level(C4) and high-level(C6)] into pooled CSF samples over three different days ( $n = 3$ ). Precision was expressed as the RSD of the peak areas of ISTD. An RSD less than 15% was within the tolerance limits of the EMA guidelines [24].

**Recovery and matrix effects** Recovery and matrix effect were evaluated by spiking ISTD solutions to pooled CSF samples ( $n = 3$ ) or water ( $n = 3$ ). Recovery was calculated as the ratio of ISTD peak areas measured before and after extraction. Matrix effect was the ratio of spiked ISTD peak areas acquired within pooled CSF and water, both spiked after extraction.

## 2.9 Data preprocessing

LabSolutions LCMS Version 5.97 SP1 (Shimadzu, Japan) and SCIEX OS version 1.6 (SCIEX, United States) were used for peak picking and integration. Absolute quantitation was calculated using the equation of the calibration curve and using the peak area ratios (peak area of targeted analyte divided by peak area of respective ISTD). F-test for linear regression was performed using Excel 2016.

## 3. Results and discussion

### 3.1 Optimization of micro-flow rates and comparison with UHPLC-MS

The main advantage of micro-LC is the ability to obtain similar or lower LODs compared with UHPLC, but with significantly reduced injection volumes, making this approach well-suited for analyzing compounds in biomass-restricted samples [26]. Another advantage of micro-LC is a higher robustness compared to nano-LC columns, which is key for clinical studies. In addition to the expected advantages of downscaling LC column diameters, such as higher sensitivity [27], micro-LC results in an improved ESI efficiency. Various flow rates were evaluated using direct infusion MS and micro-LC-MS analysis of eCBs to evaluate the improvement in ESI efficiency. With direct infusion, various flow rates at conventional (i.e.,  $550 \mu\text{L min}^{-1}$ ,  $250 \mu\text{L min}^{-1}$ ,  $100 \mu\text{L min}^{-1}$ ) and micro-level (i.e.,  $4 \mu\text{L min}^{-1}$ ,  $3 \mu\text{L min}^{-1}$ ,  $2 \mu\text{L min}^{-1}$ ,  $1 \mu\text{L min}^{-1}$ ) range were investigated, with optimized parameters on the same MS instrument. After allowing the flow rates to stabilize, a time

window of 1 min was picked and data within this window was summed. The sensitivity of each flow rate was expressed as counts per mole. As shown in **Figure 1**, significant improvements of the sensitivity were observed for both AEA and 2-AG as the flow rate decreased, especially at the low  $\mu\text{L min}^{-1}$  flow rates. This observation is in line with previously reported findings, in which the sensitivity improvement at lower flow rates was attributed to an improved ionization efficiency [28]. It is worth mentioning that, although the increasing trends were still sharp when the flow rate changed to  $1 \mu\text{L min}^{-1}$ , a noticeable increase of background noise was also observed, which may affect the signal-to-noise ratio in the LC-MS analysis.

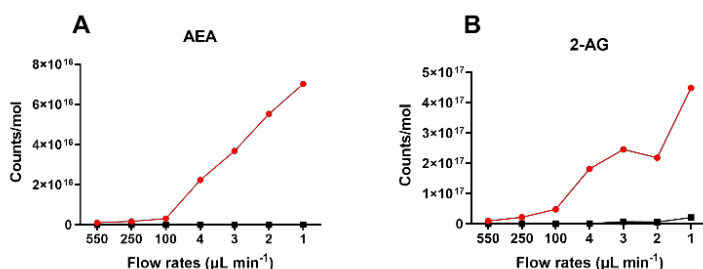


**Figure 1.** Effect of different flow rates on sensitivity of (A) AEA and (B) 2-AG with direct infusion to SCIEX Qtrap 6500+ with Sciex Turbo V ionization source (100-550  $\mu\text{L min}^{-1}$ ) and NanosprayIII ionization source (1-4  $\mu\text{L min}^{-1}$ ). Red line: infusion of standard solution I with 5 nM AEA and 50 nM 1-AG/2-AG in 70% ACN. Black line: infusion of blank sample containing 70% ACN. The y-axis shows the signal as counts per mol, x-axis shows flow rates. MS parameters are listed in **Supplemental Table S1**.

Subsequently, the effect of flow rates was investigated using three micro-LC columns of different inner diameters. Based on the column capacity, four different flow rates from 550  $\mu\text{L min}^{-1}$  to 4  $\mu\text{L min}^{-1}$  were investigated using three columns with inner diameters of 2.1 mm, 1 mm and 0.3 mm, respectively (**Table 2**). The injection volumes of standard solution II on the three columns were 10  $\mu\text{L}$ , 5  $\mu\text{L}$ , and 0.5  $\mu\text{L}$ , respectively. The dilution fold of injected sample under micro-flow rate was smaller, therefore, higher concentration of samples reached the MS interface. **Figure 2A** shows that peak areas of all compounds significantly increased as the flow rates decreased. The detector response observed at each condition is expressed as the ratio of peak area to injection volume. As an example, at a

flow rate of  $4\ \mu\text{L min}^{-1}$ , the detector responses for AEA and 1-AG/2-AG were 9.7 and 9.4 times higher compared with responses observed at a flow rate of  $550\ \mu\text{L min}^{-1}$ , respectively. The sensitivity for eCB analogues improved 5 to 22 times. The results confirm that the ionization efficiency of eCBs and eCB analogues can be enhanced by down-scaling flow rates using suitable columns.

In conclusion, a micro-flow LC-MS/MS method was able to increase the sensitivity of eCBs compared to a conventional UHPLC-MS/MS method. The MS signal is proportional to the amount of compounds reaching the detector within each unit of time, which demonstrates that micro-flow LC-MS analysis is concentration-dependent [29], where the lower the flow rate, the higher the signal. However, the robustness of the micro-flow method, when it reaches  $1\ \mu\text{L min}^{-1}$  or even the nano-flow level is crucial to consider. After taking the capacity of column, cycle time of the analysis, sensitivity required for quantification and most importantly, the method robustness into account,  $4\ \mu\text{L min}^{-1}$  was selected for the following experiments.

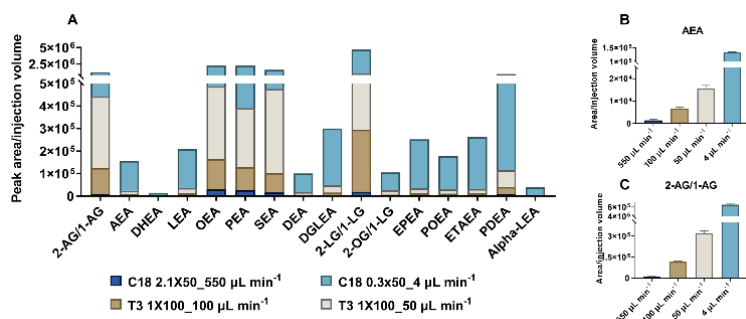


**Figure 2.** Effect of different flow rates on sensitivity of standard solution II with different I.D. columns. SCIEX QTRAP 6500+with SCIEX Turbo V ionization source ( $50 - 550\ \mu\text{L min}^{-1}$ ) and NanosprayIII ionization source ( $4\ \mu\text{L min}^{-1}$ ) was used. SCIEX QTRAP 6500+ with SCIEX Turbo V ionization source ( $50-550\ \mu\text{L min}^{-1}$ ) and NanosprayIII ionization source ( $4\ \mu\text{L min}^{-1}$ ) was used. LC-MS parameters can be found in **Table 2** and **Supplemental Table S1**. Sensitivity is shown on y-axis, expressed as the ratio of compounds peak area to injection volume. (A) Sensitivity of all the targeted compounds with different flow rates; (B) Sensitivity of AEA at different flow rates; (C) Sensitivity of 1-AG/2-AG at different flow rates.

### 3.2 Micro-LC-MS/MS method development

Clogging in the tubing or spray needle remains a major obstacle during the development of low-flow rate LC-MS methods [30]. To avoid clogging and improve the ionization efficiency of the developed micro-LC-MS/MS method, we modified the micro-spray needles on the Shimadzu 8060. In the original micro-ion source, Shimadzu used a design called “UF-link™”. As shown in **Figure 3A** and **3C**, the original micro-spray needle consisted of a metal needle (opening I.D. = 50  $\mu\text{m}$ ) and peak tubing, which were glued together. By connecting the peak tubing directly to the separation column, the dead volume from the connections and extra tubing was minimized. However, during practical use, the glued part was constantly clogged even when using standard solution injections under micro-flow rates. Since the ion source otherwise gave satisfactory performance, we decided to optimize the spray needle to fix the problem. After modification, the whole tubing part including peek part and metal part was removed and replaced by a 15-cm Metal TaperTip emitter (30- $\mu\text{m}$  tip opening and 360- $\mu\text{m}$  outer diameter). This metal emitter was able to sustain robust performance for flow rates up to 5  $\mu\text{L min}^{-1}$ . At micro-flow rates, the influence of the volume in post-column tubing and unions on peak shape, especially peak broadening, may be amplified. In this study, the spray emitter was connected to fused silica tubing (50  $\mu\text{m}$  I.D., 60-cm length) with well-fitting sleeves and a zero dead volume union. Although the total add-on volume was around 1.2  $\mu\text{L}$ , no significant peak broadening or shifting was observed during the analysis.

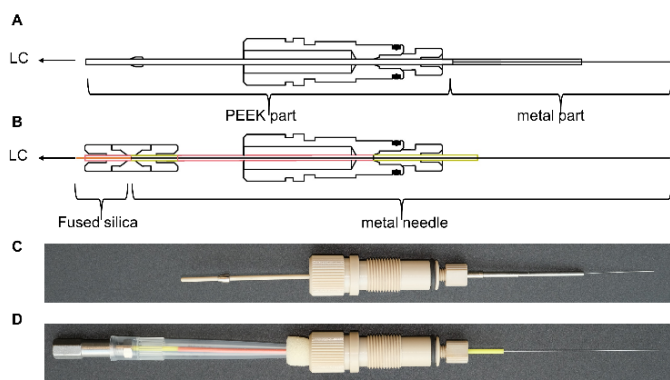


**Figure 3.** Illustration of (A) the original spray needle and (B) the optimized spray needle; Pictures of (C) original spray needle and (D) optimized spray needle.

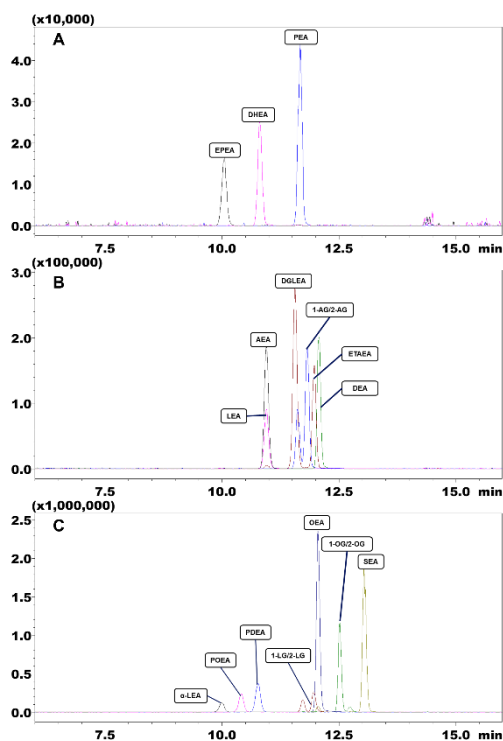


**Figure 4.** Overlay of SRM chromatograms of eCBs and eCB analogues obtained with the injection of standard solution II. The three panels represent the same chromatogram in different scales. (A) compounds with  $1 \times 10^4$  scale intensity (B) compounds with  $1 \times 10^5$  intensity scale (C) compounds with  $1 \times 10^6$  intensity scale.

The micro-LC gradient was optimized based on previous work [19]. The injection volume was evaluated based on column capacity, signal intensity and peak shape. Initial mobile phase was used as injection solvent since it resulted in the best peak shape. Next, MS parameters including nebulizing gas, heating gas, interface temperature, interface voltage, collision energy and dwell time were further optimized with standard solution. The optimized LC-MS parameters are described in **Section 2.7**. After the optimization of micro-LC-MS/MS conditions, all the targeted compounds were separated with nice peak shape by using a Phenomenex C18 (2.6  $\mu\text{m}$ ,  $0.3 \times 150$  mm) column with 16 minutes analysis time (**Figure 4**). Typical SRM chromatograms of targeted eCBs and eCB analogues in human CSF are shown in **Figure 5**. It is worth mentioning that due to the volume of mobile phase mixer, online filter, and tubings in micro-LC system, gradients could not reach the column

immediately at a flow rate of  $4 \mu\text{L min}^{-1}$ , which results in a delay of the retention time. Such delay, however, will not affect the peak shape or method repeatability.

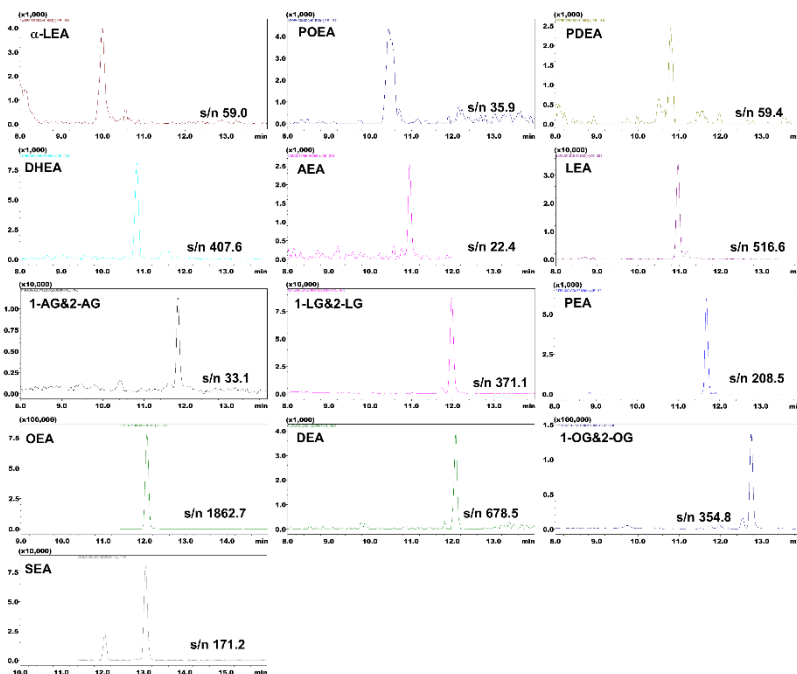


**Figure 5.** SRM chromatograms of eCBs and eCB analogues in pooled human CSF as determined by micro-LC-MS/MS using a flow rate of  $4 \mu\text{L min}^{-1}$  and an injection volume of  $3 \mu\text{L}$ . The x-axis is retention time and the y-axis is the detector response signal.

### 3.3 Analytical performance evaluation

The optimized method in **Section 2.7** was validated according to the EMA guidelines for the validation of analytical methods [24], with evaluation of linearity, precision, recovery and matrix effects. The calibration ranges were determined according to the levels observed in test samples as well as the information retrieved from the Human Metabolome Database (HMDB) and literature [11-17, 20, 31-34]. The linearity, LOD and LOQ are summarized in **Table 3**. Precision (intraday and interday) values, recovery and matrix effects are summarized in **Table 4**.

The coefficient of determination ( $R^2$ ) values were all between 0.995 and 0.999 (significance  $F < 0.05$ ), and at least 75% of the back calculated concentrations of the calibration standards

were within  $\pm 15\%$  (20% for LOQ) of the nominal value, indicating that the linearity was satisfactory for all the analytes. The LOQs were between 2.0 and 152.4 pM for most of the compounds, with the exception of PEA. A study reported that PEA contained in polyurethane foam, which is used for the wrapping material for some experimental glassware, can be absorbed by the glass and later on released to organic solvent during sample preparation [35]. Another report showed that plastic material could also be contaminated by NAEs including PEA [36]. It is important to monitor background contamination of this class to avoid jeopardizing the quantification accuracy of these compounds in biological samples. We observed noticeable PEA peaks in blank sample (50% ACN) and in the lowest calibrant of the calibration curve. Hence, the contamination of PEA from laboratory materials can explain its abnormally high LOD and LOQ values.

**Table 4.** Intraday and interday precision (RSD%).

compounds	Intraday precision (%)			Interday precision (%)		
	Low	Medium	High	Low	Medium	High
d <sub>8</sub> -AEA	10.9%	0.3%	0.1%	13.7%	2.7%	3.8%
d <sub>8</sub> -2-AG	3.2%	2.2%	4.6%	10.9%	9.6%	6.3%
d <sub>4</sub> -OEA	9.8%	8.8%	2.3%	13.7%	6.7%	2.2%
d <sub>4</sub> -LEA	0.3%	1.6%	2.3%	10.1%	5.4%	10.2%
d <sub>4</sub> -DHEA	9.2%	5.5%	9.3%	10.1%	5.4%	10.2%
d <sub>4</sub> -PEA	6.5%	6.2%	3.8%	11.0%	13.5%	6.4%
d <sub>3</sub> -SEA	4.2%	0.9%	0.2%	6.1%	8.6%	5.7%

The intraday and interday precision were assessed using three different concentrations [low-level (C2), medium-level (C4), and high-level (C6)] of internal standards spiked in pooled CSF. Triplicate samples were prepared in each batch, and three batches were measured in three consecutive days. Intra- and interday precisions varied from 0.1% to 10.9% and from 2.2% to 13.7%, respectively, which are all within 15%, indicating that the repeatability was within the tolerance limits (**Table 4**). These results are comparable to previously reported quantification methods for eCBs with nano-flow LC-MS [19], as well as some methods with conventional LC-MS. In addition, during the analysis of the 288 CSF samples, no significant signal decrease was observed, which also demonstrated the robustness of this method.



Recovery and matrix effect were determined using deuterated internal standards. The recoveries ranged from 61.5% to 114.8%. Matrix effects ranged from 24.4% to 105.2% (**Figure 6**). All compounds showed acceptable recovery. Major matrix effects were observed for several analytes, which may be caused by co-eluting phospholipids. As deuterated ISTDs were used, the quantification accuracy was ensured.

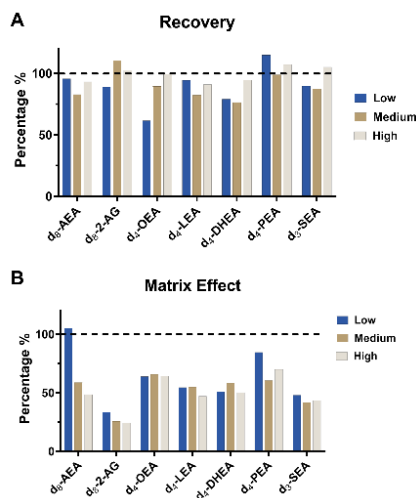


**Figure 6.** Recovery and matrix effect of deuterated internal standards in human CSF. Recovery and matrix effect values are expressed in percentages. (A) Recovery: higher values indicate better recoveries. (B) Matrix effect: values above 100% imply ion enhancement and below 100% imply ion suppression.

### 3.4 Application to the analysis of human CSF samples

As part of another study, CSF samples were collected in a population of males and females with an age ranging from 18 to 69 and measured using the developed micro-LC-MS/MS method. The study was conducted according to the criteria of the Declaration of Helsinki and was approved by the Leiden University Medical Center institutional ethics committee. All participants provided written informed consent prior to participation in the study. Data obtained from the healthy controls ( $n = 94$ ) is reported in current study. The concentration distributions of AEA and 2-AG in the 94 healthy control samples and their correlation with gender and age are shown in **Figure 7**. Concentration of AEA in this CSF study for healthy controls ranged from 1.0-7.1 pM, and for 2-AG from 87.9-658.5 pM. These levels can be

used as future reference in follow-up studies. Significant correlation was observed between age and 2-AG concentration in healthy females (p-value = 0.026). However, no clear correlation was observed between age and the concentration of AEA in human CSF. Although it should be noted that confounding factors might have affected the relation as we did not take these into account. Moreover, the quantification results showed that this method is robust and sensitive enough to be applied to future clinical studies.

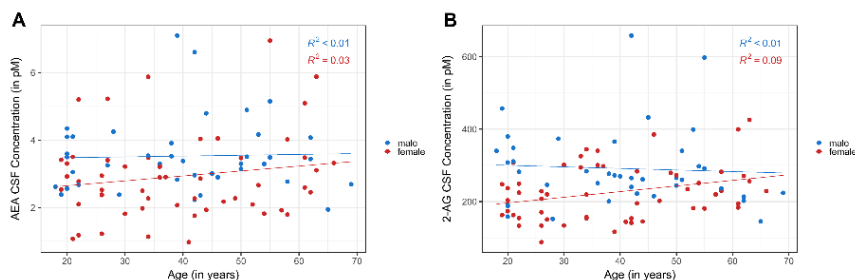


**Figure 7.** Correlation between compounds and age based on the quantification data using the validated micro-LC-MS/MS method. The colors represent male (blue) and female (red).  $R^2$  = coefficient of determination.

#### 4 Conclusion

In this study, we developed and optimized a novel micro-LC-MS/MS method for the determination of eCBs and their analogues in human CSF. By using AEA and 1-AG/2-AG as reference compounds, the comparison of conventional and micro-level flow rates highlighted the advantage of micro-flow in increasing the sensitivity for targeted compounds. The flow rate was down scaled to  $4 \mu\text{L min}^{-1}$  with a 0.3-mm inner diameter column, other setting and parameters were also optimized correspondingly to adapt the micro-flow. A minor modification on Shimadzu Mikros Micro-ESI spray needle was carried out to improve the robustness of this method. Requiring 250  $\mu\text{L}$  CSF, the method reached LODs ranging from 0.6 to 1293.4 pM and LOQs ranging from 2.0 to 4311.3 pM. The repeatability was within the tolerance limits, with intraday and interday precisions under 13.7%. The developed micro-LC-MS/MS method was found to be fit-for-purpose for the analysis of clinical CSF samples, in which 288 human CSF samples were successfully measured. With the wider coverage of eCBs and high robustness for CSF analysis, our

method showed its applicability for future clinical research of brain disorders in which a disturbance in the ECS can be expected.

### Declaration of Competing Interest

The authors declare that they have no known competing financial interests or personal relationships that could have appeared to influence the work reported in this paper.

### Acknowledgements

This study was supported by the China Scholarship Council (CSC, No. 201906390032 to Bingshu He and CSC, No. 201707060012 to Xinyu Di). Dr. Rawi Ramautar would like to acknowledge the financial support of the Vidi grant scheme of the Netherlands Organization of Scientific Research (NWO Vidi 723.016.003). This work was also supported by the Netherlands Organization for Health Research and Development (Vidi grant no. 917-11-31 to GMT), and European Community (EC) funded FP7-EUROHEADPAIN (grant no. 602633 to AMJMVdM). This research was part of the Netherlands X-omics Initiative and partially funded by NWO, project 184.034.019.

### References

- [1] F.A. Iannotti, V. Di Marzo, S. Petrosino, Endocannabinoids and endocannabinoid-related mediators: Targets, metabolism and role in neurological disorders, *Progress in Lipid Research*, 62 (2016) 107-128.
- [2] S. Ben-Shabat, E. Fride, T. Sheskin, T. Tamiri, M.-H. Rhee, Z. Vogel, T. Bisogno, L. De Petrocellis, V. Di Marzo, R. Mechoulam, An entourage effect: inactive endogenous fatty acid glycerol esters enhance 2-arachidonoyl-glycerol cannabinoid activity, *European Journal of Pharmacology*, 353 (1998) 23-31.
- [3] W.-S. Ho, D.A. Barrett, M.D. Randall, 'Entourage' effects of N-palmitoylethanolamide and N-oleoylethanolamide on vasorelaxation to anandamide occur through TRPV1 receptors, *British Journal of Pharmacology*, 155 (2008) 837-846.
- [4] R. Greco, C. Demartini, M. Francavilla, A.M. Zanaboni, C. Tassorelli, Dual Inhibition of FAAH and MAGL Counteracts Migraine-like Pain and Behavior in an Animal Model of Migraine, *Cells*, 10 (2021) 2543.
- [5] A. Della Pietra, R. Giniatullin, J.R. Savinainen, Distinct Activity of Endocannabinoid-Hydrolyzing Enzymes MAGL and FAAH in Key Regions of Peripheral and Central Nervous System Implicated in Migraine, *Int J Mol Sci*, 22 (2021) 1204.
- [6] E. Kilinc, S. Ankarali, I.E. Torun, Y. Dagistan, Receptor mechanisms mediating the anti-neuroinflammatory effects of endocannabinoid system modulation in a rat model of migraine, *European Journal of Neuroscience*, n/a.

- [7] C. Tassorelli, R. Greco, S.D. Silberstein, The endocannabinoid system in migraine: from bench to pharmacy and back, *Current Opinion in Neurology*, 32 (2019) 405-412.
- [8] J. Mulder, M. Zilberter, S.J. Pasquaré, A. Alpár, G. Schulte, S.G. Ferreira, A. Köfalvi, A.M. Martín-Moreno, E. Keimpema, H. Tanila, M. Watanabe, K. Mackie, T. Hortobágyi, M.L. de Ceballos, T. Harkany, Molecular reorganization of endocannabinoid signalling in Alzheimer's disease, *Brain*, 134 (2011) 1041-1060.
- [9] C. Altamura, M. Ventriglia, M.G. Martini, D. Montesano, Y. Errante, F. Piscitelli, F. Scarscia, C. Quattrocchi, P. Palazzo, S. Seccia, F. Vernieri, V. Di Marzo, Elevation of Plasma 2-Arachidonoylglycerol Levels in Alzheimer's Disease Patients as a Potential Protective Mechanism against Neurodegenerative Decline, *Journal of Alzheimer's Disease*, 46 (2015) 497-506.
- [10] P. Leimuranta, L. Khiroug, R. Giniatullin, Emerging Role of (Endo)Cannabinoids in Migraine, *Front Pharmacol*, 9 (2018).
- [11] M. Di Filippo, L.A. Pini, G.P. Pelliccioli, P. Calabresi, P. Sarchielli, Abnormalities in the cerebrospinal fluid levels of endocannabinoids in multiple sclerosis, *Journal of Neurology, Neurosurgery & Psychiatry*, 79 (2008) 1224-1229.
- [12] K.R. Müller-Vahl, L. Bindila, B. Lutz, F. Musshoff, T. Skripuletz, C. Baumgaertel, K.-W. Sühs, Cerebrospinal fluid endocannabinoid levels in Gilles de la Tourette syndrome, *Neuropsychopharmacology*, 45 (2020) 1323-1329.
- [13] J. Nicholson, S. Azim, M.J. Rebecchi, W. Galbavy, T. Feng, R. Reinsel, S. Rizwan, C.J. Fowler, H. Benveniste, M. Kaczocha, Leptin levels are negatively correlated with 2-arachidonoylglycerol in the cerebrospinal fluid of patients with osteoarthritis, *PloS one*, 10 (2015) e0123132-e0123132.
- [14] P. Sarchielli, L.A. Pini, F. Coppola, C. Rossi, A. Baldi, M.L. Mancini, P. Calabresi, Endocannabinoids in Chronic Migraine: CSF Findings Suggest a System Failure, *Neuropsychopharmacology*, 32 (2007) 1384-1390.
- [15] R. Jumpertz, A. Guijarro, R.E. Pratley, D. Piomelli, J. Krakoff, Central and Peripheral Endocannabinoids and Cognate Acylethanolamides in Humans: Association with Race, Adiposity, and Energy Expenditure, *The Journal of Clinical Endocrinology & Metabolism*, 96 (2011) 787-791.
- [16] A. Romigi, M. Bari, F. Placidi, M.G. Marciani, M. Malaponti, F. Torelli, F. Izzi, C. Prosperetti, S. Zannino, F. Corte, C. Chiaramonte, M. Maccarrone, Cerebrospinal fluid levels of the endocannabinoid anandamide are reduced in patients with untreated newly diagnosed temporal lobe epilepsy, *Epilepsia*, 51 (2010) 768-772.
- [17] C. Marchioni, B.L. Santos-Lobato, M.E.C. Queiroz, J.A.S. Crippa, V. Tumas, Endocannabinoid levels in patients with Parkinson's disease with and without levodopa-induced dyskinesias, *Journal of Neural Transmission*, 127 (2020) 1359-1367.
- [18] J. Nicholson, S. Azim, M.J. Rebecchi, W. Galbavy, T. Feng, R. Reinsel, S. Rizwan, C.J. Fowler, H. Benveniste, M. Kaczocha, Leptin levels are negatively correlated with 2-arachidonoylglycerol in the cerebrospinal fluid of patients with osteoarthritis, *PloS one*, 10 (2015) e0123132.
- [19] V. Kantae, S. Ogino, M. Noga, A.C. Harms, R.M. van Dongen, G.L.J. Onderwater, A.M.J.M. van den Maagdenberg, G.M. Terwindt, M. van der Stelt, M.D. Ferrari, T. Hankemeier, Quantitative profiling of endocannabinoids and related N-acylethanolamines in human CSF using nano LC-MS/MS, *Journal of Lipid Research*, 58 (2017) 615-624.
- [20] J. Czepl, J. Gdula-Argasińska, G. Biesiada, B. Bystrowska, A. Jurczyszyn, W. Perucki, K. Sroczynska, A. Zajac, T. Librowski, A. Garlicki, Fatty acids and selected endocannabinoids content in cerebrospinal fluids from patients with neuroinfections, *Metab Brain Dis*, 34 (2019) 331-339.
- [21] F.M. Leweke, A. Giuffrida, D. Koethe, D. Schreiber, B.M. Nolden, L. Kranaster, M.A. Neatby, M. Schneider, C.W. Gerth, M. Hellmich, J. Klosterkötter, D. Piomelli, Anandamide levels in cerebrospinal fluid of first-episode schizophrenic patients: Impact of cannabis use, *Schizophrenia Research*, 94 (2007) 29-36.
- [22] A.E. Kirby, M.J. Jebrail, H. Yang, A.R. Wheeler, Folded emitters for nanoelectrospray ionization mass spectrometry, *Rapid Communications in Mass Spectrometry*, 24 (2010) 3425-3431.
- [23] Y. Huang, Q. Zhang, Y. Liu, B. Jiang, J. Xie, T. Gong, B. Jia, X. Liu, J. Yao, W. Cao, H. Shen, P. Yang, Aperture-controllable nano-electrospray emitter and its application in cardiac proteome analysis, *Talanta*, 207 (2020) 120340.
- [24] E.E.M. Agency, Guidelines for the validation of analytical methods used in residue depletion studies, in: E.M. Agency (Ed.), 2009.
- [25] A. Shrivastava, V.B. Gupta, Methods for the Determination of Limit of Detection and Limit of Quantitation of the Analytical Methods, *Chron Young Sci*, 2 (2011) 15-21.
- [26] J. Zhang, W. Shou, T. Ogura, S. Li, H. Weller, Optimization of microflow LC-MS/MS and its utility in quantitative discovery bioanalysis, *Bioanalysis*, 11 (2019) 1117-1127.

- [27] M. Hilhorst, C. Briscoe, N.v.d. Merbel, Sense and nonsense of miniaturized LC–MS/MS for bioanalysis, *Bioanalysis*, 6 (2014) 3263-3265.
- [28] A. Schmidt, M. Karas, T. Dülcks, Effect of different solution flow rates on analyte ion signals in nano-ESI MS, or: when does ESI turn into nano-ESI?, *Journal of the American Society for Mass Spectrometry*, 14 (2003) 492-500.
- [29] H. Liu, G. Raffin, G. Trutt, J. Randon, Is vacuum ultraviolet detector a concentration or a mass dependent detector?, *Journal of Chromatography A*, 1530 (2017) 171-175.
- [30] K.L. Sanders, J.L. Edwards, Nano-liquid chromatography-mass spectrometry and recent applications in omics investigations, *Analytical Methods*, 12 (2020) 4404-4417.
- [31] M. Bobrich, R. Schwarz, R. Ramer, P. Borchert, B. Hinz, A simple LC-MS/MS method for the simultaneous quantification of endocannabinoids in biological samples, *Journal of Chromatography B*, 1161 (2020) 122371.
- [32] I. Mennella, M. Savarese, R. Ferracane, R. Sacchi, P. Vitaglione, Oleic acid content of a meal promotes oleoylethanolamide response and reduces subsequent energy intake in humans, *Food & Function*, 6 (2015) 203-209.
- [33] R. Ottria, A. Ravelli, F. Gigli, P. Ciuffreda, Simultaneous ultra-high performance liquid chromatography-electrospray ionization-quadrupole-time of flight mass spectrometry quantification of endogenous anandamide and related N-acylethanolamides in bio-matrices, *Journal of Chromatography B*, 958 (2014) 83-89.
- [34] P.J.H. Jones, L. Lin, L.G. Gillingham, H. Yang, J.M. Omar, Modulation of plasma N-acylethanolamine levels and physiological parameters by dietary fatty acid composition in humans, *Journal of lipid research*, 55 (2014) 2655-2664.
- [35] Identification of a Widespread Palmitoylethanolamide Contamination in Standard Laboratory Glassware, *Cannabis and Cannabinoid Research*, 2 (2017) 123-132.
- [36] S. Oddi, F. Fezza, G. Catanzaro, C. De Simone, M. Pucci, D. Piomelli, A. Finazzi-Agro, M. Maccarrone, Pitfalls and solutions in assaying anandamide transport in cells[S], *Journal of Lipid Research*, 51 (2010) 2435 - 2444.

## Supplementary Material

**Table S1(A).** MS parameters of SCIEX QTRAP 6500+ mass spectrometer used in flow rate evaluation experiment.

	Conventional flow		Micro flow					
Flow rates	550 $\mu\text{L min}^{-1}$	250 $\mu\text{L min}^{-1}$	100 $\mu\text{L min}^{-1}$	50 $\mu\text{L min}^{-1}$	4 $\mu\text{L min}^{-1}$	3 $\mu\text{L min}^{-1}$	2 $\mu\text{L min}^{-1}$	1 $\mu\text{L min}^{-1}$
Curtain gas	30	30	20	20	20	20	20	20
Ionspray voltage	5500	5500	4700	4700	2400	2300	2200	2100
Ion source gas 1	50	50	30	30	10	10	10	10
Ion source gas 2	50	50	30	0	0	0	0	0
Interface heater temperature	600	600	450	450	150	140	120	100
DP	50	50	50	50	50	50	50	50
EP	12	12	12	12	12	12	12	12
CXP	11	11	11	11	11	11	11	11

**Table S1(B).** LC gradients in LC-MS flow rates comparison.

Flow rate 550 $\mu\text{L min}^{-1}$			Flow rate 100 $\mu\text{L min}^{-1}$ and 50 $\mu\text{L min}^{-1}$			Flow rate 4 $\mu\text{L min}^{-1}$		
Time (min)	A[%]	B[%]	Time (min)	A[%]	B[%]	Time (min)	A[%]	B[%]
0	45	55	0	45	55	0	45	55
0.5	45	55	0.5	45	55	0.5	45	55
1.5	40	60	2	40	60	2	40	60
2	30	70	2.5	30	70	2.5	30	70
5.5	15	85	7.5	15	85	7.5	15	85
5.6	5	95	8	5	95	8	5	95
8	5	95	10	5	95	10	5	95
8.1	45	55	10.1	45	55	10.1	45	55
10	45	55	12	45	55	16	45	55

**Table S2.** MRM (Multiple reaction monitoring) parameters of the target compounds with Shimadzu 8060 mass spectrometer.

Compound name	ChEBI ID	Abbreviat ion	Molecular formula	MW g/mole	Precurs or ion (m/z)	Prod uct ion (m/z)	Dwell time (msec)	CE
$\alpha$ -Linolenoyl ethanolamide	89605	a-LEA	C <sub>20</sub> H <sub>35</sub> NO <sub>2</sub>	325.5	322.4	61.9	20	-16
Palmitoleoyl ethanolamide	71465	POEA	C <sub>18</sub> H <sub>35</sub> NO <sub>2</sub>	297.5	298.4	62.2	5	-16
Pentadecanoyl ethanolamide	165589	PDEA	C <sub>17</sub> H <sub>35</sub> NO <sub>2</sub>	285.5	386.4	61.9	5	-15
Linoleoyl ethanolamide	64032	LEA	C <sub>20</sub> H <sub>37</sub> NO <sub>2</sub>	323.5	324.3	62	20	-33
Anandamide	2700	AEA	C <sub>22</sub> H <sub>37</sub> NO <sub>2</sub>	347.5	348.2	62.0	20	-23
Docosahexaenoyl ethanolamide	85252	DHEA	C <sub>24</sub> H <sub>37</sub> NO <sub>2</sub>	371.6	372.4	62	20	-17
1-Arachidonoylglycerol / 2-Arachidonoylglycerol	75612 52392	1-AG/2- AG <sup>a</sup>	C <sub>23</sub> H <sub>38</sub> O <sub>4</sub>	378.5	379.2	287.0	20	-15
1-Linoleoyl glycerol / 2-Linoleoyl glycerol	75565 173124	1-LG/2- LG <sup>b</sup>	C <sub>21</sub> H <sub>38</sub> O <sub>4</sub>	354.5	355.1	263.0	10	-17
Palmitoyl ethanolamide	71464	PEA	C <sub>18</sub> H <sub>37</sub> NO <sub>2</sub>	299.5	300.4	62.0	5	-5
Dihomo- $\gamma$ -linolenoyl ethanolamide	34488	DGLEA	C <sub>22</sub> H <sub>39</sub> NO <sub>2</sub>	349.5	350.2	62	5	-17
Docosatetraenoyl ethanolamide	34478	DEA	C <sub>24</sub> H <sub>41</sub> NO <sub>2</sub>	375.6	376.2	62.0	8	-22
1-Oleoyl glycerol / 2-Oleoyl glycerol	75342 73990	1-OG/2- OG <sup>c</sup>	C <sub>21</sub> H <sub>40</sub> O <sub>4</sub>	356.5	357.3	265.3	10	-12
Stearoyl ethanolamide	85299	SEA	C <sub>20</sub> H <sub>41</sub> NO <sub>2</sub>	327.5	328.3	62.0	5	-17
Eicosapentaenoyl ethanolamide	71467	EPEA	C <sub>22</sub> H <sub>35</sub> NO <sub>2</sub>	345.5	346.2	61.9	20	-16
Mead acid ethanolamide	165588	ETAEA	C <sub>22</sub> H <sub>39</sub> NO <sub>2</sub>	349.5	350.2	62	5	-17
N-Oleoylethanolamine	71466	OEA	C <sub>20</sub> H <sub>39</sub> NO <sub>2</sub>	325.5	326.0	62.0	20	-22
N-linoleoylethanolamide - d <sub>4</sub>		d <sub>4</sub> -LEA-ISTD	C <sub>20</sub> H <sub>33</sub> D <sub>4</sub> NO <sub>2</sub>	327.5	328.3	66.2	20	-33
N-docosahexaenoyl ethanolamide- d <sub>4</sub>		d <sub>4</sub> -DHEA-ISTD	C <sub>24</sub> H <sub>33</sub> D <sub>4</sub> NO <sub>2</sub>	375.6	376.3	66.2	10	-17
N-arachidonoyl ethanolamide - d <sub>8</sub>		d <sub>8</sub> -AEA-ISTD	C <sub>22</sub> H <sub>29</sub> D <sub>8</sub> NO <sub>2</sub>	355.6	356.3	62.0	20	-23
N-arachidonoylglycerol - d <sub>8</sub>		d <sub>8</sub> -2-AG-ISTD	C <sub>23</sub> H <sub>30</sub> D <sub>8</sub> O <sub>4</sub>	386.6	387.3	294.2	20	-15
N-palmitoylethanolamide - d <sub>4</sub>		d <sub>4</sub> -PEA-ISTD	C <sub>18</sub> H <sub>33</sub> D <sub>4</sub> NO <sub>2</sub>	303.5	304.4	62.0	5	-5
N-oleoylethanolamide - d <sub>4</sub>		d <sub>4</sub> -OEA-ISTD	C <sub>20</sub> H <sub>33</sub> D <sub>4</sub> NO <sub>2</sub>	329.6	330.0	66.0	8	-22
N-stearoylethanolamide - d <sub>3</sub>		d <sub>3</sub> -SEA-ISTD	C <sub>20</sub> H <sub>38</sub> D <sub>3</sub> NO <sub>2</sub>	330.6	331.3	62.0	5	-17

**Table S3.** Accuracy and precision at lowest points of calibration curves (n=3).

Compound	Calibration ranges (pM)	Retention time (min)	R <sup>2</sup>	Nominal concentration (pM)	Calculate concentration (pM)	Accuracy	Precision
$\alpha$ -LEA	29.3-7500	10.0	0.9978	29.3	27.7	94.4%	6.3%
EPEA	58.6-7500	10.0	0.9980	58.6	57.7	98.5%	5.5%
POEA	14.6-7500	10.4	0.9970	14.6	14.5	99.2%	17.8%
PDEA	7.3-7500	10.8	0.9978	7.3	6.9	93.6%	12.4%
DHEA	58.6-7500	10.8	0.9963	58.6	61.4	104.7%	2.8%
AEA	7.3-7500	10.9	0.9982	7.3	6.9	94.6%	6.8%
LEA	29.3-7500	11.0	0.9983	29.3	28.5	97.2%	13.4%
DGLEA	29.3-7500	11.5	0.9975	29.3	25.0	85.3%	5.6%
1-AG/2-AG	146.5-75000	11.6/11.8	0.9965	146.5	159.9	109.1%	1.2%
1-LG/2-LG	1464.8-750000	11.7/11.9	0.9957	1464.8	1528.2	104.3%	5.5%
PEA	585.9-75000	11.7	0.9933	585.9	661.1	112.8%	3.6%
ETAEA	29.3-7500	11.9	0.9966	29.3	26.1	89.2%	2.9%
OEA	73.2-75000	12.0	0.9988	73.2	83.2	113.6%	3.0%
DEA	7.3-7500	12.1	0.9965	7.3	7.7	105.6%	12.6%
1-OG/2-OG	5859.4-750000	12.5/12.7	0.9976	5859.4	5747.1	98.1%	4.7%
SEA	146.5-75000	13.0	0.9963	146.5	174.2	118.9%	3.5%

\*Accuracy = calculate concentration / nominal concentration  $\times$  100%;

Precision = RSD% of calculate concentration





# Chapter IV

---

## **A micro-flow liquid chromatography-mass spectrometry method for the quantification of oxylipins in volume-limited human plasma**

### **Based on:**

Bingshu He, Rawi Ramautar, Marian Beekman, P. Eline Slagboom, Amy Harms, Thomas Hankemeier

**A micro-flow liquid chromatography-mass spectrometry method for the quantification of oxylipins in volume-limited human plasma**

ELECTROPHORESIS 2025; DOI: 10.1002/elps.202400151

## **Abstract**

Oxylipins are well-known lipid mediators in various inflammatory conditions. Their endogenous concentrations range from low picomolar to nanomolar and there are growing demands to determine their concentrations in low volume matrices for pathological studies, including blood, cerebrospinal fluids from animal disease models, infants, and microsampling devices. Most of the published quantification methods for comprehensive profiling of oxylipins still require more than 50  $\mu\text{L}$  plasma as a starting volume to detect these low levels. The aim of our study is to develop a sensitive and reliable method for the quantification of oxylipins in volume-limited human plasma samples. We established and validated a micro-LC-MS/MS method that requires only 5  $\mu\text{L}$  of human plasma for the determination of 66 oxylipins. The optimized micro-LC-MS/MS method utilized a flow rate of 4  $\mu\text{L}/\text{min}$  with a 0.3-mm inner diameter column. With an injection volume of 3  $\mu\text{L}$ , our method provides limits of detection in the range from 0.1 pM to 91.9 pM, and limits of quantification ranging from 0.3 pM to 306.2 pM. The sensitivity enhancement compared to conventional flow ranged from 1.4 to 180.7 times for 51 compounds depending on their physical-chemical properties. After validation, the method was applied to analyze 40 plasma samples from a healthy aging study to demonstrate robustness and sensitivity.

## 1. Introduction

Oxylipins are a group of signaling lipids derived from polyunsaturated fatty acids (PUFAs) through enzymatic or non-enzymatic oxidation processes. Non-esterified or free oxylipins function as important lipid mediators in multiple physiological processes as well as disease pathologies. Cardiovascular diseases, obesity, type II diabetes, and neurological disorders have been linked to abnormal oxylipin signaling [1, 2]. Oxylipins include some well-studied subclasses such as prostaglandins (PGs), arachidonic acid (AA) derived isoprostanes, AA and eicosapentaenoic acid (EPA) derived prostanoids, AA derived leukotrienes, and lipoxins, which are involved in inflammation, blood clotting, immune response, cardiovascular diseases, and tumor progression [3-7].

As the most direct and easy to sample matrix, plasma is commonly utilized for studying the onset and progression of pathological processes. Despite the increasing demand for oxylipin profiling and understanding their functions, currently available LC-MS methods for the quantification of PUFAs and their derivatives often fall short when dealing with volume-limited plasma samples [8-11]. Although plasma from adults is not normally recognized as volume-limited, when one sample set has to be aliquoted to multiple analytical platforms for a comprehensive multi-omics analysis, only a limited volume is available for each platform. On the other hand, the sampling techniques in healthcare favour sampling low volumes (below 10  $\mu\text{L}$ ) to ease the pain for patients [12, 13] and improve wellness of experimental animals [14]. The issue of volume mismatch between sampling and sample analysis can be addressed by employing a miniaturized LC-MS workflow, which allows high detection sensitivity with a minimal sample volume.

One example of how a miniaturized workflow can increase sensitivity was presented by Cebo et al. [15] who established a micro-LC-MS/MS method for accurate quantification of 42 oxylipins in plasma using a flow rate of 30  $\mu\text{L}/\text{min}$ . Although the method allowed for the quantitation of some oxylipins down to the picogram level, a relatively large volume of plasma (500  $\mu\text{L}$ ) was used, and the sample was up-concentrated to 100  $\mu\text{L}$  to achieve the required detection limits. A further down-scaling in flow rate may lead to higher sensitivity which enables the quantification of oxylipins using less starting material.

In this study, we established a micro-LC-MS workflow for the quantification of 66 oxylipins in 5  $\mu$ L human plasma. Selected reaction monitoring (SRM) was applied in a targeted method in negative ion mode. Multiple electrospray ionization sources were compared, corona discharge was minimized, and analytical performance was optimized. A reverse phase C18 column with a 0.3-mm inner diameter was used for this method at a flow rate of 4  $\mu$ L/min. The method underwent validation following the bioanalytical method validation guidelines from EMA (2009). The sensitivity enhancement was evaluated by comparing the limits of detection and limits of quantification with a published conventional flow UHPLC-MS method [16]. The validated method was applied to 40 human plasma samples from a healthy aging study with 5- $\mu$ L as starting volume. 28 oxylipins were quantified from picomolar to nanomolar level. This underscores its potential value for future studies that demand high sensitivity in determining oxylipin concentrations in volume-limited samples.

## **2. Material and methods**

### **2.1 Chemicals and materials**

Ultra-performance liquid chromatography grade acetonitrile (ACN) and methanol (MeOH) were purchased from Biosolve (Valkenswaard, Netherlands). 1-Butanol (BuOH) was acquired from Boom (Meppel, Netherlands). Methyl tert-butyl ether (MTBE), acetic acid (100%, LC-MS grade), butylated hydroxytoluene (BHT), ethylenediaminetetraacetic acid (EDTA) were from SigmaAldrich (Zwijndrecht, Netherlands). Citric acid monohydrate and disodium hydrogen phosphate were obtained from Merck (Darmstadt, Germany). Purified water was obtained from a Milli-Q PF Plus system (Merck Millipore, Burlington, Massachusetts, United States). Standards and deuterated standards for oxylipins were purchased from Cayman Chemicals (Ann Arbor, Michigan, United States). The purchasing information and abbreviations of all the targeted oxylipins and labeled standards are listed in **Supplementary Table 1**.

### **2.2 Preparation of standards solutions and calibrant solutions**

Stock solutions of oxylipins and labeled standards were dissolved in MeOH containing BHT (0.4 mg/mL) to 1 mg/mL. The oxylipins standard stock solutions were diluted to 11

calibrant points (C1 to C11) subsequently. Internal standards (ISTD) were spiked in each calibrant point and sample to reach a final concentration of 20 nM. All the stock solutions were stored at -20 °C. The compound list with their calibration concentrations can be found in **Supplementary Table 2**.

### 2.3 Sample collection and preparation

Fasted EDTA plasma samples were collected from 40 participants in the Leiden Longevity Study cohort which was enrolled between 2002 and 2006 [17]. The samples for the current study were collected at the third visit between 2009 and 2010 and stored at -80°C. The Leiden Longevity Study protocol (P09.140) was approved by the Medical Ethical Committee of the Leiden University Medical Center before the start of the study at 5th of August 2009. The first participant was enrolled at 24th of August 2009. In accordance with the Declaration of Helsinki, the Leiden Longevity Study obtained informed consent from all participants prior to their entering the study. 5 µL was taken from each plasma sample and pooled together to create a quality control (QC) sample used during method validation and bioanalysis. All plasma samples remained at -80°C until extraction.

Plasma samples, calibration samples, and QCs were thawed on ice before liquid-liquid extraction (LLE). To 5 µL plasma (or calibrant solution), 5 µL antioxidant solution, 5 µL 80 nM ISTD, 5 µL buffer solution containing 0.2 M citric acid, and 0.4 M phosphate at pH 4.5 were added in a 0.5 mL Eppendorf tube. After adding 100 µL BuOH: MTBE (1:1, v/v) and 50 µL water, oxylipins were extracted to the upper layer. Subsequently the samples were settled on ice for 20 minutes. This will facilitate the LLE because the protein layer will become more compact. After that, the samples were brought to a bullet blender to be thoroughly mixed for 4 minutes at the speed level 9. Samples were then centrifuged for 10 min at 15800 rcf under 4°C. 85 µL of the organic upper layer was collected and evaporated to dryness. Samples were reconstituted in a 20 µL mixture of MeOH: H<sub>2</sub>O (2:8, v/v) before injection.

### 2.4 Micro-LC-MS/MS instrumentation and conditions

The micro-LC-MS/MS analyses were performed using a Waters nanoAcquity LC system (Waters, Milford, Massachusetts, United States) coupled to a Sciex triple quad 7500 mass spectrometer (SCIEX, Framingham, Massachusetts, United States). A Sciex Optiflow

ionization source was equipped on the MS with a SteadySpray Low Micro Electrode (1 - 50  $\mu\text{L}/\text{min}$ ). The separation was carried out using a Phenomenex Kinetex C18 column (2.6  $\mu\text{m}$ , 150  $\times$  0.3 mm) maintained at 40  $^{\circ}\text{C}$ . The injection volume was 3  $\mu\text{L}$ . Mobile phase A consisted of 0.1% acetic acid in water, mobile phase B was 0.1% acetic acid in a mixture of 90% ACN and 10% MeOH. Using a flow rate of 4  $\mu\text{L}/\text{min}$ , the initial gradient started at 20% eluent-B and maintained for 5.0 min, eluent-B was ramped to 26% until 5.4 min, and further to 34% at 15.5 min, remained at 34% for 2 min and increased to 40% at 19.5 min, to 54% at 23.5 min, to 56% at 27.5 min, to 78% at 29.5 min, to 85% at 31.5 min, at last eluent B dropped back to 20% for re-equilibration until 40.0 min. MS data was acquired in negative ionization mode with curtain gas flow rate 32 psi, gas 1 flow rate 10 psi, gas 2 flow rate 20 psi, interface voltage at -3500 V, interface temperature at 200  $^{\circ}\text{C}$ . SRM was used for data acquisition by monitoring the precursor-product ion transitions as indicated in **Supplemental Table 3**. These instrumental conditions were used during method validation and application to plasma samples.

## 2.5 Method validation

**Linearity and limit of detection** To assess linearity, calibration lines ( $n = 3$ ) were prepared over three consecutive days, incorporating a minimum of seven calibration points for each compound. All calibration lines were fitted to a  $1/x^2$  weighted linear regression model. The limits of detection (LOD) and limits of quantification (LOQ) were calculated using the formulas  $\text{LOD} = 3 \times S_a/b$  and  $\text{LOQ} = 10 \times S_a/b$ , respectively. Here,  $S_a$  represents the standard deviation of the y-intercept,  $b$  represents the slope of the calibration curve.

**Precision** The intra- and interday precisions were evaluated by spiking three different concentrations of ISTD solutions [low-level (0.2 nM), medium-level (2.0 nM) and high-level (20 nM)] into pooled plasma samples over three different days ( $n = 3$ ). Precision was expressed as the RSD of the peak areas of ISTD. An RSD less than 15% was within the tolerance limits of the EMA guidelines [18].

**Recovery and matrix effects** Recovery was investigated by spiking ISTD solution before LLE and after LLE. Matrix effect was evaluated by spiking ISTD solutions to pooled plasma samples ( $n = 3$ ) or water ( $n = 3$ ). Recovery was calculated as the ratio of ISTD peak

areas spiked before and after extraction. The Matrix effect was determined by calculating the ratio of the peak areas of ISTD spiked in pooled plasma and water samples.

## 2.6 Comparison to conventional UHPLC-MS/MS method

The performance of the optimized micro-LC-MS/MS method was compared to a conventional UHPLC-MS/MS described in a previous study [16]. The sample preparation procedure and starting volume (5  $\mu$ L plasma) were same in both methods as described in **section 2.3**. A Shimadzu Nexera X2 LC-30AD system (Shimadzu corporation., Kyoto, Japan) was coupled to a SCIEX triple quad 7500 mass spectrometer (SCIEX, Framingham, Massachusetts, United States). An OptiFlow ionization source with spray emitters for high flow (>200  $\mu$ L/min) was employed. The separation was carried out on a Waters Acquity® BEH C18 column (50 mm  $\times$  2.1 mm, 1.7  $\mu$ m) maintained at 40 °C with a 5- $\mu$ L injection volume. The detailed UHPLC gradient can be found in **Supplementary table 4**. MS data was acquired in negative ionization mode with curtain gas flow rate of 45 psi, gas 1 flow rate of 65 psi, gas 2 flow rate of 65 psi, interface voltage of -4500 V, interface temperature of 600 °C.

## 2.7 Data preprocessing

SCIEX OS version 1.6 (SCIEX, United States) was used for peak integration. Absolute quantitation was calculated using the equation of the calibration curve and using the peak area ratios (peak area of targeted analyte divided by peak area of respective ISTDs).


# 3. Results and discussion

## 3.1 micro-LC-MS/MS method development

Significant sensitivity enhancement was achieved by employing a nanoAcquity LC coupled with Shimadzu 8060 MS and a homemade spray emitter under micro-level flow rate as indicated in previous study [19]. Negative mode was used for the analysis of oxylipins. However, applying a negative voltage resulted in damage to the tip of the spray emitter due to severe corona discharge. Although the discharge problem could be mitigated by moving the emitter tip away from the MS orifice, sensitivity was sacrificed in this process. To address the discharge issue while maintaining high sensitivity under micro-flow rates, we compared several MS systems and micro-flow ionization sources, including SCIEX



nanoSprayIII with a Metal TaperTip spray emitter, Shimadzu MIKRO ionization source with a homemade spray needle, and SCIEX OptiFlow with a SteadySpray electrode (**Figure 1**). All MS parameters were optimized for the optimal performance of each system. Based on its advantages in robustness and sensitivity (**Figure 2A**), a Sciex triple quad 7500 MS with the Optiflow ionization source was ultimately selected for further method development. The SteadySpray needle also provided more flexibility with its tolerance of a wide range of flow rates.

MS	 Shimadzu LCMS8060	 SCIEX Qtrap 6500 +	 SCIEX Triple quad 7500
Ionization Source	 Shimadzu MIKRO	 SCIEX nanoSprayIII	 SCIEX OptiFlow
Spray Needle	 Modified based on Shimadzu Mikros spray needle I.D. 30 $\mu\text{m}$	 New Objective, Metal TaperTip, I.D. 30 $\mu\text{m}$	 SCIEX, SteadySpray Electrode Low Micro
Flow Rate	Up to 4 $\mu\text{L}/\text{min}$	Up to 4 $\mu\text{L}/\text{min}$	1 - 50 $\mu\text{L}/\text{min}$

**Figure 1.** Mass spectrometers, Ionization sources, and micro-flow spray needles used for performance comparison

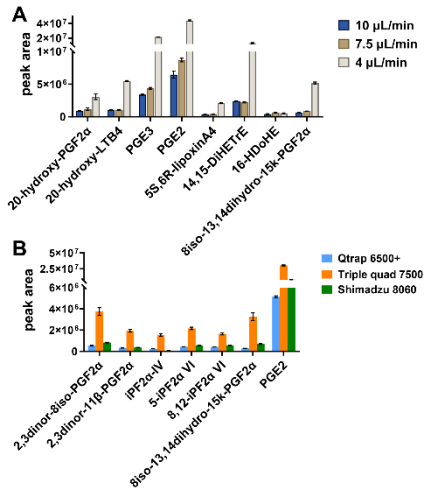


**Figure 2.** (A) Comparison of the performance from different MS systems using 4  $\mu\text{L}/\text{min}$ ; (B) optimization of micro flow rate on SCIEX triple quad 7500 MS.

To enhance the sensitivity of targeted compounds, we initially compared several flow rates. **Figure 2B** illustrates that the peak area of selected compounds increased with lower flow rate. It is also predictable that with 4  $\mu\text{L}/\text{min}$  flow rate, the dilution factor of injected samples is lower. Simultaneously, a lower flow rate facilitates more efficient ionization of target compounds.

In order to improve the separation of isomers with same SRM transitions, including 8-iso-PGE<sub>2</sub>, PGE<sub>2</sub>, 11 $\beta$ -PGE<sub>2</sub>, PGD<sub>2</sub> (Q1/Q3 351.1/271.2), and 8iso-15R-PGF<sub>2</sub> $\alpha$ , 8iso-PGF<sub>2</sub> $\alpha$ , 11 $\beta$ -PGF<sub>2</sub> $\alpha$ , PGF<sub>2</sub> $\alpha$  (Q1/Q3 353.1/193.1), a 15-cm length Phenomenex Kinetex C18 column was used. In addition, a 5-min isocratic time at the beginning of the gradient with 80% mobile phase A was applied. This step is also crucial to prevent peak tailing in early eluting compounds, such as 20-hydroxy-PGE<sub>2</sub> and 20-hydroxy-PGF<sub>2</sub> $\alpha$  (**Supplementary Figure 1**).

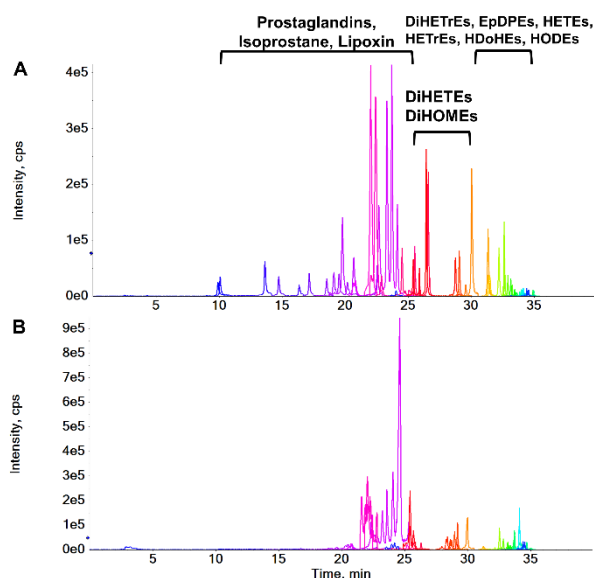


**Figure 3.** Overlay of SRM chromatograms of oxylipins obtained with the injection of (A) standard solution C7 and (B) 5  $\mu\text{L}$  pooled plasma

Following the optimization of micro-LC-MS/MS conditions, all targeted compounds exhibited excellent resolution using a Phenomenex Kinetex C18 (2.6  $\mu\text{m}$ , 0.3  $\times$  150 mm) column with a 40-minute analysis time. The injection volume was set at 3  $\mu\text{L}$ . Typical SRM

chromatograms of targeted oxylipins in standard solution and pooled human plasma are shown in **Figure 3**. Prostaglandins, isoprostane, and lipoxins eluted before 30 min, while dihydroxy- eicosatrienoic acids (DiHETrEs), epoxy- docosapentaenoic acid (EpDPes), hydroxy- eicosatrienoic acid (HETrEs), and hydroxyeicosatetraenoic acids (HETEs) with lower polarity eluted between 30 min to 35 min. The optimized condition ensures robust analysis of the diverse oxylipin classes.

### 3.2 Sensitivity enhancement compared to a UHPLC-MS/MS method

The sensitivity enhancement of micro-LC-MS/MS method was evaluated by comparing its LODs and LOQs with those of conventional UHPLC-MS/MS using calibration solutions. 5  $\mu$ L extracted sample was injected on a Waters Acquity® BEH C18 column (50 mm  $\times$  2.1 mm, 1.7  $\mu$ m) for conventional method, and 3  $\mu$ L was injected on a Phenomenex Kinetex C18 column (2.6  $\mu$ m , 150  $\times$  0.3 mm) for micro-LC-MS/MS method. The same MS and ionization source were utilized for a fair comparison. In **Figure 4**, the fold changes in LOD and LOQ for the micro flow method over the conventional method are depicted for targeted oxylipins. For 13-HODE, 8,12-iPF $2\alpha$ -VI, and 13,14-dihydro-15keto-PGE $2$ , the calibration points within the same concentration ranges of the micro-LC-MS method were insufficient for calculating LOD and LOQ compared with the UHPLC-MS/MS method.

Among the other 63 oxylipins, sensitivity increased from 1.4 to 180.7 times in 51 compounds (orange bars in **Figure 4**). However, due to differences in the compounds physical-chemical properties, for 10 compounds (depicted as green bars in **Figure 4**), including 9-HETE, 11-HDoHE, 10-HDoHE, 9-HODE, 16-HDoHE, 5-HEPE, 12-HETE, 17-HDoHE, 20-HDoHE, and 8-HDoHE, micro-LC-MS performance was found to be inferior to that of the UHPLC-MS/MS method. Different reconstitution solvents and LC gradients were used for the micro-LC-MS and UHPLC-MS methods, resulted in change of chromatographic selectivity, and lead to changes in ion suppression for those compounds due to the matrix effect. The ion suppression subsequently resulted in higher LOD and lower signal to noise ratio for micro-LC-MS. For detailed LOD and LOQ values for both methods, refer to **Supplementary table 5**.

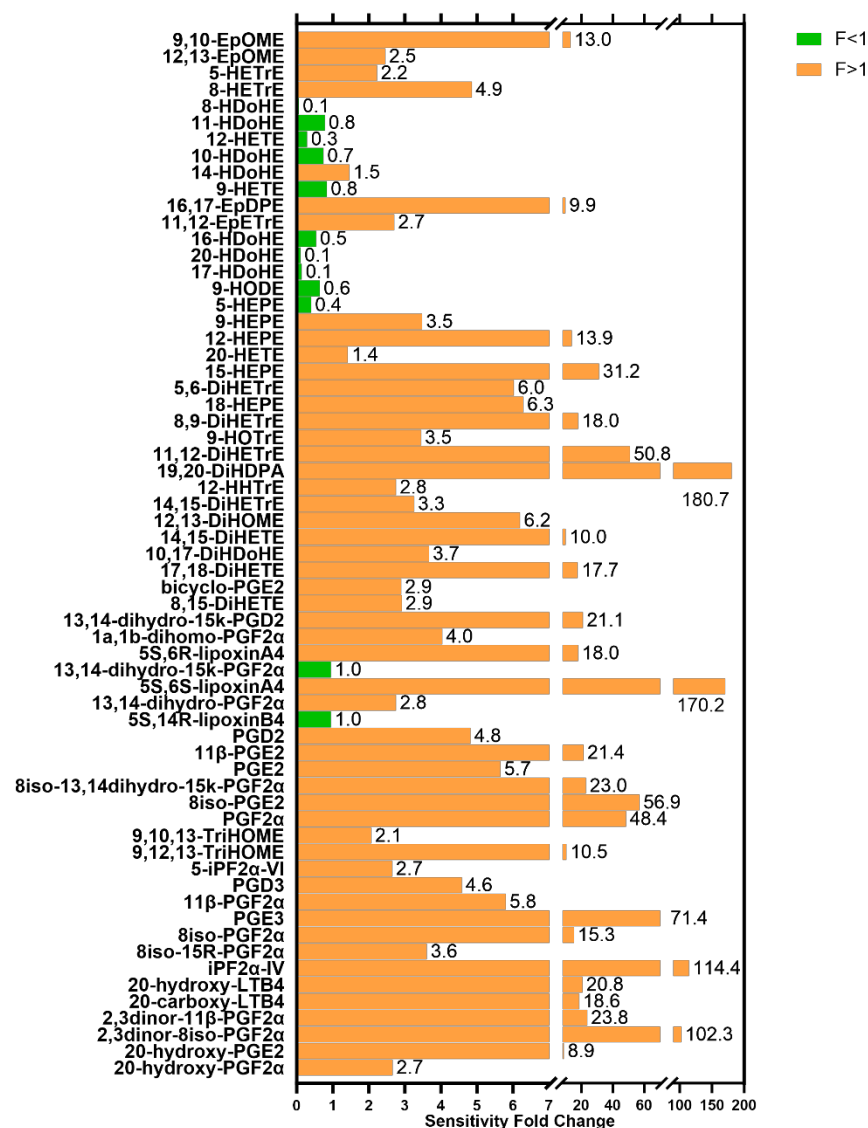


**Figure 4.** Sensitivity fold change (F) calculated by LOD (LOQ) of micro-LC-MS/MS divided by LOD (LOQ) from UHPLC-MS/MS, compounds arranged in elution order from bottom to top.

### 3.3 Method validation

The optimized method outlined in **Section 2.4** was validated with the evaluation of linearity, precision, recovery and matrix effects. To cater to the demands of quantification in 5  $\mu$ L

human plasma, the calibration solutions were diluted to picomolar level near the detection limits.

The linearity of all compounds was established using calibrant solutions, yielding coefficient of determination ( $R^2$ ) values ranging from 0.9930 to 0.9999. Back-calculated concentrations of the calibration standards fell within  $\pm 15\%$  (20% for LOQ) of the nominal values, indicating satisfactory linearity for all analytes. The LOQs were determined to be between 0.3 pM and 306.2 pM, as summarized in **Table 1**.

**Table 1.** Validation parameters: calibration range, LODs, and LOQs.

Compound name	Linearity range (nM)	$R^2$	LOD (pM)	LOQ (pM)
20-hydroxy-PGF2 $\alpha$	0.12 -29.93	0.9976	1.9	6.2
20-hydroxy-PGE2	0.02 -21.3	0.9986	0.3	1.0
2,3dino-8iso-PGF2 $\alpha$	0.07 -37.5	0.9996	0.3	1.1
20-carboxy-LTB4	0.08 -20.63	0.9988	1.3	4.2
2,3dino-11 $\beta$ -PGF2 $\alpha$	0.07 -37.5	0.9989	1.2	4.1
20-hydroxy-LTB4	0.04 -20.85	0.9987	0.8	2.6
iPF2 $\alpha$ -IV	0.07 -37.5	0.9979	0.2	0.8
8iso-15R-PGF2 $\alpha$	0.07 -37.5	0.9994	0.8	2.8
8iso-PGF2 $\alpha$	0.07 -37.5	0.9995	2.1	6.8
11 $\beta$ -PGF2 $\alpha$	0.12 -29.63	0.9989	1.1	3.8
PGF2 $\alpha$	0.04 -37.5	0.9991	0.2	0.8
PGE3	0.04 -37.5	0.9989	0.1	0.3
PGD3	0.04 -37.5	0.9991	0.6	1.8
8iso-PGE2	0.04 -37.5	0.9994	0.1	0.3
PGE2	0.04 -37.5	0.9988	0.9	2.9
11 $\beta$ -PGE2	0.03 -29.78	0.9995	0.3	0.9
PGD2	0.04 -37.5	0.9990	0.4	1.3
5-iPF2 $\alpha$ -VI	0.15 -37.5	0.9989	2.5	8.3
8,12-iPF2 $\alpha$ -VI	1.17 -37.5	0.9991	23.0	76.5
9,12,13-TriHOME	0.12 -30.11	0.9988	6.6	22.0
9,10,13-TriHOME	0.06 -30.11	0.9990	4.6	15.4
8iso-13,14dihydro-15keto-PGF2 $\alpha$	0.15 -37.5	0.9996	1.1	3.6
13,14dihydro-15keto-PGF2 $\alpha$	0.12 -14.81	0.9984	2.5	8.5
13,14dihydro-PGF2 $\alpha$	0.03 -14.74	0.9987	3.5	11.7
13,14dihydro-15keto-PGE2	0.03 -14.89	0.9996	0.3	0.9
13,14dihydro-15keto-PGD2	0.03 -29.78	0.9993	0.3	1.1
5S,6R-lipoxinA4	0.04 -20.85	0.9993	1.0	3.4
5S,6S-lipoxinA4	0.02 -10.43	0.9987	0.1	0.3
1a,1b-dihomo-PGF2 $\alpha$	0.03 -27.45	0.9993	0.6	2.1
bicyclo-PGE2	0.03 -31.43	0.9991	0.9	3.0
8,15-DiHETE	0.33 -20.93	0.9985	6.1	20.5
10,17-DiHDoHE	0.16 -21	0.9984	4.7	15.8
17,18-DiHETE	0.12 -30	0.9991	2.4	8.0
14,15-DiHETE	0.03 -30	0.9989	0.7	2.3
12,13-DiHOME	0.16 -41.4	0.9986	2.3	7.6
14,15-DiHETrE	0.02 -21.08	0.9988	0.9	3.0
12-HHTrE	0.02 -21	0.9989	4.4	14.7
19,20-DiHDPA	0.02 -20.85	0.9987	0.1	0.4
11,12-DiHETrE	0.02 -10.54	0.9991	0.1	0.4
9-HOTrE	0.04 -21.41	0.9982	2.6	8.8

Compound name	Linearity range (nM)	R <sup>2</sup>	LOD (pM)	LOQ (pM)
8,9-DiHETrE	0.02 -21	0.9986	0.5	1.6
18-HEPE	0.09 -11.55	0.9975	3.0	9.9
15-HEPE	0.04 -21.15	0.9983	0.4	1.5
20-HETE	0.08 -21	0.9965	8.8	29.3
5,6-DiHETrE	0.16 -10.54	0.9973	2.2	7.4
12-HEPE	0.17 -21.15	0.9957	0.4	1.5
9-HEPE	0.18 -11.55	0.9948	3.9	12.9
13-HODE	1.33 -42.53	0.9981	59.0	196.6
12,13-EpOME	0.16 -20.55	0.9984	4.3	14.4
5-HEPE	0.17 -10.58	0.9978	5.7	19.1
9-HODE	0.66 -21.26	0.9981	27.7	92.3
9,10-EpOME	0.08 -20.55	0.9984	2.2	7.3
17-HDoHE	1.34 -21.38	0.9936	47.3	157.6
20-HDoHE	1.34 -21.38	0.9832	91.9	306.2
16-HDoHE	0.33 -21	0.9982	3.4	11.5
16,17-EpDPE	0.17 -10.69	0.9967	5.1	16.8
9-HETE	0.48 -30.53	0.9970	8.3	27.8
11,12-EpETrE	0.33 -21	0.9968	0.6	1.8
14-HDoHE	0.04 -5.25	0.9946	7.1	23.6
10-HDoHE	0.33 -21.38	0.9980	12.8	42.6
12-HETE	0.17 -21.38	0.9942	21.9	72.9
11-HDoHE	0.66 -21	0.9944	8.8	29.2
8-HDoHE	0.33 -21.38	0.9964	76.4	254.6
8-HETrE	1.34 -21.38	0.9981	4.4	14.5
5-HETrE	0.18 -22.8	0.9961	4.7	15.6
5S,14R-lipoxinB4	0.18 -22.8	0.9972	11.6	38.6

Intra- and interday precisions varied from 0.5% to 11.7% and from 2.5% to 14.1%, respectively. All values were within the 15% tolerance limit, underscoring the repeatability of the method, as detailed in **Table 2**.

**Table 2.** Intraday and interday precision (RSD%) of oxylipins spiked to plasma

Compounds	Intraday precision (%)			Interday precision (%)		
	Low	Medium	High	Low	Medium	High
d <sub>4</sub> -8iso-PGF2 $\alpha$	11.4	9.6	5.2	5.8	6.0	3.5
d <sub>4</sub> -PGF2 $\alpha$	14.1	3.6	6.3	2.3	4.9	2.8
d <sub>11</sub> -5-iPF2 $\alpha$ -VI	9.6	8.0	6.2	2.9	2.5	5.5
d <sub>11</sub> -8,12-iso-iPF2 $\alpha$ -VI	2.5	4.5	3.5	2.9	4.2	3.6
d <sub>4</sub> -8iso-PGE2	5.8	2.9	3.7	2.0	1.2	1.7
d <sub>4</sub> -PGE2	14.1	3.6	4.6	7.4	4.0	3.4
d <sub>4</sub> -PGD2	7.1	6.5	6.9	1.5	2.1	2.9
d <sub>9</sub> -PGE2	2.5	2.6	5.9	1.0	1.4	0.7
d <sub>4</sub> -LTB4	7.1	5.3	9.0	1.6	1.4	0.7
d <sub>4</sub> -12,13-DiHOME	8.7	6.0	9.0	11.7	2.8	4.3
d <sub>4</sub> -9,10-DiHOME	5.8	6.6	2.6	1.7	1.3	1.8
d <sub>11</sub> -14,15-DiHETrE	4.3	8.7	7.4	0.5	3.3	2.3
d <sub>6</sub> -20-HETE	13.5	6.8	12.1	9.8	10.0	12.5

Matrix effect suggests ion enhancement or suppression during MS ionization due to matrix components. Matrix effects above 100% indicate ion enhancement, suggesting that components in the matrix positively influence the ionization of analytes, leading to higher signal intensities. Conversely, matrix effects below 100% suggest ion suppression, where the matrix components hinder the ionization of analytes, resulting in reduced signal intensities. Deuterated internal standards were employed for the determination of recovery and matrix effect. The recoveries ranged from 64.6% to 99.6%. Matrix effect ranged from 79.2% to 130.3% (**Figure 5**). Particularly, ion enhancement was observed in LTB4-d4. All compounds demonstrated acceptable recovery rates and consistent matrix effects across three concentration levels, affirming the applicability of the sample preparation method for quantitative analysis. The results collectively emphasize the robustness and reliability of the validated method for the sensitive and accurate quantification of oxylipins in volume-limited human plasma.

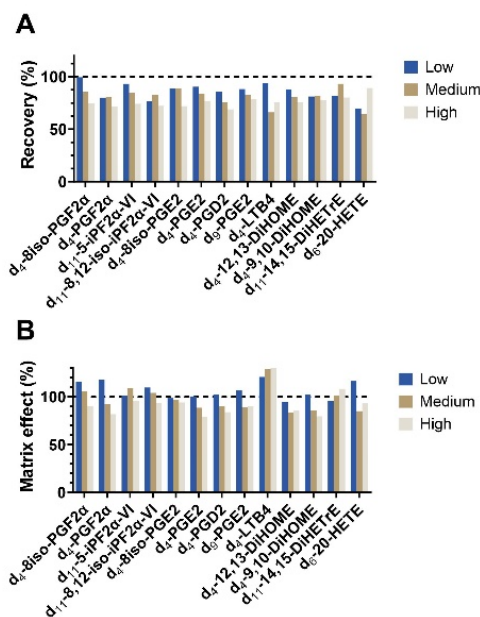


**Figure 5.** Recovery and matrix effect of deuterated internal standards in human plasma. Recovery and matrix effect values are expressed in percentages. (A) Recovery: higher values indicate better recoveries. (B) Matrix effect: values above 100% indicate ion enhancement and below 100% imply ion suppression.

### 3.4 Application in a sample-limited clinical study modeling healthy aging

The validated method was applied to a healthy aging study involving 40 human plasma samples grouped by genders. Three samples were excluded due to technical errors. 4 pooled plasma samples were analyzed along with the study samples as QC samples. Compounds with >80% missing values in study samples or >50% missing values in QCs were also excluded for data reliability. As presented in **Table 3**, a total of 28 oxylipins were successfully quantified in study samples, revealing a broad concentration range spanning from  $51.8 \pm 21.8$  pM (8,9-DiHETrE in male samples) to  $30.9 \pm 8.9$  nM (13-HODE). These findings underscore the applicability of the developed micro-LC-MS/MS method in analyzing oxylipins within volume-limited plasma samples, particularly in the context of studies focused on healthy aging. It is worth noting that the current results serve as a promising indication of the method's suitability for oxylipin studies in volume-limited plasma, given the diverse range of concentrations successfully determined.

**Table 3.** Average concentrations of oxylipins in two groups of study samples (Mean  $\pm$  SD)

Oxylipins	Female (n=18, pM)	Male (n=19, pM)
5-iPF $\alpha$ -VI	152 $\pm$ 73	153 $\pm$ 80
8,12-iso-iPF2 $\alpha$ -VI	4115 $\pm$ 1930	4258 $\pm$ 1920
9,12,13-TriHOME	1241 $\pm$ 737	2297 $\pm$ 1725
9,10,13-TriHOME	230 $\pm$ 184	227 $\pm$ 102
17,18-DiHETE	2014 $\pm$ 896	1922 $\pm$ 765
14,15-DiHETE	267 $\pm$ 121	243 $\pm$ 81
12,13-DiHOME	3373 $\pm$ 1900	3845 $\pm$ 1816
14,15-DiHETrE	148 $\pm$ 49	147 $\pm$ 30
12-HHTrE	71 $\pm$ 20	206 $\pm$ 319
19,20-DiHDPA	468 $\pm$ 182	473 $\pm$ 252
11,12-DiHETrE	124 $\pm$ 41	120 $\pm$ 31
9-HOTrE	1052 $\pm$ 638	850 $\pm$ 407
8,9-DiHETrE	64 $\pm$ 26	52 $\pm$ 22
18-HEPE	135 $\pm$ 63	127 $\pm$ 61
15-HEPE	148 $\pm$ 91	119 $\pm$ 29
20-HETE	306 $\pm$ 154	243 $\pm$ 90
5,6-DiHETrE	196 $\pm$ 80	198 $\pm$ 107
12-HEPE	71 $\pm$ 41	100 $\pm$ 84



Oxylipins	Female (n=18, pM)	Male (n=19, pM)
13-HODE	30852±8892	29356±11859
12,13-EpOME	2239±1534	2011±806
5-HEPE	302±346	317±137
9-HODE	20316±7779	23773±13832
9,10-EpOME	475±314	427±179
20-HDoHE	779±624	543±278
16-HDoHE	191±218	142±61
16,17-EpDPE	341±135	353±169
11,12-EpETrE	170±55	181±73
8-HETrE	181±69	162±65

#### 4. Conclusion

In this study, we developed a micro-LC-MS/MS method tailored for the precise determination of oxylipins in volume-limited human plasma. Requiring only 5 µL plasma, the method achieved LODs ranging from 0.1 pM to 91.9 pM, and LOQs ranging from 0.3 pM to 306.2 pM. The method exhibited good repeatability, with intraday and interday precisions consistently below 14.1%. To assess its sensitivity enhancement, the developed micro-LC-MS/MS method underwent a thorough comparison with a conventional flow UHPLC-MS/MS method. The results demonstrated that our method is not only sensitive but also well-suited for bioanalysis in volume-limited plasma. We subsequently applied the validated method to analyze 40 human plasma samples for oxylipin determination. Although the difference between the two gender groups is not significant among current sample set, the method is robust and could contribute to cohort studies with volume-limited samples. With the wide coverage of concentration levels in different oxylipins and robustness for plasma analysis, our method is instrumental in its ability for future research in oxylipins, especially when confronted with volume-limited samples. To pave the way for its broader utility in clinical and research settings, further development of the method should prioritize expanding the targets to other signaling lipids such as fatty acids, bile acids, etc., and evaluating its performance in extensive sample cohorts under diverse health conditions.

## Declaration of Competing Interest

The authors declare that they have no known competing financial interests or personal relationships that could have appeared to influence the work reported in this paper.

## Acknowledgements

The authors would like to thank Faiza Guled for valuable discussions and technical assistance with the laboratory work. This research was supported by DuSRA-VOILA (Vitality Oriented Innovation for the Lifecourse of the Ageing Society), project number 457001001. The construction and maintenance of the Leiden Longevity Study biomaterial and data has received funding from the European Union's Seventh Framework Programme (FP7/2007-2011; grant agreement number 259679), the Innovation-Oriented Research Program on Genomics (SenterNovem IGE05007), and the Netherlands Consortium for Healthy Ageing (050-060-810). Dr. Amy Harms would like to acknowledge the financial support from The Netherlands X-omics Initiative NWO (project 184.034.019). This study was also supported by the China Scholarship Council (CSC, No. 201906390032 to Bingshu He) and the Vidi grant scheme of the Dutch Research Council (NWO Vidi 723.016.003 to Rawi Ramautar).

## References

- [1] M. Misheva, J. Johnson, J. McCullagh, Role of Oxylipins in the Inflammatory-Related Diseases NAFLD, Obesity, and Type 2 Diabetes, *Metabolites*, 12 (2022) 1238.
- [2] M.A. Nayeem, Role of oxylipins in cardiovascular diseases, *Acta Pharmacologica Sinica*, 39 (2018) 1142-1154.
- [3] Á. Jara-Gutiérrez, V. Baladrón, The Role of Prostaglandins in Different Types of Cancer, *Cells*, 10 (2021) 1487.
- [4] U.N. Das, Essential Fatty Acids and Their Metabolites in the Pathobiology of Inflammation and Its Resolution, *Biomolecules*, 11 (2021) 1873.
- [5] G.L. Milne, Q. Dai, L.J. Roberts, The isoprostanes—25 years later, *Biochimica et Biophysica Acta (BBA) - Molecular and Cell Biology of Lipids*, 1851 (2015) 433-445.
- [6] I. Ferreira, C.S. Maier, S. Kaul, Plasma Oxylipins: A Potential Risk Assessment Tool in Atherosclerotic Coronary Artery Disease, *Frontiers in Cardiovascular Medicine*, 8 (2021).
- [7] D.E. Le, M. García-Jaramillo, G. Bobe, A. Alcazar Magana, A. Vaswani, J. Minnier, D.B. Jump, D. Rinkevich, N.J. Alkayed, C.S. Maier, S. Kaul, Plasma Oxylipins: A Potential Risk Assessment Tool in Atherosclerotic Coronary Artery Disease, *Frontiers in Cardiovascular Medicine*, 8 (2021).
- [8] X. Fu, M. Anderson, Y. Wang, J.C. Zimring, LC-MS/MS-MRM-Based Targeted Metabolomics for Quantitative Analysis of Polyunsaturated Fatty Acids and Oxylipins, in: A. D'Alessandro (Ed.) *High-Throughput Metabolomics: Methods and Protocols*, Springer New York, New York, NY, 2019, pp. 107-120.

- [9] T. Wang, H. Li, Y. Han, Y. Wang, J. Gong, K. Gao, W. Li, H. Zhang, J. Wang, X. Qiu, T. Zhu, A rapid and high-throughput approach to quantify non-esterified oxylipins for epidemiological studies using online SPE-LC-MS/MS, *Analytical and Bioanalytical Chemistry*, 412 (2020) 7989-8001.
- [10] K. Strassburg, A.M.L. Huijbrechts, K.A. Kortekaas, J.H. Lindeman, T.L. Pedersen, A. Dane, R. Berger, A. Brenkman, T. Hankemeier, J. van Duynhoven, E. Kalkhoven, J.W. Newman, R.J. Vreeken, Quantitative profiling of oxylipins through comprehensive LC-MS/MS analysis: application in cardiac surgery, *Analytical and Bioanalytical Chemistry*, 404 (2012) 1413-1426.
- [11] I. Liakh, A. Pakiet, T. Sledzinski, A. Mika, Methods of the Analysis of Oxylipins in Biological Samples, *Molecules*, 25 (2020) 349.
- [12] W. Jung, C.H. Ahn, A micro blood sampling system for catheterized neonates and pediatrics in intensive care unit, *Biomedical Microdevices*, 15 (2013) 241-253.
- [13] J. Kovač, G. Panic, A. Neodo, I. Meister, J.T. Coulibaly, J.D. Schulz, J. Keiser, Evaluation of a novel micro-sampling device, Mitra™, in comparison to dried blood spots, for analysis of praziquantel in *Schistosoma haematobium*-infected children in rural Côte d'Ivoire, *Journal of Pharmaceutical and Biomedical Analysis*, 151 (2018) 339-346.
- [14] N.A. Karp, L. Coleman, P. Cotton, N. Powles-Glover, A. Wilson, Impact of repeated micro and macro blood sampling on clinical chemistry and haematology in rats for toxicokinetic studies, *Regulatory Toxicology and Pharmacology*, 141 (2023) 105386.
- [15] M. Cebo, X. Fu, M. Gawaz, M. Chatterjee, M. Lämmerhofer, Micro-UHPLC-MS/MS method for analysis of oxylipins in plasma and platelets, *Journal of Pharmaceutical and Biomedical Analysis*, 189 (2020) 113426.
- [16] W. Yang, J.C. Schoeman, X. Di, L. Lamont, A.C. Harms, T. Hankemeier, A comprehensive UHPLC-MS/MS method for metabolomics profiling of signaling lipids: Markers of oxidative stress, immunity and inflammation, *Analytica Chimica Acta*, 1297 (2024) 342348.
- [17] R.G.J. Westendorp, D. Van Heemst, M.P. Rozing, M. Frölich, S.P. Mooijaart, G.-J. Blauw, M. Beekman, B.T. Heijmans, A.J.M. De Craen, P.E. Slagboom, f.t.L.L.S. Group, Nonagenarian Siblings and Their Offspring Display Lower Risk of Mortality and Morbidity than Sporadic Nonagenarians: The Leiden Longevity Study, *Journal of the American Geriatrics Society*, 57 (2009) 1634-1637.
- [18] E.E.M. Agency, Guidelines for the validation of analytical methods used in residue depletion studies, in: E.M. Agency (Ed.), 2009.
- [19] B. He, X. Di, F. Guled, A.V.E. Harder, A.M.J.M. van den Maagdenberg, G.M. Terwindt, E.H.J. Krekels, I. Kohler, A. Harms, R. Ramautar, T. Hankemeier, Quantification of endocannabinoids in human cerebrospinal fluid using a novel micro-flow liquid chromatography-mass spectrometry method, *Analytica Chimica Acta*, 1210 (2022) 339888.

## Supporting Information

Supplementary Table 1. Abbreviations and purchasing information of oxylipins and labeled standards

Abbr.	Common Name	Systematic name	Molecular formula	Cayman	CAS	Mass	HMDB
20-hydroxy-PGF2 $\alpha$	20-hydroxy Prostaglandin F2 $\alpha$	9 $\alpha$ ,11 $\alpha$ ,15S,20-etrahydroxy-prosta-5Z,13E-dien-1-oic acid	C <sub>20</sub> H <sub>34</sub> O <sub>6</sub>	16950	57930-92-4	370.2355	HMDB0004049
20-hydroxy-PGE2	20-Hydroxy-PGE2	9-oxo-11 $\alpha$ ,15S,20-trihydroxy-prosta-5Z,13E-dien-1-oic acid	C <sub>20</sub> H <sub>32</sub> O <sub>6</sub>	14950	57930-95-7	368.2199	HMDB0003247
2,3-dinor-8-iso-PGF2 $\alpha$	2,3-dinor-8-iso Prostaglandin F2 $\alpha$	9 $\alpha$ ,11 $\alpha$ ,15S-trihydroxy-2,3-dinor-(8 $\beta$ )-prosta-5Z,13E-dien-1-oic acid	C <sub>18</sub> H <sub>30</sub> O <sub>5</sub>	16290	221664-05-7	326.4000	NA
20-carboxy-LTB4	20-Carboxy-leukotriene B4	5S,12R-dihydroxy-6Z,8E,10E,14Z-icosatetraene-1,20-dioic acid	C <sub>20</sub> H <sub>30</sub> O <sub>6</sub>	20180	80434-82-8	366.2042	HMDB0006059
2,3-dinor-11 $\beta$ -PGF2 $\alpha$	2,3-dinor-11 $\beta$ -Prostaglandin F2 $\alpha$	9 $\alpha$ ,11 $\beta$ ,15S-trihydroxy-2,3-dinor-prosta-5Z,13E-dien-1-oic acid	C <sub>18</sub> H <sub>30</sub> O <sub>5</sub>	16530	240405-20-3	326.4000	NA
20-hydroxy-LTB4	20-Hydroxy-leukotriene B4	5S,12R,20-trihydroxy-6Z,8E,10E,14Z-icosatetraenoic acid	C <sub>20</sub> H <sub>32</sub> O <sub>5</sub>	20190	79516-82-8	352.2249	HMDB0001509
iPF2 $\alpha$ -IV	iPF2 $\alpha$ pha-IV	(8S)-10-[(1R,2S,3S,5R)-3,5-Dihydroxy-2-pentylcyclopentyl]-8-hydroxydeca-5,9-dienoic acid	C <sub>29</sub> H <sub>50</sub> O <sub>5</sub>	16395	331962-00-6	354.2000	NA
8-iso-15-R-PGF2 $\alpha$	8-iso-15(R)-Prostaglandin F2 $\alpha$	9 $\alpha$ ,11 $\alpha$ ,15R-trihydroxy-(8 $\beta$ )-prosta-5Z,13E-dien-1-oic acid	C <sub>20</sub> H <sub>34</sub> O <sub>5</sub>	16350	214748-65-9	354.2406	NA
8-iso-PGF2 $\alpha$	8-iso-15(S)-Prostaglandin F2 $\alpha$	9 $\alpha$ ,11 $\alpha$ ,15S-trihydroxy-(8 $\beta$ )-prosta-5Z,13E-dien-1-oic acid	C <sub>20</sub> H <sub>34</sub> O <sub>5</sub>	16350	27415-26-5	354.2406	HMDB0005083
11 $\beta$ -PGF2 $\alpha$	11 $\beta$ -Prostaglandin F2 $\alpha$	9 $\alpha$ ,11 $\beta$ ,15S-trihydroxy-prosta-5Z,13E-dien-1-oic acid	C <sub>20</sub> H <sub>34</sub> O <sub>5</sub>	16520	38432-87-0	354.2406	NA
PGF2 $\alpha$	Prostaglandin F2 $\alpha$	9 $\alpha$ ,11 $\alpha$ ,15S-trihydroxy-prosta-5Z,13E-dien-1-oic acid	C <sub>20</sub> H <sub>34</sub> O <sub>5</sub>	16010	551-11-1	354.2406	HMDB0001139
PGE3	Prostaglandin E3	9-oxo-11 $\alpha$ ,15S-dihydroxy-prosta-5Z,13E,17Z-trien-1-oic acid	C <sub>20</sub> H <sub>30</sub> O <sub>5</sub>	14990	802-31-3	350.2093	HMDB0002664
PGD3	Prostaglandin D3	9 $\alpha$ ,15S-dihydroxy-11-oxo-prosta-5Z,13E,17Z-trien-1-oic acid	C <sub>20</sub> H <sub>30</sub> O <sub>5</sub>	12990	71902-47-1	350.2093	HMDB0003034
8-iso-PGE2	8-iso Prostaglandin E2	9-oxo-11 $\alpha$ ,15S-dihydroxy-(8 $\beta$ )-prosta-5Z,13E-dien-1-oic acid	C <sub>20</sub> H <sub>32</sub> O <sub>5</sub>	14350	27415-25-4	352.2250	HMDB0005844
PGE2	Prostaglandin E2	9-oxo-11 $\alpha$ ,15S-dihydroxy-prosta-5Z,13E-dien-1-oic acid	C <sub>20</sub> H <sub>32</sub> O <sub>5</sub>	14010	363-24-6	352.2250	HMDB0001220
11 $\beta$ -PGE2	11 $\beta$ -Prostaglandin E2	9-oxo-11 $\beta$ ,15S-dihydroxy-prosta-5Z,13E-dien-1-oic acid	C <sub>20</sub> H <sub>32</sub> O <sub>5</sub>	14510	38310-90-6	352.2250	HMDB0006041
PGD2	Prostaglandin D2	9 $\alpha$ ,15S-dihydroxy-11-oxo-prosta-5Z,13E-dien-1-oic acid	C <sub>20</sub> H <sub>32</sub> O <sub>5</sub>	12010	41598-07-6	352.2250	HMDB0001403

Abbr.	Common Name	Systematic name	Molecular formula	Cayman	CAS	Mass	HMDB
5- $\alpha$ PF2 $\alpha$ VI	( $\pm$ )-5- $\alpha$ PF2 $\alpha$ -VI	(8 $\beta$ )-5,9 $\alpha$ ,11 $\alpha$ -trihydroxy-prosta-6E,14Z-dien-1-oic acid	C <sub>20</sub> H <sub>34</sub> O <sub>5</sub>	16300	179094-11-2	354.2406	NA
8,12- $\alpha$ PF2 $\alpha$ VI	8,12-iso- $\alpha$ PF2 $\alpha$ -VI-1,5-lactone	6-(E)-2-(1R,2S,3R,5S)-3,5-dihydroxy-2-((Z)-oct-2-enyl) cyclopentyl tetrahydro-2H-pyran-2-one	C <sub>28</sub> H <sub>42</sub> O <sub>4</sub>	10312		336.5000	NA
9,12,13-TriHOME	9(S),12(S),13(S)-TriHOME	9S,12S,13S-trihydroxy-11E-octadecenoic acid	C <sub>18</sub> H <sub>34</sub> O <sub>5</sub>	10005143	97134-11-7	330.2406	HMDB0004708
9,10,13-TriHOME	9(S),10(S),13(S)-TriHOME	9S,10S,13S-trihydroxy-11E-octadecenoic acid	C <sub>18</sub> H <sub>34</sub> O <sub>5</sub>	26768	135214-44-7	330.2406	
8-iso-13,14-dihydro-15-keto-PGF2 $\alpha$	8-iso-13,14-dihydro-15-keto Prostaglandin F2 $\alpha$	9 $\alpha$ ,11 $\alpha$ -dihydroxy-15-oxo-(8 $\beta$ )-prost-5Z-en-1-oic acid	C <sub>20</sub> H <sub>34</sub> O <sub>5</sub>	16380	191919-02-5	354.2406	HMDB0006562
13,14-dihydro-15-keto-PGF2 $\alpha$	13,14-dihydro-15-keto Prostaglandin F2 $\alpha$	9 $\alpha$ ,11 $\alpha$ -dihydroxy-15-oxo-prost-5Z-en-1-oic acid	C <sub>20</sub> H <sub>34</sub> O <sub>5</sub>	16670	27376-76-7	354.2406	HMDB0004685
13,14-dihydro-PGF2 $\alpha$	13,14-dihydro Prostaglandin F2 $\alpha$	9 $\alpha$ ,11 $\alpha$ ,15S-trihydroxy-prost-5Z-en-1-oic acid	C <sub>20</sub> H <sub>34</sub> O <sub>5</sub>	16660	27376-74-5	356.2563	HMDB0004239
13,14-dihydro-15-keto-PGE2	13,14-dihydro-15-keto Prostaglandin E2	9,15-dioxo-11 $\alpha$ -hydroxy-prost-5Z-en-1-oic acid	C <sub>20</sub> H <sub>32</sub> O <sub>5</sub>	14650	363-23-5	352.2250	HMDB0002776
13,14-dihydro-15-keto-PGD2	13,14-dihydro-15-keto Prostaglandin D2	9 $\alpha$ -hydroxy-11,15-dioxo-prost-5Z-en-1-oic acid	C <sub>20</sub> H <sub>32</sub> O <sub>5</sub>	12610	59894-07-4	352.2250	HMDB0000042
5S,6R-lipoxinA4	Lipoxin A4	5S,6R,15S-trihydroxy-7E,9E,11Z,13E-eicosatetraenoic acid	C <sub>20</sub> H <sub>32</sub> O <sub>5</sub>	90410	89663-86-5	352.2250	HMDB0004385
5S,6S-lipoxinA4	6(S)-Lipoxin A4	5S,6S,15S-trihydroxy-7E,9E,11Z,13E-eicosatetraenoic acid	C <sub>20</sub> H <sub>32</sub> O <sub>5</sub>	10049	94292-80-5	352.2250	NA
1 $\alpha$ ,1 $\beta$ -dihomo-PGF2 $\alpha$	1 $\alpha$ ,1 $\beta$ -dihomo Prostaglandin F2 $\alpha$	9 $\alpha$ ,11 $\alpha$ ,15S-trihydroxy-1 $\alpha$ ,1 $\beta$ -dihomo-prosta-5Z,13E-dien-1-oic acid	C <sub>22</sub> H <sub>38</sub> O <sub>5</sub>	16050	57944-39-5	382.2719	NA
bicyclo-PGE2	Bicyclo Prostaglandin E2	11-deoxy-13,14-dihydro-15-keto-11 $\beta$ ,16 $\alpha$ ,1-cycloprostaglandin E2	C <sub>20</sub> H <sub>30</sub> O <sub>4</sub>	14530	74158-09-1	334.2144	HMDB0000054
8,15-DIHETE	8(S),15(S)-DIHETE	8S,15S-dihydroxy-5Z,9E,11Z,13E-eicosatetraenoic acid	C <sub>20</sub> H <sub>32</sub> O <sub>4</sub>	35370	80234-65-7	336.5000	NA
10,17-DiHDoHE	10(S),17(S)-DIHDHA	10(S),17(S)-dihydroxy-4Z,7Z,11E,13Z,15E,19Z-docosahexaenoic acid	C <sub>22</sub> H <sub>32</sub> O <sub>4</sub>	10008128	871826-47-0	360.2301	NA
17,18-DIHETE	( $\pm$ )-17(18)-DIHETE	( $\pm$ )-17,18-dihydroxy-5Z,8Z,11Z,14Z-eicosatetraenoic acid	C <sub>20</sub> H <sub>32</sub> O <sub>4</sub>	10006999		336.2301	HMDB0010211
14,15-DIHETE	( $\pm$ )-14(15)-DIHETE	( $\pm$ )-14,15-dihydroxy-5Z,8Z,11Z,17Z-eicosatetraenoic acid	C <sub>20</sub> H <sub>32</sub> O <sub>4</sub>	10006998		336.2301	HMDB0010204
12,13-DiHOME	( $\pm$ )-12(13)-DiHOME	( $\pm$ )-12,13-dihydroxy-9Z-octadecenoic acid	C <sub>18</sub> H <sub>34</sub> O <sub>4</sub>	10009832	263399-35-5	314.2457	HMDB0004705
14,15-DiHETE	( $\pm$ )-14(15)-DIHET	( $\pm$ )-14,15-dihydroxy-5Z,8Z,11Z-eicosatetraenoic acid	C <sub>22</sub> H <sub>34</sub> O <sub>4</sub>	51651	77667-09-5	338.2457	HMDB0002265

Abbr.	Common Name	Systematic name	Molecular formula	Ca <sub>m</sub> n	CAS	Mass	HMDB
12-HHTe	12(S)-HHTe	12S-hydroxy-5Z,8E,10E-heptadecatrienoic acid	C <sub>17</sub> H <sub>32</sub> O <sub>3</sub>	34590	54397-84-1	280.2038	HMDB001 2535
19,20-DHDPa	(±)19(20)-DHDPa	(±)19,20-dihydroxy-4Z,7Z,10Z,13Z,16Z-docosapentaenoic acid	C <sub>22</sub> H <sub>38</sub> O <sub>4</sub>	1000700		362.2457	HMDB001 0214
11,12-DHETe	(±)11(12)-DHETe	(±)11,12-dihydroxy-5Z,8Z,14Z-eicosatrienoic acid	C <sub>20</sub> H <sub>34</sub> O <sub>4</sub>	51511	192461-95-3	338.2457	HMDB000 2314
9-HOTe	9(S)-HOTe	9S-hydroxy-10E,12Z,15Z-octadecatrienoic acid	C <sub>18</sub> H <sub>32</sub> O <sub>3</sub>	39420	89886-42-0	294.2195	HMDB003 1934
8,9-DHETe	(±)8(9)-DHETe	(±)8,9-dihydroxy-5Z,11Z,14Z-eicosatrienoic acid	C <sub>20</sub> H <sub>34</sub> O <sub>4</sub>	51351	192461-96-4	338.2457	HMDB000 2311
18-HEPe	(±)18-HEPe	(±)18-hydroxy-5Z,8Z,11Z,14Z,16E-eicosapentaenoic acid	C <sub>20</sub> H <sub>36</sub> O <sub>3</sub>	32840	141110-17-0	318.2195	HMDB001 2611(R)
15-HEPe	(±)15-HEPe	(±)15-hydroxy-5Z,8Z,11Z,13E,17Z-eicosapentaenoic acid	C <sub>20</sub> H <sub>36</sub> O <sub>3</sub>	32700	88852-33-9	318.2195	HMDB001 0209
20-HETe	(±)20-HETe	20-hydroxy-5Z,8Z,11Z,14Z-eicosatetraenoic acid	C <sub>20</sub> H <sub>34</sub> O <sub>3</sub>	90030	79551-86-3	320.2351	HMDB000 5998
5,6-DHETe	(±)5(6)-DHETe	(±)5,6-dihydroxy-8Z,11Z,14Z-eicosatrienoic acid	C <sub>20</sub> H <sub>34</sub> O <sub>4</sub>	51211	213382-49-1	338.2457	HMDB000 2343
12-HEPe	(±)12-HEPe	(±)12-hydroxy-5Z,8Z,10E,14Z,17Z-eicosapentaenoic acid	C <sub>20</sub> H <sub>36</sub> O <sub>3</sub>	32540	81187-21-5	318.2195	HMDB102 02
9-HEPe	(±)9-HEPe	(±)9-hydroxy-5Z,7E,11Z,14Z,17Z-eicosapentaenoic acid	C <sub>20</sub> H <sub>36</sub> O <sub>3</sub>	32400	286390-03-2	318.2195	HMDB006 0053
13-HODE	(±)13-HODE	(±)13-hydroxy-9Z,11E-octadecadienoic acid	C <sub>18</sub> H <sub>32</sub> O <sub>3</sub>	38600	18104-45-5	296.2351	HMDB011 2194
12,13-EpOME	(±)12(13)-EpOME	(±)12(13)epoxy-9Z-octadecenoic acid	C <sub>18</sub> H <sub>32</sub> O <sub>3</sub>	52450		296.2351	HMDB000 4702
5-HEPe	(±)5-HEPe	(±)5-hydroxy-6E,8Z,11Z,14Z,17Z-eicosapentaenoic acid	C <sub>20</sub> H <sub>36</sub> O <sub>3</sub>	32200	83952-40-3	318.2195	HMDB000 5081
9-HODE	(±)9-HODE	(±)9-hydroxy-10E,12Z-octadecadienoic acid	C <sub>18</sub> H <sub>32</sub> O <sub>3</sub>	38400	98524-19-7	296.2351	HMDB001 0223
9,10-EpOME	(±)9(10)-EpOME	(±)9,10-epoxy-12Z-octadecenoic acid	C <sub>18</sub> H <sub>32</sub> O <sub>3</sub>	52400		296.2351	HMDB000 4701
17-HDoHE	(+/-)17-HDoHE	(±)17-hydroxy-4Z,7Z,10Z,13Z,15E,19Z-docosahexaenoic acid	C <sub>22</sub> H <sub>38</sub> O <sub>3</sub>	33650	90780-52-2	344.2351	HMDB001 0213
20-HDoHE	(+/-)20-HDoHE	(±)20-hydroxy-4Z,7Z,10Z,13Z,16Z,18E-docosahexaenoic acid	C <sub>22</sub> H <sub>38</sub> O <sub>3</sub>	33750	90906-41-5	344.2351	HMDB006 0048
16-HDoHE	(+/-)16-HDoHE	(±)16-hydroxy-4Z,7Z,10Z,13Z,17E,19Z-docosahexaenoic acid	C <sub>22</sub> H <sub>38</sub> O <sub>3</sub>	33600	90780-51-1	344.2351	HMDB006 0047

Abbr.	Common Name	Systematic name	Molecular formula	Ca <sub>yma</sub> n	CAS	Mass	HMDB
16,17-EpDPE	(±)16(17)-EpDPA	(±)16,17-epoxy-4Z,7Z,10Z,13Z,19Z-docosapentaenoic acid	C <sub>22</sub> H <sub>32</sub> O <sub>3</sub>	10174	155073-46-4	344.2351	HMDB00013621
9-HETE	(±)9-HETE	(±)9-hydroxy-5Z,7E,11Z,14Z-eicosatetraenoic acid	C <sub>20</sub> H <sub>32</sub> O <sub>3</sub>	34400	79495-85-5	320.2351	HMDB00010222
11,12-EpETe	(±)11,12-EpETe	(±)11,(12)-epoxy-5Z,8Z,14Z-eicosatrienoic acid	C <sub>20</sub> H <sub>32</sub> O <sub>3</sub>	50511	123931-40-8	320.2351	HMDB0004673
14-HDoHE	(+/-)14-HDoHE	(±)14-hydroxy-4Z,7Z,10Z,12E,16Z,19Z-docosahexaenoic acid	C <sub>22</sub> H <sub>32</sub> O <sub>3</sub>	33550	87042-40-8	344.2351	HMDB00060044
10-HDoHE	(+/-)10-HDoHE	(±)10-hydroxy-4Z,7Z,11E,13Z,16Z,19Z-docosahexaenoic acid	C <sub>22</sub> H <sub>32</sub> O <sub>3</sub>	33400	90780-50-0	344.2351	HMDB00060037
12-HETE	(±)12-HETE	(±)12-hydroxy-5Z,8Z,10E,14Z-eicosatetraenoic acid	C <sub>20</sub> H <sub>32</sub> O <sub>3</sub>	34550	71030-37-0	320.2351	HMDB0006111
11-HDoHE	(+/-)11-HDoHE	(±)11-hydroxy-4Z,7Z,9E,13Z,16Z,19Z-docosahexaenoic acid	C <sub>22</sub> H <sub>32</sub> O <sub>3</sub>			344.2351	HMDB00060040
8-HDoHE	(+/-)8-HDoHE	(±)8-hydroxy-4Z,6E,10Z,13Z,16Z,19Z-docosahexaenoic acid	C <sub>22</sub> H <sub>32</sub> O <sub>3</sub>	33350	90780-54-4	344.2351	HMDB00060051
8-HETE	8(S)-HETE	8S-hydroxy-9E,11Z,14Z-eicosatrienoic acid	C <sub>20</sub> H <sub>32</sub> O <sub>3</sub>	36360	889573-69-7	322.2508	NA
5-HETE	5(S)-HETE	5S-hydroxy-6E,8Z,11Z-eicosatrienoic acid	C <sub>20</sub> H <sub>32</sub> O <sub>3</sub>	36230	195061-94-0	322.2508	NA
5S-14R-lipoxin B4	Lipoxin B4	5S,14R,15S-trihydroxy-6E,8Z,10E,12E-eicosatetraenoic acid	C <sub>20</sub> H <sub>32</sub> O <sub>3</sub>	90420	98049-69-5	352.2250	HMDB0005082
d-8-iso-PGF2α	8-iso Prostaglandin F2α-d <sub>4</sub>	9α,11α,15S-trihydroxy-(8β)-prosta-5Z,13E-dien-1-oi-c-3,3,4,4-d4 acid	C <sub>20</sub> H <sub>30</sub> D <sub>4</sub> O <sub>3</sub>	316350	211105-40-7	358.48	
d-α-PGF2α	Prostaglandin F2α-d <sub>4</sub>	9α,11α,15S-trihydroxy-prosta-5Z,13E-dien-1-oi-c-3,3,4,4-d4 acid	C <sub>20</sub> H <sub>30</sub> D <sub>4</sub> O <sub>3</sub>	316010	34210-11-2	358.48	
d <sub>11</sub> -5-IPF2α-VI	(±)5-IPF2α-VI-d <sub>11</sub>	(±)5,9α,11α-trihydroxy-(8β)-prosta-6E,14Z-dien-1-oi-c-16,16,17,17,18,18,19,19,20,20,20-d11 acid	C <sub>20</sub> H <sub>32</sub> D <sub>11</sub> O <sub>3</sub>	10006654	936565-17-2	365.57	
d <sub>11</sub> -8,12-iso-IPF2α-VI	8,12-iso-IPF2α-VI-d <sub>11</sub>	(12α)-5,9α,11α-trihydroxy-prosta-6E,14Z-dien-1-oi-c-16,16,17,17,18,18,19,19,20,20,20-d11 acid	C <sub>20</sub> H <sub>32</sub> D <sub>11</sub> O <sub>3</sub>	10006878	1616977-85-5	365.6	
d-8-iso-PGE2	8-iso Prostaglandin E2-d <sub>4</sub>	9-oxo-11α,15S-dihydroxy-(8β)-prosta-5Z,13E-dien-1-oi-c-3,3,4,4-d4 acid	C <sub>20</sub> H <sub>32</sub> D <sub>4</sub> O <sub>3</sub>	10011321	34210-10-1	356.5	
d-α-PGE2	Prostaglandin E2-d <sub>4</sub>	9-oxo-11α,15S-dihydroxy-prosta-5Z,13E-dien-1-oi-c-3,3,4,4-d4 acid	C <sub>20</sub> H <sub>32</sub> D <sub>4</sub> O <sub>3</sub>	314010	1356347-42-6	361.5	
d-α-PGD2	Prostaglandin D2-d <sub>4</sub>	9α,15S-dihydroxy-11-oxo-prosta-5Z,13E-dien-1-oi-c-3,3,4,4-d4 acid	C <sub>20</sub> H <sub>32</sub> D <sub>4</sub> O <sub>3</sub>	312010	211105-29-2	356.5	
d-α-PGE2	Prostaglandin E2-d <sub>6</sub>	9-oxo-11α,15S-dihydroxy-prosta-5Z,13E-dien-1-oi-c-17,17,18,18,19,19,20,20,20-d9 acid	C <sub>20</sub> H <sub>32</sub> D <sub>6</sub> O <sub>3</sub>	10581	1356347-42-6	361.5	

Abbr.	Common Name	Systematic name	Molecular formula	Cayman	CAS	Mass	HMDB
d <sub>4</sub> -L-TB4	Leukotriene B <sub>4</sub> -d <sub>4</sub>	5S,12R-dihydroxy-6Z,8E,10E,14Z- <i>eicosatetraenoic-6,7,14,15-d4 acid</i>	C <sub>20</sub> H <sub>32</sub> D <sub>4</sub> O <sub>4</sub>	320110	124629-74-9	340.5	
d <sub>4</sub> -12,13-DHOMIE	(±)12(13)-DHOMIE-d <sub>4</sub>	(±)12,13-dihydroxy-9Z-octadecenoic-9,10,12,13-d4 acid	C <sub>18</sub> H <sub>30</sub> D <sub>4</sub> O <sub>4</sub>	1000999		318.5	
d <sub>4</sub> -9,10-DHOMIE	(±)9(10)-DHOMIE-d <sub>4</sub>	(±)9,10-dihydroxy-12Z-octadecenoic-9,10,12,13-d4 acid	C <sub>18</sub> H <sub>30</sub> D <sub>4</sub> O <sub>4</sub>	1000999		318.5	
d <sub>11</sub> -14,15-DHETTE	(±)14(15)-DHETT-d <sub>11</sub>	(±)14,15-dihydroxy-5Z,8Z,11Z- <i>eicosatrienoic-16,16,17,17,18,18,19,20,20,20-d11 acid</i>	C <sub>20</sub> H <sub>32</sub> D <sub>11</sub> O <sub>4</sub>	1000804		349.6	
d <sub>6</sub> -20-HETE	20-HETE-d <sub>6</sub>	20-hydroxy-5Z,8Z,11Z,14Z- <i>eicosatetraenoic-16,16,17,17,18,18-d6 acid</i>	C <sub>20</sub> H <sub>32</sub> D <sub>6</sub> O <sub>3</sub>	390030	2548939-89-3	326.5	



Supplementary Table 2. Calibrant concentrations of oxylipins

Calibration concentrations (pM)	C11	C10	C9	C8	C7	C6	C5	C4	C3	C2	C1
20-hydroxy-PGF2 $\alpha$	29925.0	14962.5	7481.3	3740.6	1870.3	935.2	467.6	233.8	116.9	58.4	29.2
20-hydroxy-PGE2	21300.0	10650.0	5325.0	2662.5	1331.3	665.6	332.8	166.4	83.2	41.6	20.8
2,3-dimor-8iso-PGF2 $\alpha$	37500.0	18750.0	9375.0	4687.5	2343.8	1171.9	585.9	293.0	146.5	73.2	36.6
20-carboxy-LTB4	20625.0	10312.5	5156.3	2578.1	1289.1	644.5	322.3	161.1	80.6	40.3	20.1
2,3-dimor-1 $\beta$ -PGF2 $\alpha$	37500.0	18750.0	9375.0	4687.5	2343.8	1171.9	585.9	293.0	146.5	73.2	36.6
20-hydroxy-LTB4	20850.0	10425.0	5212.5	2606.3	1303.1	651.6	325.8	162.9	81.4	40.7	20.4
iPF2 $\alpha$ -IV	37500.0	18750.0	9375.0	4687.5	2343.8	1171.9	585.9	293.0	146.5	73.2	36.6
8iso-13R-PGF2 $\alpha$	37500.0	18750.0	9375.0	4687.5	2343.8	1171.9	585.9	293.0	146.5	73.2	36.6
8iso-PGF2 $\alpha$	37500.0	18750.0	9375.0	4687.5	2343.8	1171.9	585.9	293.0	146.5	73.2	36.6
1 $\beta$ -PGF2 $\alpha$	29625.0	14812.5	7406.3	3703.1	1851.6	925.8	462.9	231.4	115.7	57.9	28.9
PGF2 $\alpha$	37500.0	18750.0	9375.0	4687.5	2343.8	1171.9	585.9	293.0	146.5	73.2	36.6
PGE3	37500.0	18750.0	9375.0	4687.5	2343.8	1171.9	585.9	293.0	146.5	73.2	36.6
PGD3	37500.0	18750.0	9375.0	4687.5	2343.8	1171.9	585.9	293.0	146.5	73.2	36.6
8iso-PGE2	37500.0	18750.0	9375.0	4687.5	2343.8	1171.9	585.9	293.0	146.5	73.2	36.6
PGE2	37500.0	18750.0	9375.0	4687.5	2343.8	1171.9	585.9	293.0	146.5	73.2	36.6
1 $\beta$ -PGE2	29775.0	14887.5	7443.8	3721.9	1860.9	930.5	465.2	232.6	116.3	58.2	29.1
PGD2	37500.0	18750.0	9375.0	4687.5	2343.8	1171.9	585.9	293.0	146.5	73.2	36.6
5-iPF2 $\alpha$ -VI	37500.0	18750.0	9375.0	4687.5	2343.8	1171.9	585.9	293.0	146.5	73.2	36.6
8,12-iPF2 $\alpha$ -VI	37500.0	18750.0	9375.0	4687.5	2343.8	1171.9	585.9	293.0	146.5	73.2	36.6
9,12,13-TriHOME	60225.0	30112.5	15056.3	7528.1	3764.1	1882.0	941.0	470.5	235.3	117.6	58.8
9,10,13-TriHOME	60375.0	30187.5	15093.8	7546.9	3773.4	1886.7	943.4	471.7	235.8	117.9	59.0
8iso-13,14dihydro-15keto-PGF2 $\alpha$	37500.0	18750.0	9375.0	4687.5	2343.8	1171.9	585.9	293.0	146.5	73.2	36.6
13,14dihydro-15keto-PGF2 $\alpha$	29625.0	14812.5	7406.3	3703.1	1851.6	925.8	462.9	231.4	115.7	57.9	28.9
13,14dihydro-PGF2 $\alpha$	29475.0	14737.5	7368.8	3684.4	1842.2	921.1	460.5	230.3	115.1	57.6	28.8
13,14dihydro-15keto-PGE2	29775.0	14887.5	7443.8	3721.9	1860.9	930.5	465.2	232.6	116.3	58.2	29.1
13,14dihydro-15keto-PGD2	29775.0	14887.5	7443.8	3721.9	1860.9	930.5	465.2	232.6	116.3	58.2	29.1

Calibration concentrations (pM)	C11	C10	C9	C8	C7	C6	C5	C4	C3	C2	C1
5S,6R-lipoxinA4	20850.0	10425.0	5212.5	2606.3	1303.1	651.6	325.8	162.9	81.4	40.7	20.4
5S,6S-lipoxinA4	20850.0	10425.0	5212.5	2606.3	1303.1	651.6	325.8	162.9	81.4	40.7	20.4
1a,1b-dihomo-PGF2 $\alpha$	27450.0	13725.0	6862.5	3431.3	1715.6	857.8	428.9	214.5	107.2	53.6	26.8
bicyclo-PGE2	31425.0	15712.5	7856.3	3928.1	1964.1	982.0	491.0	245.5	122.8	61.4	30.7
8,15-DHETE	20925.0	10462.5	5231.3	2615.6	1307.8	653.9	327.0	163.5	81.7	40.9	20.4
10,17-DHDoHE	21000.0	10500.0	5250.0	2625.0	1312.5	656.3	328.1	164.1	82.0	41.0	20.5
17,18-DHETE	30000.0	15000.0	7500.0	3750.0	1875.0	937.5	468.8	234.4	117.2	58.6	29.3
14,15-DHETE	30000.0	15000.0	7500.0	3750.0	1875.0	937.5	468.8	234.4	117.2	58.6	29.3
12,13-DHOME	41400.0	20700.0	10350.0	5175.0	2587.5	1293.8	646.9	323.4	161.7	80.9	40.4
14,15-DHETe	21075.0	10537.5	5268.8	2634.4	1317.2	658.6	329.3	164.6	82.3	41.2	20.6
12-HHTe	21000.0	10500.0	5250.0	2625.0	1312.5	656.3	328.1	164.1	82.0	41.0	20.5
19,20-DHHPA	20850.0	10425.0	5212.5	2606.3	1303.1	651.6	325.8	162.9	81.4	40.7	20.4
11,12-DHETe	21075.0	10537.5	5268.8	2634.4	1317.2	658.6	329.3	164.6	82.3	41.2	20.6
9-HOTe	42825.0	21412.5	10706.3	5353.1	2676.6	1338.3	669.1	334.6	167.3	83.6	41.8
8,9-DHETe	21000.0	10500.0	5250.0	2625.0	1312.5	656.3	328.1	164.1	82.0	41.0	20.5
18-HEPE	23100.0	11550.0	5775.0	2887.5	1443.8	721.9	360.9	180.5	90.2	45.1	22.6
15-HEPE	21150.0	10575.0	5287.5	2643.8	1321.9	660.9	330.5	165.2	82.6	41.3	20.7
20-HEPE	21000.0	10500.0	5250.0	2625.0	1312.5	656.3	328.1	164.1	82.0	41.0	20.5
5,6-DHETe	21075.0	10537.5	5268.8	2634.4	1317.2	658.6	329.3	164.6	82.3	41.2	20.6
12-HEPE	21150.0	10575.0	5287.5	2643.8	1321.9	660.9	330.5	165.2	82.6	41.3	20.7
9-HEPE	23100.0	11550.0	5775.0	2887.5	1443.8	721.9	360.9	180.5	90.2	45.1	22.6
13-HODE	42525.0	21262.5	10631.3	5315.6	2657.8	1328.9	664.5	332.2	166.1	83.1	41.5
12,13-EpOME	41100.0	20550.0	10275.0	5137.5	2568.8	1284.4	642.2	321.1	160.5	80.3	40.1
5-HEPE	21150.0	10575.0	5287.5	2643.8	1321.9	660.9	330.5	165.2	82.6	41.3	20.7
9-HODE	42525.0	21262.5	10631.3	5315.6	2657.8	1328.9	664.5	332.2	166.1	83.1	41.5
9,10-EpOME	41100.0	20550.0	10275.0	5137.5	2568.8	1284.4	642.2	321.1	160.5	80.3	40.1

Calibration concentrations (pM)	C11	C10	C9	C8	C7	C6	C5	C4	C3	C2	C1
17-HDoHE	21375.0	10687.5	5343.8	2671.9	1335.9	668.0	334.0	167.0	83.5	41.7	20.9
20-HDoHE	21375.0	10687.5	5343.8	2671.9	1335.9	668.0	334.0	167.0	83.5	41.7	20.9
16-HDoHE	21375.0	10687.5	5343.8	2671.9	1335.9	668.0	334.0	167.0	83.5	41.7	20.9
16,17-EpDPE	30525.0	15262.5	7631.3	3815.6	1907.8	953.9	477.0	238.5	119.2	59.6	29.8
9-HETE	21000.0	10500.0	5250.0	2625.0	1312.5	656.3	328.1	164.1	82.0	41.0	20.5
11,12-EpETE	21000.0	10500.0	5250.0	2625.0	1312.5	656.3	328.1	164.1	82.0	41.0	20.5
14-HDoHE	21375.0	10687.5	5343.8	2671.9	1335.9	668.0	334.0	167.0	83.5	41.7	20.9
10-HDoHE	21375.0	10687.5	5343.8	2671.9	1335.9	668.0	334.0	167.0	83.5	41.7	20.9
12-HETE	21000.0	10500.0	5250.0	2625.0	1312.5	656.3	328.1	164.1	82.0	41.0	20.5
11-HDoHE	21375.0	10687.5	5343.8	2671.9	1335.9	668.0	334.0	167.0	83.5	41.7	20.9
8-HDoHE	21375.0	10687.5	5343.8	2671.9	1335.9	668.0	334.0	167.0	83.5	41.7	20.9
8-HEtE	22800.0	11400.0	5700.0	2850.0	1425.0	712.5	356.3	178.1	89.1	44.5	22.3
5-HEtE	22800.0	11400.0	5700.0	2850.0	1425.0	712.5	356.3	178.1	89.1	44.5	22.3
5S,14R-lipoxinB4	20850.0	10425.0	5212.5	2606.3	1303.1	651.6	325.8	162.9	81.4	40.7	20.4

**Supplementary Table 3.** Mass spectrometer parameters in the developed micro-LC-MS/MS method

Compound Name	Q1 mass	Q3 mass	Dwell time	EP	CE	CXP	Q0D	Retention time (min)
20-hydroxy-PGF2 $\alpha$	369.2	325.2	200.00	-12	-28	-15	-25	10.02
20-hydroxy-PGE2	367.2	287.2	200.00	-11	-22	-14	-25	10.16
2,3dinor-8iso-PGF2 $\alpha$	325.1	237.2	200.00	-9	-16	-15	-25	13.67
2,3dinor-11 $\beta$ -PGF2 $\alpha$	325	145.2	200.00	-9	-23	-13	-25	14.77
20-carboxy-LTB4	365.2	347.2	200.00	-10	-23	-16	-25	16.35
20-hydroxy-LTB4	351.2	195.2	200.00	-7	-23	-10	-25	17.17
iPF2 $\alpha$ -IV	353.3	127.1	200.00	-11	-29	-14	-25	18.55
d <sub>4</sub> -8iso-PGF2 $\alpha$ -ISTD	357.3	197.15	200.00	-10	-33	-13	-25	19.46
PGE3; PGD3	349.2	269.2	200.00	-10	-21	-12	-25	20.0
d <sub>11</sub> -5-iPF2 $\alpha$ -VI-ISTD	364.2	115.05	169.25	-10	-30	-13	-25	20.45
5-iPF $\alpha$ -VI	353.2	115.05	162.12	-10	-28	-10	-25	20.8
8iso-15R-PGF2 $\alpha$ ;8iso-PGF2 $\alpha$ ;11 $\beta$ -PGF2 $\alpha$ ;PGF2 $\alpha$	353.1	193.1	200.00	-10	-33	-10	-25	21.0
9,12,13-TriHOME	329.2	211.1	170.46	-9	-29	-10	-50	22.03
9,10,13-TriHOME	329.2	171.1	127.11	-10	-33	-11	-50	22.43
d <sub>4</sub> -PGF2 $\alpha$ -ISTD	357.3	197.15	125.20	-10	-33	-13	-25	22.5
8iso-13,14dihydro-15keto-PGF2 $\alpha$	353.3	183.1	135.84	-8	-32	-9	-25	22.88
d <sub>9</sub> -PGE2-ISTD	360.3	280.25	152.01	-10	-21	-13	-25	23.13
d <sub>4</sub> -8iso-PGE2-ISTD;d <sub>4</sub> -PGE2-ISTD;d <sub>4</sub> -PGD2-ISTD	355.3	275.25	183.42	-10	-21	-13	-25	23.2
8iso-PGE2; PGE2; 11 $\beta$ -PGE2; PGD2	351.1	271.15	165.78	-8	-23	-14	-25	23.5
5S,14R-lipoxinB4	351.2	221.2	200.00	-14	-20	-10	-35	24.05
13,14dihydro-PGF2 $\alpha$	355.2	311.3	189.05	-13	-31	-17	-25	24.51
d <sub>11</sub> -8,12-iso-iPF2 $\alpha$ -VI-ISTD	364.21	115.05	148.55	-10	-30	-13	-25	25.1
8,12-iso-iPF2 $\alpha$ -V1	353.21	115.05	144.80	-7	-25	-13	-25	25.2
5S,6S-LipoxinA4	351.21	115.2	153.12	-13	-20	-13	-35	25.41
13,14dihydro-15keto-PGE2	351.2	175.1	160.38	-13	-30	-8	-25	25.52
13,14dihydro-15keto-PGF2 $\alpha$	353.31	183.1	161.00	-11	-35	-16	-25	25.53
5S,6R-LipoxinA4	351.2	115.2	200.00	-14	-35	-10	-35	25.91
1a-1b-dihomo-PGF2 $\alpha$	381.1	337.45	200.00	-13	-29	-13	-25	26.43
13,14dihydro-15keto-PGD2	351.21	175.1	200.00	-11	-27	-13	-25	26.59
8,15-DiHETE	335.2	235.1	200.00	-13	-12	-11	-50	28.47
bicyclo-PGE2	333.2	113.15	200.00	-13	-33	-13	-25	28.75
17,18-DiHETE	335.2	247.1	185.52	-8	-24	-11	-50	28.98
10,17-DiHDoHE	359.2	153.1	176.57	-13	-24	-14	-50	29.06
d <sub>4</sub> -LTB4-ISTD	339.5	197.1	171.63	-10	-20	-13	-50	29.18

14,15-DiHETE	335.2	207.1	161.35	-7	-22	-10	-50	29.57
d <sub>4</sub> -12,13-DiHOME-ISTD	317.2	185.1	142.71	-10	-30	-13	-50	29.95
12,13-DiHOME	313.2	183.1	144.99	-11	-30	-11	-50	30.04
d <sub>4</sub> -9,10-DiHOME-ISTD	317.2	203.1	151.84	-10	-30	-13	-50	30.38
d <sub>11</sub> -14,15-DiHETrE-ISTD	348.2	207.1	176.19	-10	-24	-13	-50	31.2
14,15-DiHETrE	337.2	207.1	178.48	-9	-24	-9	-50	31.3
12-HHTrE	279.2	179.1	189.13	-11	-18	-10	-50	31.4
19,20-DiHDPa	361.2	273.2	200.00	-10	-21	-13	-50	31.5
11,12-DiHETrE	337.2	167.3	200.00	-7	-24	-14	-50	32.2
9-HOTrE	293.2	171.2	162.00	-9	-22	-10	-50	32.64
8,9-DiHETrE	337.2	127.2	152.47	-10	-27	-14	-50	32.67
18-HEPE	317.2	299.2	98.84	-11	-18	-14	-50	32.92
5,6-DiHETrE	337.2	145.15	59.84	-8	-24	-13	-50	33.16
d <sub>6</sub> -20-HETE-ISTD	325.2	279.2	55.36	-10	-21	-13	-50	33.24
15-HEPE	317.2	219.2	54.70	-8	-18	-11	-50	33.26
20-HETE	319.2	289.2	53.90	-8	-24	-13	-50	33.28
12-HEPE	317.2	179.1	48.05	-9	-18	-14	-50	33.45
9-HEPE	317.2	167.25	46.42	-13	-18	-14	-50	33.51
5-HEPE	317.2	115.2	43.36	-8	-12	-13	-50	33.64
d <sub>4</sub> -9-HODE-ISTD	299.2	172.1	40.81	-10	-27	-13	-50	33.74
9-HODE	295.21	171.1	40.81	-8	-15	-15	-50	33.74
13-HODE	295.2	195.2	40.81	-10	-15	-14	-50	33.75
20-HDoHE	343.21	299.2	40.25	-15	-18	-16	-50	33.85
16-HDoHE	343.2	233.2	39.63	-12	-18	-10	-45	34.02
16,17-EpDPE	343.21	233.2	39.63	-10	-15	-11	-50	34.02
11,12-EpETrE	319.22	167.1	40.61	-10	-18	-15	-45	34.12
9-HETE	319.21	167.1	40.91	-9	-10	-15	-50	34.13
10-HDoHE	343.21	153.1	42.16	-14	-21	-15	-40	34.17
14-HDoHE	343.2	205.1	42.16	-7	-18	-15	-50	34.18
d <sub>8</sub> -12-HETE-ISTD	327.2	184.1	43.76	-10	-21	-13	-50	34.21
12-HETE	319.2	179.2	47.17	-12	-10	-14	-50	34.28
11-HDoHE	343.2	121.1	47.17	-11	-18	-14	-45	34.28
8-HDoHE	343.2	189.1	55.57	-14	-15	-15	-45	34.4
8-HETrE	321.2	303.2	55.57	-12	-18	-16	-40	34.4
17-HDoHE	343.2	281.2	103.43	-13	-16	-13	-50	34.5
5-HETrE	321.21	303.2	79.86	-7	-18	-15	-50	34.55
12,13-EpOME	295.21	195.2	167.46	-7	-21	-13	-45	34.9
9,10-EpOME	295.22	171.1	200.00	-8	-21	-9	-50	34.98

**Supplementary Table 4.** UHPLC gradients used in the comparison experiment

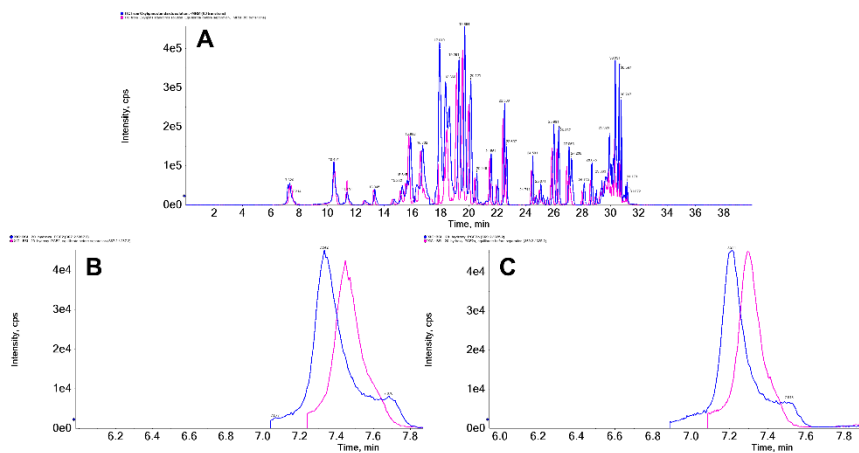
Mobile phase A: H<sub>2</sub>O with 0.1 % acetic acid; mobile phase B: 90 % ACN/10 % MeOH with 0.1 % acetic acid; mobile phase C: IPA with 0.1 % acetic acid with pH ranges between 3.2 and 3.5

Time [min]	Flow [mL/min]	B.Conc [%]	C.Conc [%]
0.75	0.70	20.0	1.0
0.95	0.70	26.0	1.0
6.00	0.70	34.0	1.0
8.00	0.70	40.0	1.0
10.00	0.70	54.0	1.0
11.00	0.70	55.0	1.0
12.00	0.70	56.0	3.0
13.00	0.70	78.0	6.0
14.00	0.70	85.0	15.0
14.50	0.70	85.0	15.0
14.80	0.70	20.0	1.0
16.00	0.70	20.0	1.0

**Supplementary Table 5.** Comparison of LODs and LOQs of micro flow-LC-MS/MS and UHPLC-MS/MS methods

Compounds	LOD (pM)		Fold Change	LOQ (pM)	
	micro flow-LC-MS/MS	UHPLC-MS/MS		micro flow-LC-MS/MS	UHPLC-MS/MS
13-HODE	59.0	-	-	196.6	-
8,12-iPF2 $\alpha$ -IV	23.0	-	-	76.5	-
13,14dihydro-15keto-PGE2	0.3	-	-	0.9	-
19,20-DiHDP A	0.1	19.9	180.7	0.4	66.3
5S,6S-LipoxinA4	0.1	16.9	170.2	0.3	56.2
iPF2 $\alpha$ -IV	0.2	28.0	114.4	0.8	93.2
2,3dino r-8iso-PGF2 $\alpha$	0.3	34.6	102.3	1.1	115.4
PGE3	0.1	7.4	71.4	0.3	24.7
8iso-PGE2	0.1	4.9	56.9	0.3	16.3
11,12-DiHETrE	0.1	5.6	50.8	0.4	18.6
PGF2 $\alpha$	0.2	11.6	48.4	0.8	38.7
15-HEPE	0.4	13.7	31.2	1.5	45.8
2,3dino r-11 $\beta$ -PGF2 $\alpha$	1.2	29.4	23.8	4.1	98.1
8iso-13,14dihydro-15keto-PGF2 $\alpha$	1.1	24.7	23.0	3.6	82.5
11 $\beta$ -PGE2	0.3	6.1	21.4	0.9	20.2
13,14dihydro-15keto-PGD2	0.3	6.7	21.1	1.1	22.2
20-hydroxy-LTB4	0.8	16.1	20.8	2.6	53.8
20-carboxy-LTB4	1.3	23.5	18.6	4.2	78.4
8,9-DiHETrE	0.5	8.5	18.0	1.6	28.2
5S,6R-lipoxinA4	1.0	18.1	18.0	3.4	60.4
17,18-DiHETE	2.4	42.7	17.7	8.0	142.4
8iso-PGF2 $\alpha$	2.1	31.3	15.3	6.8	104.3
12-HEPE	0.4	6.1	13.9	1.5	20.3
9,10-EpOME	2.2	28.5	13.0	7.3	94.9

9,12,13-TriHOME	6.6	69.1	10.5	22.0	230.5
14,15-DiHETE	0.7	6.8	10.0	2.3	22.5
16,17-EpDPE	5.1	50.1	9.9	16.8	167.1
20-hydroxy-PGE2	0.3	2.5	8.9	1.0	8.5
18-HEPE	3.0	18.7	6.3	9.9	62.4
12,13-DiHOME	2.3	14.2	6.2	7.6	47.2
5,6-DiHETrE	2.2	13.3	6.0	7.4	44.3
11 $\beta$ -PGF2 $\alpha$	1.1	6.6	5.8	3.8	22.0
PGE2	0.9	4.9	5.6	2.9	16.2
8-HETrE	4.4	21.2	4.9	14.5	70.5
PGD2	0.4	1.8	4.8	1.3	6.1
PGD3	0.6	2.5	4.6	1.8	8.4
1a,1b-dihomo-PGF2 $\alpha$	0.6	2.5	4.0	2.1	8.4
10,17-DiHDoHE	4.7	17.4	3.7	15.8	57.9
8iso-15R-PGF2 $\alpha$	0.8	3.0	3.6	2.8	9.9
9-HEPE	3.9	13.5	3.5	12.9	45.0
9-HOTrE	2.6	9.1	3.4	8.8	30.4
14,15-DiHETrE	0.9	2.9	3.3	3.0	9.8
8,15-DiHETE	6.1	17.9	2.9	20.5	59.8
bicyclo-PGE2	0.9	2.6	2.9	3.0	8.8
13,14dihydro-PGF2 $\alpha$	3.5	9.7	2.8	11.7	32.4
12-HHTrE	4.4	12.2	2.8	14.7	40.7
11,12-EpETrE	0.6	1.5	2.7	1.8	5.0
20-hydroxy-PGF2 $\alpha$	1.9	5.0	2.7	6.2	16.6
5-iPF2 $\alpha$ -VI	2.5	6.6	2.6	8.3	22.0
12,13-EpOME	4.3	10.6	2.5	14.4	35.3
5-HETrE	4.7	10.4	2.2	15.6	34.7
9,10,13-TriHOME	4.6	9.5	2.1	15.4	31.8
14-HDoHE	7.1	10.4	1.5	23.6	34.5
20-HETE	8.8	12.5	1.4	29.3	41.8
13,14dihydro-15keto-PGF2 $\alpha$	2.5	2.4	1.0	8.5	8.1
5S,14R-lipoxinB4	11.6	11.0	0.9	38.6	36.7
9-HETE	8.3	7.0	0.8	27.8	23.3
11-HDoHE	8.8	6.8	0.8	29.2	22.8
10-HDoHE	12.8	9.4	0.7	42.6	31.3
9-HODE	27.7	17.8	0.6	92.3	59.3
16-HDoHE	3.4	1.9	0.5	11.5	6.2
5-HEPE	5.7	2.3	0.4	19.1	7.7
12-HETE	21.9	6.3	0.3	72.9	21.0
17-HDoHE	47.3	6.4	0.1	157.6	21.5
20-HDoHE	91.9	10.3	0.1	306.2	34.5
8-HDoHE	76.4	4.7	0.1	254.6	15.8



**Supplementary Figure 1.** Effect of equilibration time on early eluted compounds. A. Total ion chromatogram from injections of oxylipins standard solution; B. Extracted SRM chromatograms of 20-hydroxy-PGE2; C. Extracted SRM chromatograms of 20-hydroxy-PGF2α. Blue line represents the analysis with 1.5-min initial gradient, red line represents analysis with 5.5-min initial gradient.





# Chapter V

---

## **Capillary Electrophoresis-Mass Spectrometry for Creatinine Analysis in Residual Clinical Plasma Samples and Comparison with Gold Standard Assay**

### **Based on:**

Marlien van Mever, Bingshu He, Mariam van Veen, Jeroen Slaats, Madelon M. Buijs, Joanne E. Wieringa, Thomas Hankemeier, Peter de Winter, Rawi Ramautar

**Capillary electrophoresis–mass spectrometry for creatinine analysis in residual clinical plasma samples and comparison with gold standard assay**

ELECTROPHORESIS 2024; DOI: 10.1002/elps.20230026

## **Abstract**

When hospitalized, infants, particularly preterm, are often subjected to multiple painful needle procedures to collect sufficient blood for metabolic screening or diagnostic purposes using standard clinical tests. For example, at least 100  $\mu\text{L}$  of whole blood is required to perform one creatinine plasma measurement with enzymatic colorimetric assays. Since capillary electrophoresis-mass spectrometry (CE-MS) utilizing a sheathless porous tip interface only requires limited amounts of sample for in-depth metabolic profiling studies, the aim of this work was to assess the utility of this method for the determination of creatinine in low amounts of plasma using residual blood samples from adults and infants. By using a starting amount of 5  $\mu\text{L}$  of plasma and an injection volume of only 6.7 nL, a detection limit ( $S/N=3$ ) of 30 nM could be obtained for creatinine, and intra- and interday precisions (for peak area ratios) were below 3.2%. To shorten the electrophoretic separation time, a multi-segment injection strategy was employed to analyze up to seven samples in one electrophoretic run. The findings obtained by CE-MS for creatinine in pre-treated plasma were compared with the values acquired by an enzymatic colorimetric assay typically used in clinical laboratories for this purpose. The comparison revealed that CE-MS could be used in a reliable way for the determination of creatinine in residual plasma samples from infants and adults. Nevertheless, to underscore the clinical efficacy of this method, a subsequent investigation employing an expanded pool of plasma samples is imperative. This will not only enhance the method's diagnostic utility but also contribute to minimizing both the amount and frequency of blood collecting required for diagnostic purposes.

## 1. Introduction

In neonates, such as asphyxiated newborns, creatinine levels are frequently monitored multiple times per week upon admission to the hospital, requiring repeated blood sampling procedures involving heel lances or venipunctures [1, 2]. These procedures are not limited to sick infants; even healthy infants undergo approximately 12 needle procedures within their first year of life [3, 4]. Although necessary, these painful procedures can have immediate adverse effects, such as pain and enhanced anemia in preterm neonates, potentially necessitating blood transfusions [5, 6]. Furthermore, long-term effects were also observed regarding the changes in immune and cognition function, adaptations in brain development, such as cortical thickness and negative impacts on stress responsiveness and emotional health [7-9]. One of the solutions for reducing the required (starting) sample amount and subsequently easing the painful procedure for children is considering the use of microscale analytical methods that are well-suited for analyzing small-volume biological samples.

Our group has developed CE-MS methods employing a sheathless porous tip interface for the selective and sensitive profiling of polar ionogenic metabolites, including creatinine, in various volume-restricted biological samples over the past few years [10-12]. More recently, the Metabo-ring trial revealed that our CE-MS method can be used in a reproducible and robust way for compound annotation when using effective electrophoretic mobilities [13]. Moreover, a simulated metabolomics study using human plasma revealed that the right chemical information could be obtained when comparing two artificial sample sets based on their recorded metabolic profiles by CE-MS [14]. Another interesting feature of CE-MS, notably in the context of analyzing clinical samples, is the possibility of using a multi-segment approach, which allows the analysis of up to ten samples within a single electrophoretic run, thereby improving sample throughput without compromising separation resolution [15-18]. Recently, CE-MS utilizing a multi-segment injection approach has been used for the analysis of creatinine [19], polyamines [20], untargeted profiling of lipids [21], and for the monitoring of drug metabolism [17].

Based on the encouraging CE-MS studies reported until now for the profiling of charged metabolites in volume-restricted samples, the aim of this study was to assess the utility of our previously developed sheathless CE-MS method for the determination of creatinine in

minute amounts of human plasma. Small aliquots of pooled human plasma were used for the initial part of the study to examine whether creatinine could be determined reliably when using the complete analytical workflow and isotope-labeled internal standards. A multi-segment injection strategy was also considered in order to speed up the electrophoretic analysis. Then, creatinine levels were determined in low amounts of residual plasma from adults and children, and the obtained findings have been compared with an enzymatic colorimetric analyzer (Architect c4000, Abbott Laboratories), which is typically used in clinical chemistry laboratories for creatinine measurements. Though used in a routine way, this approach requires at least 100  $\mu\text{L}$  of blood for a single creatinine measurement.

## **2 Materials and methods**

### **2.1 Chemicals and Materials**

LC-MS-grade methanol, chloroform, and acetic acid were purchased from Biosolve B.V. (Valkenswaard, Netherlands). Purified water was obtained from a Milli-Q PF Plus system (Merck Millipore, Burlington, Massachusetts, United States). Amicon Ultra-0.5 Centrifugal Filter Unit, standard reagent creatinine (anhydrous,  $\geq 98\%$ ), proline, valine, leucine, isoleucine, hypoxanthine, methionine, arginine, tryptophan, creatine, tyrosine, threonine, serine, alanine, asparagine, glycine, glutamic acid, histidine, lysine, glutamine, phenylalanine, and deuterated standard Creatinine-methyl- $^{13}\text{C}$  was purchased from Sigma-Aldrich (St. Louis, Missouri, United States). Deuterated standard Creatinine-methyl- $\text{d}_3$  was purchased from Cayman Chemical (Ann Arbor, Michigan, United States).

### **2.2 Preparation of standard solutions**

All the amino acid standards mentioned above were dissolved in Milli-Q water to a concentration of 1 mg / mL as a single standard solution. Subsequently, they were mixed into a mixture solution with five  $\mu\text{M}$  of each compound upon qualitative analysis.

Creatinine, Creatinine- $^{13}\text{C}$ , and Creatinine- $\text{d}_3$  were weighed and dissolved in Milli-Q water to 1 mg/mL stock solutions. Creatinine stock solution (1 mg/mL) was then diluted in water, resulting in seven calibration concentration levels. Creatinine- $^{13}\text{C}$  solution was spiked as internal standard (ISTD) for each calibration level to reach a final concentration of 5  $\mu\text{M}$ . The concentration of ISTD was chosen to be in the middle of the dynamic range, i.e.,

equivalent to C4 concentration. Final calibrant concentrations are shown in **Table 1**. When it comes to method validation, Creatinine-d<sub>3</sub> was spiked in plasma in three different concentration levels [low-level (1 µM), medium-level (10 µM) and high-level (40 µM)] as a substitute for endogenous creatinine.

**Table 1.** Concentrations of creatinine, creatinine-d<sub>3</sub>, and creatinine-<sup>13</sup>C in calibrant solutions

Compound Name	Concentration (µM)								
	C0	C1	C2	C3	C4	C5	C6	C7	C8
Creatinine	0	0.5	1	2.5	5	10	20	40	60
Creatinine-d <sub>3</sub>	0	0.5	1	2.5	5	10	20	40	60
Creatinine- <sup>13</sup> C	5	5	5	5	5	5	5	5	5

### 2.3 Collection of clinical samples

Children were eligible for inclusion when their physician decided that a plasma creatinine measurement was necessary. All physicians working at the children's department of Spaarne Gasthuis were asked to alert one of the researchers when they requested a creatinine measurement for a child under five years of age. When alerted, one of the researchers would inform the parents for written consent. Children could only be included if written consent was obtained and if there was plasma left over after all measurements requested by the treating physician were finished. From the leftover material, at least 20 µL plasma was taken. A maximum of three samples (each from a different creatinine measurement) per patient was set to prevent confounding. The samples were stored and transferred at -20 °C. The Advisory Committee on Local Feasibility of Spaarne Gasthuis tested and approved this study. Because only leftover material was used and the participants did not undergo any extra procedures, testing of the protocol by the Medical Ethical Review Committee was not needed.

For the development of the CE-MS method, adult leftover samples were used from Atalmedial Medical Diagnostics Centre. Leftover samples in this clinical laboratory can be used anonymously for quality improvement and method development without the need for explicit written consent. Atalmedial routinely informs patients about this procedure, with the possibility to object against the use of their biomaterials for method development.

The sheathless CE-MS measurements were blinded to the outcome of the first creatinine measurement as well as to the participants' personal and health data.

## **2.4 Sample preparation**

The plasma samples were prepared through protein precipitation, Bligh & Dyer extraction, and an extra ultra-filtration step to gain clean samples for sheathless CE-MS analysis. For the purpose of method validation and adult sample quantification, 10  $\mu\text{L}$  plasma was subsequently spiked with 10  $\mu\text{L}$  water, 10  $\mu\text{L}$  50  $\mu\text{M}$  Creatinine- $^{13}\text{C}$ , and 10  $\mu\text{L}$  Creatinine- $\text{d}_3$  solutions. Followed by 160  $\mu\text{L}$  methanol for protein precipitation. Samples were vortexed thoroughly for 5 min and centrifuged at 15,800 g for 10 min. Once the supernatant was collected, 90  $\mu\text{L}$  water and 120  $\mu\text{L}$  chloroform was added for the extraction of creatinine. After another round of vortex and centrifugation, 200  $\mu\text{L}$  sample was taken from the water/methanol layer. Finally, the ultra-filtered centrifugation step was applied with Amicon Ultra-0.5 Centrifugal Filter Unit at 13,000 g, 4  $^{\circ}\text{C}$  for 60 min. The centrifugal filter was prerinsed with water prior to use. Considering the compatibility of the filter material, 200  $\mu\text{L}$  methanol and 100  $\mu\text{L}$  water were added in the filter tube together with the supernatant from the last step. Samples were evaporated to dry and reconstituted in 100  $\mu\text{L}$  water for sheathless CE-MS analysis. For the quantification analysis in children samples, 5  $\mu\text{L}$  plasma was used in the sample preparation, and the processed samples were reconstituted in 25  $\mu\text{L}$  water. The volume of ISTD solution and other solvents were also adjusted in order to align with other samples.

## **2.5 CE-MS instruments and conditions**

Sheathless CE-MS analyses were performed on CESI 8000 Plus System (AB sciex, Inc., Redwood City, CA, U.S.A.) coupled to a Sciex TripleTOF 6600 MS via a Sciex Nanospray III ionization source. The multi-segment injection (MSI) separation was carried out using an OptiMS fused-silica capillary cartridge (id is 30  $\mu\text{m}$  across the whole capillary, 91 cm length in total; od is 150  $\mu\text{m}$ ), which was regulated at 25  $^{\circ}\text{C}$  with recirculating liquid coolant. 10% acetic acid (1.75 M, pH = 2.2) was used as background electrolyte (BGE). Sheathless CE-MS separation was started with a rinsing procedure including 1 min water rinse at 75 psi (517106.8 Pa), 1 min 0.1 M NaOH rinse at 75 psi (517106.8 Pa), and another 1 min water rinse at 85 psi (586054.4 Pa); Followed by BGE flushing for 2.5 min on separation

capillary at 85 psi (586054.4 Pa), and 1 min on conductive capillary at 80 psi (551580.6 Pa). Seven samples and in total six BGE spacers were injected alternately using hydrodynamic injection [2 psi (13789.5 Pa) for 20 s] and short rinsing procedure [20 psi (137895.1 Pa) for 0.3 min], respectively. On completion of multi-segment injection, a voltage of 30 kV for electrophoresis separation was applied on the capillary for 25 min. BGE was refilled into the capillary at 85 psi (586054.4 Pa) for 2.5 min after each measurement.

TOF-MS was operated in positive ionization mode with an ionspray voltage floating (ISVF) at 1530 V. Ion source gas 1, gas 2 were set to 0 psi, and Curtain gas at 5 psi (34473.8 Pa). Data was recorded at a  $m/z$  range from 65 to 500. Mass accuracy was calibrated daily using an ESI-positive calibration solution prior to analysis.

## 2.6 Method validation

### 2.6.1 Linearity of detector response and limit of detection

The Linearity of detector response was evaluated by injecting academic calibration solutions ( $n = 3$ ) on three consecutive days. The calibration range is shown in **Table 1**. The recorded calibration lines of creatinine were fitted to a  $1/x^2$  weighted linear regression model. The limits of detection (LOD) and limits of quantification (LOQ) were calculated as  $LOD = 3 \times S_a/b$ ,  $LOQ = 10 \times S_a/b$ , where  $S_a$  stands for the standard deviation of the y-intercept,  $b$  is the slope of the calibration curve.

### 2.6.2 Precision and accuracy

The intra- and interday precisions and accuracy were evaluated by spiking three different concentrations of creatinine- $d_3$  [low-level (1  $\mu$ M), medium-level (10  $\mu$ M) and high-level (40  $\mu$ M)] into pooled plasma samples over three different days ( $n = 5$  per day). Precision was expressed as the relative standard deviations (RSD) of the peak area ratio of creatinine- $d_3$  and creatinine- $^{13}C$ . An RSD of less than 15% was within the tolerance limits of the EMA guidelines. Accuracy was evaluated by back-calculation of creatinine- $d_3$  concentrations based on the linear regression equation. A criterion of 15 % relative error (RE) compared with their nominal concentrations was employed according to the EMA guideline.



### 2.6.3 Recovery and matrix effects

Recovery, and matrix effects were evaluated by spiking creatinine-<sup>13</sup>C and creatinine-d<sub>3</sub> solutions to pooled plasma samples (n = 5) or water (n = 5). Recovery was calculated using the peak area ratio of creatinine-d<sub>3</sub> and Creatinine-<sup>13</sup>C measured before and after extraction. Similarly, the matrix effect was calculated by the peak area ratio of creatinine-d<sub>3</sub> and Creatinine-<sup>13</sup>C spiked within pooled plasma and water, both spiked before extraction.

### 2.7 Data pre-processing

SCIEX MultiQuant version 3.0.3 (SCIEX, United States) were used for peak integration and identification. The precursor ions selected for peak picking were *m/z* 114.0662, 115.0662, 117.0850 for creatinine, creatinine-<sup>13</sup>C, and creatinine-d<sub>3</sub>, respectively. Mass tolerance was set to 5 ppm. Absolute quantitation was calculated using the equation of the calibration curve and peak area ratios between creatinine and creatinine-<sup>13</sup>C. For method performance comparison, creatinine concentrations from CE-MS were compared to the Architect c4000 results using Bland-Altman plots. To compute their disparities, statistical analysis was performed on GraphPad Prism 10. The following formulas were utilized:

Difference = Conc. Architect – Conc. CE-MS (**Figure 2A, D**)

Difference% =  $100\% \times (\text{Conc. Architect} - \text{Conc. CE-MS}) / \text{Conc. Architect}$  (**Figure 2B, E**).

## 3 Results and discussion

As indicated in the Introduction and considered a logical next step given our previous studies, the aim of this work was to assess the utility of sheathless CE-MS for diagnostic purposes in a clinical setting by performing the determination of creatinine in low amounts of plasma, using residual samples from the clinic, as a test case. To achieve this goal, method development was focused on describing performance metrics for creatinine analysis, including sample preparation and adjustment on multi-segment injection. A key aspect was the comparison of the creatinine concentration values obtained by CE-MS in plasma with an assay typically employed in clinical chemistry labs for this purpose in order to assess whether the same findings can be obtained by CE-MS but with significantly less blood material.

### 3.1 CE-MS method for creatinine determination

Zi-Ao Huang et al. proposed a CE-MS method using multi-segment injection for the quantification of urinary creatinine using a simple dilute-and-shoot sample preparation [19]. However, in this study, the aim was to determine creatinine in residual human plasma samples. For the latter matrix, rigorous sample preparation is needed prior to CE-MS analysis, in particular when using porous tip capillaries which have an inner diameter of only 30  $\mu\text{m}$ . Therefore, sample preparation was comprised of Bligh & Dyer extraction and ultra-filtration, including 5 to 50 times dilution of the residual plasma samples from children and adults to avoid detector saturation. In the case of using multi-segment injection, two pooled plasma segments were injected at the beginning and the end as quality control (QC) samples. As for the academic calibrant line, C0 samples were injected. Creatinine- $^{13}\text{C}$  and Creatinine- $\text{d}_3$  were spiked in the QC samples as internal standards to correct potential migration time shifts of creatinine. In order to obtain good peak shapes for creatinine when using multi-segment injection, the hydrodynamic injection time was optimized. As a result, samples were injected under 2.0 psi for 20 s, which corresponds to about 6.7 nL, followed by a BGE plug of 20 psi for 0.3 min (corresponding to 9.4% of the total capillary volume) between sample segments. The BGE plug length was also optimized for baseline separation of peaks when using the injection of seven discrete sample plugs in a single electrophoretic run.

The modified sheathless CE-MS method was validated according to the EMA guidelines for the validation of analytical methods, including linearity, precision, accuracy, recovery, and quantification. Typical electropherograms obtained for creatinine in academic calibrant solutions with multi-segment CE-MS are shown in **Supplementary Figure 1**. The 8 calibrant points were able to run within two measurements. Within a linear range from 0.5 to 40  $\mu\text{M}$ , the coefficient of determination ( $R^2$ ) value reached 0.998, and all the back calculation concentrations of the calibration standards were within  $\pm 10\%$  of the nominal value, indicating an acceptable response function satisfactory for creatinine within the calibration range. The LOD and LOQ of creatinine were 0.03  $\mu\text{M}$  and 0.09  $\mu\text{M}$ , respectively (**Table 2**), when using an injection volume of 6.7 nL, which enabled the reliable determination of endogenous creatinine plasma levels. Although no peak tailing was observed for 60  $\mu\text{M}$  creatinine, the accuracy of back calculation concentration was above

15%, presumably attributed to detector saturation and as such, this calibrant solution was excluded from the calibration range.

The intraday and interday precision were assessed using three different concentrations [low-level (1  $\mu\text{M}$ ), medium-level (10  $\mu\text{M}$ ), and high-level (40  $\mu\text{M}$ ),  $n=5$  for each concentration] of internal standards spiked in pooled plasma. Triplicate samples were prepared for each level, and samples were measured on three consecutive days. Intra- and interday precisions were below 3.16%, indicating that the repeatability was within the tolerance limits (**Table 3**). In addition, during method development and sample measurement, no significant signal decrease was observed, which demonstrated stable performance over time.

Recovery and matrix effects were determined using creatinine- $\text{d}_3$  and were above 87% for the three concentration levels. Matrix effects were around 50% (**Table 3**), and deuterated creatinine was therefore employed to compensate for matrix effects and ensure quantification accuracy.

**Table 2.** Overview of validation parameters determined for creatinine and creatinine- $\text{d}_3$  by CE-MS

Compound	Calibration ranges ( $\mu\text{M}$ )	$m/z$	slope	$R^2$	LOD ( $\mu\text{M}$ )	LOQ ( $\mu\text{M}$ )
Creatinine	1-40	114.0662	0.16	0.998	0.03	0.09
Creatinine- $\text{d}_3$	1-40	115.0662	0.15	0.997	0.05	0.15

<sup>a)</sup>  $R^2$ , coefficient of determination

**Table 3.** Intra-day ( $n=5$ ) and inter-day ( $n=15$ ) precision (RSD%), accuracy (RE%), matrix effect, and recovery of creatinine- $\text{d}_3$  calculated by using creatinine- $^{13}\text{C}$  as internal standard in plasma by CE-MS

Concentration levels	1 $\mu\text{M}$	10 $\mu\text{M}$	40 $\mu\text{M}$
<b>Intraday precision</b>	3.0%	2.7%	1.8%
<b>Interday precision</b>	3.2%	2.8%	2.5%
<b>Accuracy</b>	0.6%	8.5%	15.1%
<b>Matrix effect</b>	51.1%	33.3%	43.7%
<b>Recovery</b>	94.4%	94.4%	87.6%

### 3.2 Comparison with enzymatic colorimetric assay

To determine whether our CE-MS method yielded the right creatinine values in the plasma samples obtained from our clinical collaborators, a comparison with the gold standard assay for creatinine measurements is required, in this case, an enzymatic colorimetric assay using

the Architect c4000. For the reliable determination of creatinine, both creatinine- $^{13}\text{C}$  and creatinine- $\text{d}_3$  were spiked into human plasma samples and QC samples were injected as the first and last sample plugs. As shown in **Figure 1**, the isotope-labeled internal standards showed a similar variation trend to endogenous creatinine during the electrophoretic run, indicating that analyte response fluctuations during CE-MS analysis can be corrected by using peak area ratio for quantification.

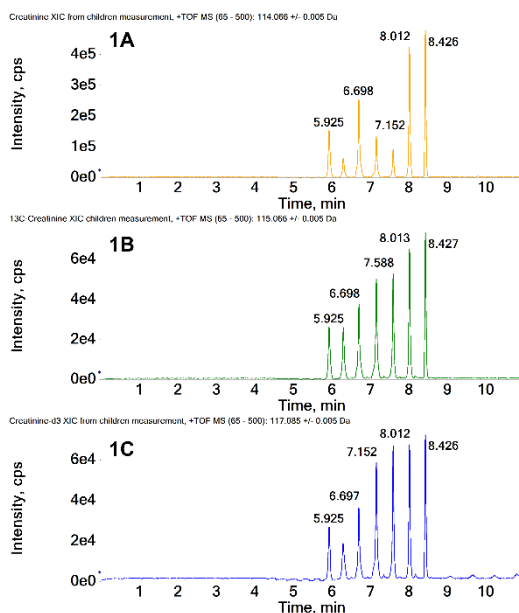


**Figure 1.** Extracted ion electropherogram of creatinine, creatinine- $^{13}\text{C}$ , and creatinine- $\text{d}_3$  obtained with sheathless CE-MS in children's plasma samples

For a comprehensive comparison between sheathless CE-MS and Architect c4000, Bland-Altman plots and regression lines were constructed to illustrate concentration disparities relative to the standard concentrations determined with Architect c4000.

In adult samples, the mean creatinine concentration difference is  $7.12 \mu\text{M}$  (0.73%), which is indicated by the red line in **Figure 2A** and **B**. The difference values were distributed close to zero and mean difference line, particularly in cases of lower creatinine concentrations. For the higher concentration levels, larger differences were observed most presumably attributed to MS detector saturation. The determination coefficient ( $R^2$ ) for adult sample concentrations was 0.9789 while the correlation of concentrations for children samples

appears to be suboptimal due to the presence of an outlier (**Figure 2C, F**). However, if we exclude the outlier, concentration differences of children samples are clustered around the mean difference line as well (**Figure 2D, E**). The important notion that only 5  $\mu\text{L}$  of plasma as starting material is needed for CE-MS, whereas 100  $\mu\text{L}$  is required for the enzymatic colorimetric assay. Most of the data points are closely aligned with the mean difference line and remain within the limits of agreement ( $\pm 2\text{SD}$ ), indicating a good agreement between the two methodologies.

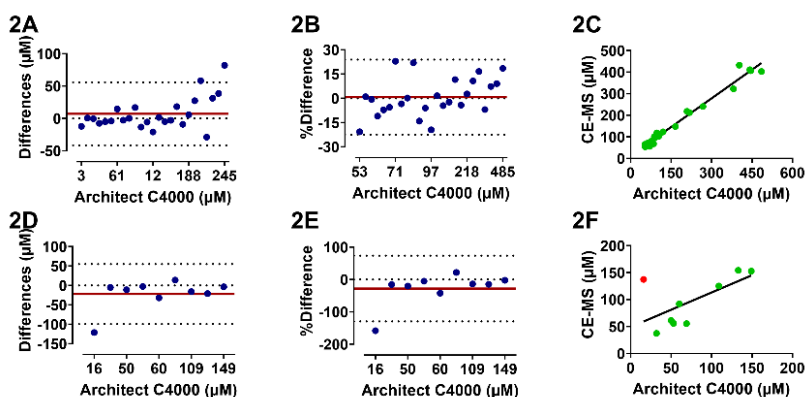


**Figure 2.** Correlation between creatinine concentrations measured with sheathless CE-MS and Architect C4000 for 25 adult (A-C) and 9 children samples (D-F). Bland-Altman plots where concentration differences are presented as micromolar (A, D) and (B, E) as a percentage; (C, F) Regression line between the two methods

### 3.3 CE-MS for metabolic profiling of residual plasma samples

Along with the ability for creatinine quantification, utilization of high-resolution TOF-MS in full scan mode and low-pH BGE condition in CE enabled a wide range of polar ionogenic metabolites to be detected in the plasma sample. Some amino acids were identified based on their accurate mass and migration time paired with authentic standards. Extracted ion electropherograms of these amino acids and some compounds that still need to be identified are shown in **Figure 3**. Data was acquired from QC plasma samples. Despite seven sample plugs being injected in the same electrophoretic run, the peaks from the same compound were baseline separated except for a few isomers, such as leucine and isoleucine. However, as these two compounds were partially overlaid in the electropherogram (**Figure 3C**),

better separation could be potentially gained by adjusting the composition of the BGE (i.e. the viscosity and thus the electrophoretic mobility). Using a longer capillary is not an option with our sheathless CE-MS, as the capillaries from the vendor have a defined capillary length. The main purpose of this part of the study was to solely demonstrate that, next to creatinine, many more metabolites could be detected by CE-MS in plasma, offering the possibility of further exploring the role of the proposed CE-MS method for biomarker discovery studies using metabolomics in a neonatology/pediatric context.

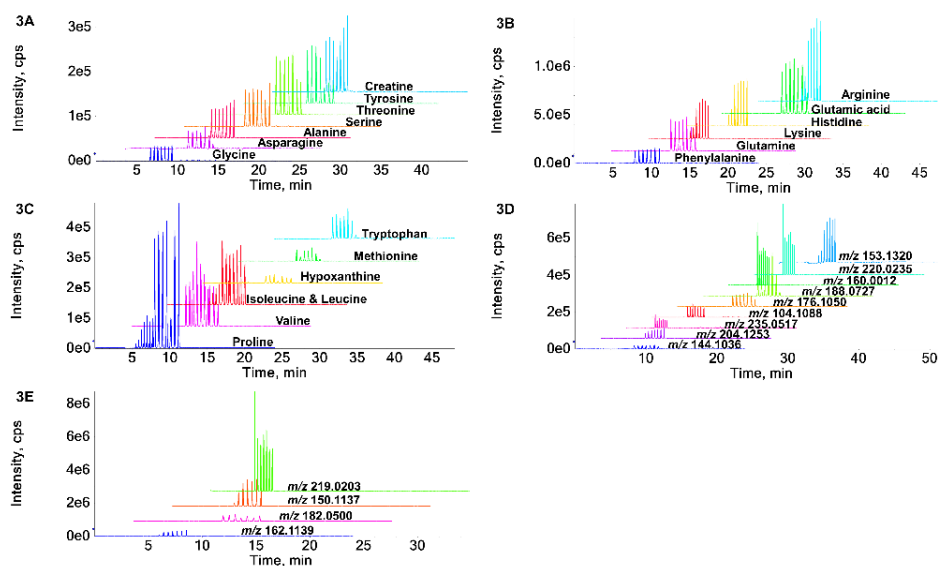


**Figure 3.** Multiple extracted ion electropherograms for a selected number of analytes detected in human plasma next to creatinine (using starting amount of 5  $\mu$ L) by sheathless CE-MS in positive ion mode. (A) (B) (C) Amino acids identified by accurate mass and migration time. (D)(E) Identity of compounds is unknown at this stage. Separation conditions: BGE, 10% acetic acid (1.75 M, pH 2.2); Separation voltage, 30 kV

## 4 Concluding remarks

In this study, sheathless CE-MS was used for the determination of creatinine in volume-limited plasma samples with the aim of assessing its utility for clinical studies, in particular for samples originating from a neonatology/pediatric context. A comparison with a gold standard assay has been made and revealed that sheathless CE-MS yielded comparable

creatinine concentration values but with the use of significantly less plasma sample, i.e. 5  $\mu$ L versus 100  $\mu$ L required for the clinical assay. Still, a follow-up study with many more plasma samples is needed for the comparison with the clinical assay in order to determine whether CE-MS is ready for handling samples from pediatrics, in particular for biomarker discovery studies, as the current study clearly revealed that, apart from creatinine, many more polar and charged metabolites could be observed by CE-MS in the volume-limited plasma sample.

### Acknowledgements

Bingshu He would like to acknowledge the China Scholarship Council (CSC, No. 201906390032). Dr. Rawi Ramautar would like to acknowledge the financial support of the Vidi grant scheme of the Netherlands Organization of Scientific Research (NWO Vidi 723.016.003).

### Conflict of interest

The authors have declared no conflict of interest.

### Data Availability Statement

The data that support the findings of this study are available on request from the corresponding author. The data are not publicly available due to privacy or ethical restrictions.

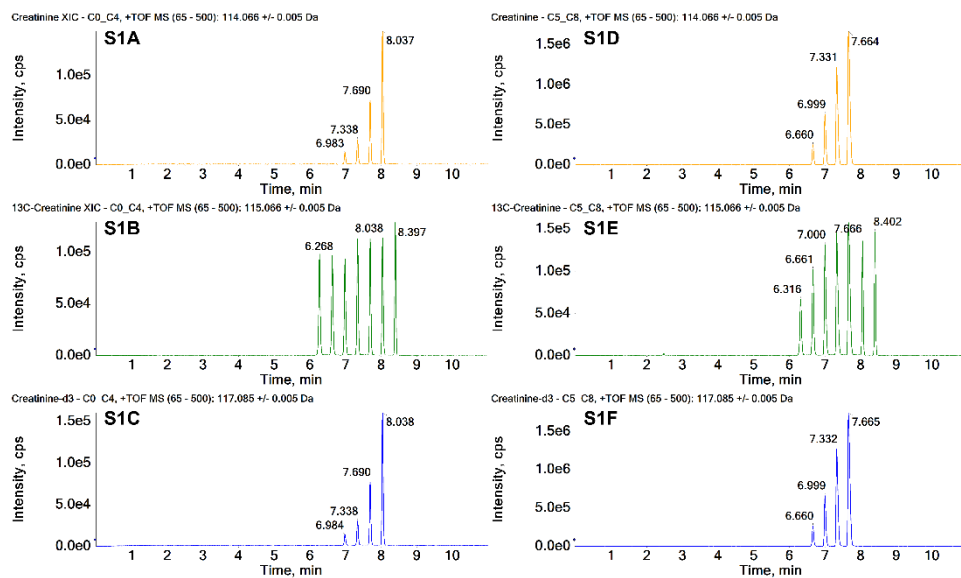
### References

- [1] Kastl JT. Renal function in the fetus and neonate – the creatinine enigma. *Seminars in Fetal and Neonatal Medicine*. 2017;22(2):83-9.
- [2] Sulemanji M, Vakili K. Neonatal renal physiology. *Seminars in Pediatric Surgery*. 2013;22(4):195-8.
- [3] McNair C, Campbell-Yeo M, Johnston C, Taddio A. Nonpharmacologic Management of Pain During Common Needle Puncture Procedures in Infants: Current Research Evidence and Practical Considerations: An Update. *Clinics in Perinatology*. 2019;46(4):709-30.

- [4] Uman LS, Birnie KA, Noel M, Parker JA, Chambers CT, McGrath PJ, Kisely SR. Psychological interventions for needle-related procedural pain and distress in children and adolescents. *Cochrane Database of Systematic Reviews*. 2013(10).
- [5] Shah VS, Ohlsson A. Venepuncture versus heel lance for blood sampling in term neonates. *Cochrane Database of Systematic Reviews*. 2011(10).
- [6] Widness JA. Pathophysiology of Anemia During the Neonatal Period, Including Anemia of Prematurity. *NeoReviews*. 2008;9(11):e520-e5.
- [7] Victoria NC, Murphy AZ. Exposure to early life pain: long term consequences and contributing mechanisms. *Current Opinion in Behavioral Sciences*. 2016;7:61-8.
- [8] Friedrichsdorf SJ, Goubert L. Pediatric pain treatment and prevention for hospitalized children. *PAIN Reports*. 2020;5(1):e804.
- [9] Ranger M, Grunau RE. Early repetitive pain in preterm infants in relation to the developing brain. *Pain Management*. 2014;4(1):57-67.
- [10] Ramautar R. Sheathless Capillary Electrophoresis-Mass Spectrometry for the Profiling of Charged Metabolites in Biological Samples. In: Theodoridis GA, Gika HG, Wilson ID, editors. *Metabolic Profiling: Methods and Protocols*. New York, NY: Springer New York; 2018. p. 183-92.
- [11] Zhang W, Hankemeier T, Ramautar R. Capillary Electrophoresis-Mass Spectrometry for Metabolic Profiling of Biomass-Limited Samples. In: Phillips TM, editor. *Clinical Applications of Capillary Electrophoresis: Methods and Protocols*. New York, NY: Springer New York; 2019. p. 165-72.
- [12] Sánchez-López E, Kammeijer GSM, Crego AL, Marina ML, Ramautar R, Peters DJM, Mayboroda OA. Sheathless CE-MS based metabolic profiling of kidney tissue section samples from a mouse model of Polycystic Kidney Disease. *Scientific Reports*. 2019;9(1):806.
- [13] Drouin N, van Mever M, Zhang W, Tobolkina E, Ferre S, Servais A-C, Gou M-J, Nyssen L, Fillet M, Lageveen-Kammeijer GSM, Nouta J, Chetwynd AJ, Lynch I, Thorn JA, Meixner J, Löfner C, Taverna M, Liu S, Tran NT, Francois Y, Lechner A, Nehmé R, Al Hamoui Dit Banni G, Nasreddine R, Colas C, Lindner HH, Faserl K, Neusüß C, Nelke M, Lämmerer S, Perrin C, Bich-Muracciole C, Barbas C, González ÁL, Guttman A, Szigeti M, Britz-McKibbin P, Kroezen Z, Shanmuganathan M, Nemes P, Portero EP, Hankemeier T, Codesido S, González-Ruiz V, Rudaz S, Ramautar R. Capillary Electrophoresis-Mass Spectrometry at Trial by Metabo-Ring: Effective Electrophoretic Mobility for Reproducible and Robust Compound Annotation. *Analytical Chemistry*. 2020;92(20):14103-12.
- [14] Zhang W, Segers K, Mangelings D, Van Eeckhaut A, Hankemeier T, Vander Heyden Y, Ramautar R. Assessing the suitability of capillary electrophoresis-mass spectrometry for biomarker discovery in plasma-based metabolomics. *ELECTROPHORESIS*. 2019;40(18-19):2309-20.
- [15] Shanmuganathan M, Kroezen Z, Gill B, Azab S, de Souza RJ, Teo KK, Atkinson S, Subbarao P, Desai D, Anand SS, Britz-McKibbin P. The maternal serum metabolome by multisegment injection-capillary electrophoresis-mass spectrometry: a high-throughput platform and standardized data workflow for large-scale epidemiological studies. *Nature Protocols*. 2021;16(4):1966-94.
- [16] Gill B, Jobst K, Britz-McKibbin P. Rapid Screening of Urinary 1-Hydroxypyrene Glucuronide by Multisegment Injection–Capillary Electrophoresis–Tandem Mass Spectrometry: A High-Throughput Method for Biomonitoring of Recent Smoke Exposures. *Analytical Chemistry*. 2020;92(19):13558-64.
- [17] Au - Shanmuganathan M, Au - Macklai S, Au - Barrenas Cárdenas C, Au - Kroezen Z, Au - Kim M, Au - Zizek W, Au - Lee H, Au - Britz-McKibbin P. High-throughput and Comprehensive Drug Surveillance Using Multisegment Injection-Capillary Electrophoresis-Mass Spectrometry. *JoVE*. 2019(146):e58986.
- [18] Kuehnbaum NL, Kormendi A, Britz-McKibbin P. Multisegment Injection-Capillary Electrophoresis-Mass Spectrometry: A High-Throughput Platform for Metabolomics with High Data Fidelity. *Analytical Chemistry*. 2013;85(22):10664-9.
- [19] Huang Z-A, Scotland KB, Li Y, Guo J-P, McGeer PL, Lange D, Chen DDY. Application of multisegment injection on quantification of creatinine and standard addition analysis of urinary 5-hydroxyindoleacetic acid simultaneously with creatinine normalization. *ELECTROPHORESIS*. 2020;41(3-4):183-93.
- [20] Igarashi K, Ota S, Kaneko M, Hirayama A, Enomoto M, Katumata K, Sugimoto M, Soga T. High-throughput screening of salivary polyamine markers for discrimination of colorectal cancer by multisegment injection capillary electrophoresis tandem mass spectrometry. *Journal of Chromatography A*. 2021;1652:462355.
- [21] Ly R, Ly N, Sasaki K, Suzuki M, Kami K, Ohashi Y, Britz-McKibbin P. Nontargeted Serum Lipid Profiling of Nonalcoholic Steatohepatitis by Multisegment Injection–Nonaqueous Capillary Electrophoresis–Mass Spectrometry: A Multiplexed Separation Platform for Resolving Ionic Lipids. *Journal of Proteome Research*. 2022;21(3):768-77.



## Supporting information



**Supplementary Figure 1.** Extracted ion electropherograms obtained for creatinine, <sup>13</sup>C-creatinine, and creatinine-d<sub>3</sub> in academic calibrant solutions with sheathless CE-M

# Chapter VI

---

## Conclusions and perspectives

## Conclusions

Reversed-phase UHPLC-MS has become a routine analytical technique for both academic and pharmaceutical research in recent decades [1]. While widely employed for highly sensitive and high-throughput analysis, its detection and quantification ability are still compromised when analyzing biomass-restricted matrices. When the sensitivity of a method is not sufficient for a biomass limited sample like zebrafish larvae, single cells or minimal amount of body fluids, the commonly used strategy to reach the (required) detection limits is to pool several samples together, which results in sacrificing the heterogeneity of the sample set. However, collecting data for an individual (or single) sample is pivotal for metabolomics and for future personalized treatment strategies. Additionally, the development of non-invasive sampling techniques allows for the collection of a few picoliters to microliters blood or cytoplasm at a time, yet the lack of sensitive analytical methods for these trace amount samples leaves a gap between sampling and analysis. Addressing this volume-mismatch will further our understanding of disease pathology, drug metabolism and dose assessment.

The underlying idea of this thesis is to reduce sample dilution in the ionization source and improve MS sensitivity by down-scaling the flow rate to micro/nanoliter level. The robustness and applicability of micro flow-LC-MS and CE-MS for the analysis of biomass-restricted samples were demonstrated. While nano flow LC-MS provides superior sensitivity, it often sacrifices robustness compared to conventional LC-MS methods. Micro flow LC-MS offers a balanced approach, providing sufficient sensitivity for biomass-restricted samples while offering greater robustness compared to nano flow methods. Additionally, CE-MS is an ideal technique for volume-limited samples due to its zero dead volume, which maximizes system efficiency. The use of sheathless CE-MS further enhances sensitivity, making it a perfect fit for analyzing small sample sizes without compromising performance.

In this thesis, miniaturized MS-based analytical methods are established to address the volume-mismatch issue between sampling and analysis, as well as enabling the analysis of concentration-limited compounds in matrices including human plasma and cerebrospinal fluids. The significance of miniaturized MS-based workflows, including sampling and sample preparation methods, separation techniques and ionization sources, was emphasized

at the beginning of the thesis (**Chapter 2**). The applications showcasing recently reported miniaturized methods were discussed. In **Chapters 3** and **4**, micro-LC-MS methods were developed and successfully applied to biomass-restricted samples after evaluating various MS ionization source designs. To enhance the robustness and sensitivity, a spray needle was developed for positive mode analysis of endocannabinoids. For analysis of oxylipins in negative ionization mode, an OptiFlow ionization source was utilized for obtaining optimal performance. These two methods demonstrated that robustness is no longer an obstacle when the correct instrumentation is selected.

CE-MS has its advantage in analyzing polar and charged compounds, especially for volume-limited samples [2-4]. A sheathless CE-MS method was developed in **chapter 5** with high sensitivity for the quantification of creatinine in residual children plasma. Although the fixed length of the sheathless capillary compromises flexibility to some extent, this method managed to improve analysis throughput by employing a multi-segment injection strategy, enabling seven samples to be measured in one electrophoretic run. The measured creatinine values correlated well with the results from clinical measurements.

### Sensitivity enhancement

Miniaturized analytical methods operate on a significantly smaller scale compared to conventional methods, utilizing reduced flow rates and sample volumes. This miniaturization enhances sensitivity with low flow rates, which reduces the dilution within ionization source, making micro-flow LC-MS ideal for analyzing biomass-restricted samples. By optimizing chromatographic conditions and mass spectrometry parameters, micro-flow LC-MS enables the precise quantification of analytes even at ultra-low concentrations.

In **Chapter 3**, our focus was on the detection and quantification of endocannabinoids in 250  $\mu\text{L}$  human CSF. The trace levels of endogenous concentrations make this challenging for conventional methods. **Chapter 4** presents a negative quantification method for oxylipins in 5  $\mu\text{L}$  human plasma. Both of these methods were developed with 4  $\mu\text{L}/\text{min}$  flow rate and were compared with conventional flow LC-MS methods (i.e. flow rate above 0.5  $\text{mL}/\text{min}$ ). The sensitivity for endocannabinoids and their analogues improved 5 to 22 times, notably enhancing the ionization efficiency of AEA and 1-AG/2-AG by about nine

times compared to conventional flow rates (550  $\mu\text{L}/\text{min}$ ). For oxylipins, sensitivity increased by 1.4 to 180.7 times with 4  $\mu\text{L}/\text{min}$  compared to 700  $\mu\text{L}/\text{min}$ . Although enhancement values varied for each compound, comparing results indicated that micro flow-LC-MS significantly enhances detection of both concentration-limited and volume-limited sample compared to conventional LC-MS.

In **Chapter 5**, a sheathless CE-MS method was developed for the profiling of hydrophilic compounds in residual plasma samples. The method was validated for quantification of creatinine in 5  $\mu\text{L}$  plasma. Results from 25 adults and 9 children samples were compared with the golden standard enzymatic colorimetric assay used in clinics. Good alignment was observed between these two methods. This method holds promise as an alternative quantification tool in clinics, particularly in pediatric contexts, due to its significantly improved sensitivity and minimal sample volume requirement.

By establishing these three methods with micro flow LC-MS and sheathless CE-MS, we have demonstrated with solid data that miniaturized analytical methods significantly enhance sensitivity regardless of whether under positive or negative ionization, and whether for hydrophilic or hydrophobic compounds.

On the other hand, the required volume in the injection vials for LC and CE injections could be further miniaturized. For the micro-flow LC-MS and CE-MS methods used in **Chapter 4&5**, 5  $\mu\text{L}$  of plasma was used as the starting volume, and samples were reconstituted in 20  $\mu\text{L}$  and 25  $\mu\text{L}$  solvents before injection due to lack of proper miniaturized vials, respectively, which resulted in unnecessary sample dilution. Optimization of injection strategy such as using online sample preparation and loading samples directly to the column could be benefit for higher sensitivity.

### **Robustness**

Miniaturized techniques necessitate the downscaling of various components such as LC columns, CE capillaries, tubing, pumps, spray needles, and ionization sources in MS. Optimizing these miniaturized components enhances ionization efficiency and sensitivity. However, system robustness can be compromised, as smaller components are more prone to clogging by matrices. In addition, miniaturization can lead to other issues like discharge for nanospray in negative mode if conditions are not properly chosen. To mitigate this issue,

it is crucial to focus on two aspects: ensuring clean sample preparation and developing robust analytical systems.

For metabolite analysis, clogging is often caused by the residue proteins or salts from the matrices. In **Chapter 5**, an intensive sample preparation method was used for CE-MS analysis, including protein precipitation (PP) and one-hour centrifugation with an ultra-filter. This extraction procedure ensured good recovery (>87.6%) for creatinine and robust analysis using the capillary cartridge with a 30  $\mu\text{m}$  inner diameter (i.d.). Given the CE-MS flow rate of only a few nanoliters, an ultraclean sample preparation is pivotal. Over 700 samples were injected using the same capillary cartridge during the method development and application to human plasma, proving the robustness of the sample preparation procedure. The intra- and interday precision of this method was below 3.2%.

Compared to the CE-MS method with nano-flow rate (around 30 nL/min), micro flow LC-MS methods in **Chapter 3&4** were developed using micro-level flow rate (4  $\mu\text{L}/\text{min}$ ), wider inner diameters of tubings (50-60  $\mu\text{m}$ ) and column (i.d. 300  $\mu\text{m}$ ). These properties decrease the chance of clogging during sample analysis. To further improve method robustness, the focus was on selecting the optimal instrument and plumbing parts. The spray emitter was modified for positive mode analysis in **Chapter 3**. Along with well-fitting sleeves and zero dead volume connections, the modified needle enabled the quantification of endocannabinoids in 288 human CSF samples with precision under 13.7%. For the analysis of oxylipins in **Chapter 4**, discharge issues in electrospray sources with negative mode makes it more challenging than positive ionization method. An OptiFlow ionization source with SteadySpray electrode was selected for optimal performance as well as avoiding the corona discharge during analysis.

With the development and application of these three miniaturized methods, we can conclude that the poor robustness of miniaturized techniques is a misconception. By employing efficient sample preparation to obtain clean sample injection solutions, appropriately optimized instruments, and plumbing parts, micro flow LC-MS and CE-MS methods are promising for various metabolomics, clinical, and pharmaceutical studies involving large cohort and diverse sample types.

Future efforts to improve the robustness of micro-flow LC-MS should be putting on eliminating too many connections in the system to avoid dead volume and possible leakage.

For sheathless CE-MS, the capillary cartridge should be more robust if extra coating can be applied on the fused silica tubing to make it less fragile.

### **The optimal choice for biomass-restricted samples**

MS-based metabolomics has been a crucial part of biomarker discovery for the in-depth deciphering of various disease pathophysiologies. However, conventional methods fall short in dealing with biomass-restricted samples due to the higher sensitivity required. For the application in academic and clinical studies, high coverage for biomarker detection, good precision and accuracy for quantification are key requirements. In this thesis, in order to show the applicability of miniaturized methods, conventional LC-MS methods and clinical enzymatic method were used as standards for comparison. The established methods showed their robustness and accuracy when applied to various matrices. Among all biomass-restricted samples, those from infants and children are the most valuable due to their limited total blood volume and vulnerability.

In **Chapter 5**, the comparison between CE-MS and golden standard enzymatic method indicated the applicability of CE-MS for quantifying creatinine in plasma. The quantification accuracy was below 8.5% for concentrations from 1  $\mu\text{M}$  to 10  $\mu\text{M}$ , aligning well with the enzymatic method. For clinical utilization, this means significantly less sample volume from children is required with equivalent measurement ability, which also leads to reduced pain from the sampling procedure.

Beyond higher sensitivity, miniaturized LC-MS and CE-MS enable wider compound coverage than current biochemical methods in clinics. **Chapter 3 & 4** determined 16 endocannabinoids and 66 oxylipins in biomass-restricted samples, respectively. The CE-MS method also allows for profiling a broad range of hydrophilic compounds. The metabolomics data provided by these methods could aid in more comprehensive monitoring of healthy or diseased conditions, enabling pharmacokinetic profiling, biomarker discovery, and the development of personalized medicine.

In addition, LLE was used for the extraction of endocannabinoids and oxylipins for micro-flow LC-MS analysis. In this case, only extracts from organic layer were injected and the aqueous extracts were disposed, while both of them could be utilized by injecting the aqueous extraction to CE-MS. In this way, more comprehensive information could be obtained from one aliquot of sample, and enables higher throughput analysis. Miniaturized

SPE could also be considered as hydrophilic and hydrophobic compounds could be eluted separately from the SPE column, hence preventing the contamination from proteins.

## Future perspectives

### Combine miniaturized analytical methods with other miniaturized techniques

For the analysis of biomass-restricted samples, sensitivity enhancement is crucial when designing the experimental workflow. However, the volume mismatch between sample handling and the minimal requirement for injection still jeopardizes the measurement. While sample preparation is imperative for miniaturized MS-based techniques, two aspects can be improved to avoid unnecessary sample loss, which is especially critically when small volumes are in contact with large surfaces. One of them is reducing sample transfer steps during sample preparation. In this thesis, PP and LLE were used for CSF and plasma sample preparation. Sample loss due to manually transferring is inevitable, pipetting error could also be significant when the required volume is below 5  $\mu\text{L}$  depends on the viscosity of matrix sample[5]. By using deuterated internal standards and online sample preparation techniques, the repeatability and robustness could be improved.

So far, some online sample preconcentration methods have been developed to avoid unnecessary sample loss and gain more signal abundance for MS analysis. In our lab, a three-phase electroextraction (EE) method was reported for the fast online analysis of trace-level pharmaceuticals in plasma [6]. By applying 40-400V extraction voltage, acidic compounds were concentrated to a 0.3  $\mu\text{L}$  aqueous acceptor droplet and directly injected to LC-MS. The enrichment factor ranged from 70 to 190 for the targeted compounds. This electroextraction is currently fully automated and promises to gain even higher sensitivity by connecting to micro flow LC-MS. Given that the electromigration-based separation principle is similar to CE, this method is also suitable for coupling with CE-MS [7].

Another potential online preconcentration approach is a hanging droplet evaporator. This technique concentrates the sample on-the-fly in a hanging droplet exposed to heated nitrogen gas flow enriching up to tens of microlitres into a hanging droplet of less than one microlitre, without evaporation to dryness. The solvent evaporation rate and droplet volume are measured and controlled by a camera and real-time image processing. A 15-fold preconcentration can be obtained in less than 3 min. **Figure 1** shows the SRM



chromatograms obtained with an evaporator module coupled to a micro flow LC-MS system. A 10  $\mu\text{L}$  endocannabinoid standard solution was evaporated into a 2.5  $\mu\text{L}$  droplet and injected. The repeatability for 12 injections were 2.7% for LEA and 3.0% for EPEA. Although further optimization is still required for better robustness, the combination of online evaporation and micro-flow LC-MS is anticipated to benefit the analysis of biomass-restricted samples. For examples, samples can be enriched via evaporation without the need to redissolve the analytes after evaporation.

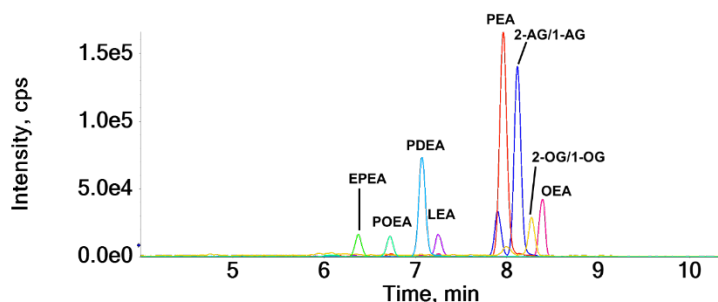


**Figure 1.** Typical SRM chromatograms from endocannabinoids standard solution obtained with an online evaporator module coupled with micro flow LC-MS

### Further improvement in instrument design

Down-scaling flow rates and plumbing volume enhances sensitivity. This benefit has been proven and increasingly utilized in proteomics study. However, the application of miniaturized methods for small molecule is still rare due to concerns about method robustness and relatively long analysis time. To address this issue, many users have modified their own micro- or nano-flow systems, including tubing, connections, columns, flow generators, ionization sources, and CE-MS interfaces (**Chapter 2**). In **chapter 3** of this thesis, a commercialized spray needle was modified to avoid clogging from matrix samples. Additionally, the sizes of tubing and connection fittings were carefully selected to prevent possible leakage and dead volume within the system. These innovations enable more sensitive and robust analysis with miniaturized techniques. However, the lack of standardized (or ready-for-use) techniques including miniaturized ionization sources, spray emitters, miniaturized LC tubings and connections has hindered their widespread application in academic and clinical studies. In-house designs of these instruments also require extra training for other researchers to operate.

Efforts have been made in recent years to standardize miniaturized device design. Examples include the EVOSEP+ method from EVOSEP (Denmark), which is a standardized method for detecting stanzolol in equine hair and urine, specially designed for a ReproSil-Pur C18 (8 cm x 100  $\mu$ m, 3  $\mu$ m) column. Additionally, chip-based LC-MS devices have been developed by companies such as Agilent (HPLC-Chip/MS), Waters (TRIZAIC™ nano tile), Sciex (cHiPLC®-Nanoflex), and New Objectives (PicoChip) [8]. These devices require appropriate connection among the pumps, columns, and detector to fully release their advantages in miniaturized analysis. Further development of miniaturized techniques should focus more on the communication and connection among all the parts, minimizing the volume within system to improve the throughput. Moreover, the design of more user-friendly and robust instruments should be promoted for their broader adoption and reproducibility in research and clinical settings.

### **Translation to clinical studies**

Miniaturized LC-MS and CE-MS methods offer a transformative solution to the analytical challenges posed by biomass-restricted samples in clinical and pharmaceutical studies. By leveraging their high sensitivity, these miniaturized methods enable researchers to extract maximal information from minimal sample amount, thereby advancing our understanding of disease mechanisms, guiding therapeutic interventions, and accelerating drug discovery and development.

In this thesis, the potential of CE-MS for clinical analyses was demonstrated for creatinine analysis by comparison of the findings with the gold-standard enzymatic assay employed in clinical chemistry labs. The reliable quantification ability of CE-MS using only 5  $\mu$ L of plasma as starting volume, instead of the traditional 100  $\mu$ L (due to the void volume), showed its potential for translation to clinical, especially pediatric, studies. In addition to higher sensitivity, the multi-segment injection strategy allowed seven samples to be analyzed in a single run, contributing to the high-throughput analysis of targeted compounds for clinical practice.

Similarly, micro-flow LC-MS methods were capable of measuring oxylipins and endocannabinoids in biomass-restricted samples with higher sensitivity compared to conventional methods. Their applications on biomass-restricted human CSF and plasma

proved their capability of adapting to future clinical practice. Additionally, in both academia and clinical settings, the welfare of patients and experimental animals is a primary concern. Consequently, microsampling techniques such as microdialysis, volumetric absorptive microsampling (VAMS), and capillary blood sampling are becoming more prevalent [9]. Miniaturized methods are therefore worth promoting for use in both academic and clinical contexts. Moreover, the cost of analyzing samples is lower with miniaturized flow rates due to significantly reduced solvent consumption.

Repeatability and accuracy are crucial for the application of analytical methods. Micro-flow LC-MS methods and CE-MS methods developed in this thesis highlight the importance of clean and efficient sample preparation procedure and connection of robust instruments to ensure robust, accurate, and sensitive measurements. While the high sensitivity of miniaturized techniques is widely known, future studies should focus on standardization of methodologies, optimization of online or automated sample preparation procedures, and development of robust and high-throughput instruments to realize their full potential in clinical and pharmaceutical research. Furthermore, interdisciplinary collaboration and the integration of miniaturized methods with complementary analytical techniques hold promise for addressing complex analytical problems and driving innovation in the field.

## References

- [1] C. Seger, L. Salzmann, After another decade: LC–MS/MS became routine in clinical diagnostics, *Clinical Biochemistry*, 82 (2020) 2-11.
- [2] M. van Mever, T. Hankemeier, R. Ramautar, CE–MS for anionic metabolic profiling: An overview of methodological developments, *ELECTROPHORESIS*, 40 (2019) 2349-2359.
- [3] E. Nevedomskaya, R. Ramautar, R. Derks, I. Westbroek, G. Zondag, I. van der Pluijm, A.M. Deelder, O.A. Mayboroda, CE-MS for Metabolic Profiling of Volume-Limited Urine Samples: Application to Accelerated Aging TTD Mice, *Journal of Proteome Research*, 9 (2010) 4869-4874.
- [4] J. Li, L. Huang, Y. Guo, K.A. Cupp-Sutton, S. Wu, An automated spray-capillary platform for the microsampling and CE-MS analysis of picoliter- and nanoliter-volume samples, *Analytical and Bioanalytical Chemistry*, 415 (2023) 6961-6973.
- [5] X.L. Guan, D.P.S. Chang, Z.X. Mok, B. Lee, Assessing variations in manual pipetting: An under-investigated requirement of good laboratory practice, *Journal of Mass Spectrometry and Advances in the Clinical Lab*, 30 (2023) 25-29.
- [6] Y. He, N. Drouin, B. Wouters, P. Miggiels, T. Hankemeier, P.W. Lindenburg, Development of a fast, online three-phase electroextraction hyphenated to fast liquid chromatography–mass spectrometry for analysis of trace-level acid pharmaceuticals in plasma, *Analytica Chimica Acta*, 1192 (2022) 339364.
- [7] A. Oedit, B. Duivelshof, P.W. Lindenburg, T. Hankemeier, Integration of three-phase microelectroextraction sample preparation into capillary electrophoresis, *Journal of Chromatography A*, 1610 (2020) 460570.
- [8] D.A. Vargas Medina, E.V.S. Maciel, F.M. Lanças, Miniaturization of liquid chromatography coupled to mass spectrometry. 3. Achievements on chip-based LC–MS devices, *TrAC Trends in Analytical Chemistry*, 131 (2020) 116003.
- [9] M.S.F. Hoffman, J.W. McKeage, J. Xu, B.P. Ruddy, P.M.F. Nielsen, A.J. Taberner, Minimally invasive capillary blood sampling methods, *Expert Review of Medical Devices*, 20 (2023) 5-16.

# Appendix

---

**Summary**

**Nederlandse samenvatting**

**Curriculum vitae**

**List of publications**

**Acknowledgements**

## Summary

Mass spectrometry (MS)-based analytical methods are widely utilized in both academic and clinical research, providing critical insights into biological and disease mechanisms. Despite their high sensitivity and throughput, conventional MS methods face significant challenges when analyzing biomass-restricted samples. Pooling such samples to meet detection limits compromises sample heterogeneity—an essential factor in metabolomics and personalized medicine. Additionally, non-invasive sampling techniques often yield only picoliters to microliters of sample volume, creating a mismatch between available sample quantities and the capabilities of standard analytical methods.

To address these challenges, this thesis explores miniaturized analytical techniques that enhance sensitivity and performance while maintaining robustness. By optimizing micro-flow liquid chromatography-mass spectrometry (micro-LC-MS) and sheathless capillary electrophoresis-mass spectrometry (CE-MS), analytical workflows are tailored for specific metabolite classes based on their physicochemical properties. Micro-LC-MS is employed for lipid analysis, while sheathless CE-MS is applied to polar and charged metabolites such as amino acids. These methods are validated and applied to various biomass-restricted biospecimens, demonstrating their feasibility for biological and clinical research.

**Chapter 1** outlines the limitations of conventional MS methods for biomass-restricted samples and introduces miniaturized MS workflows as a solution. It also provides an overview of the thesis structure and objectives.

**Chapter 2** critically reviews microscale analytical techniques, emphasizing their relevance in metabolomics and small-volume biological sample analysis. It discusses recent advancements in micro-LC-MS, nano-LC-MS, and CE-MS, highlighting their sensitivity, robustness, and feasibility. While these miniaturized methods show great promise, further optimization of sampling and sample preparation is necessary to fully harness their potential. The chapter also underscores the importance of system components—such as low-flow LC and optimized MS ionization sources—designed for minimal sample amount.

Endocannabinoids play a crucial role in brain function and pathology, but their analysis in biomass-restricted samples such as human cerebrospinal fluid (CSF) remains challenging.

**Chapter 3** details the development of a micro-LC-MS workflow for the selective and sensitive determination of endocannabinoids and their analogs in CSF. A modified micro-electrospray ionization (micro-ESI) spray needle (Shimadzu Mikros) was employed to enhance sensitivity and durability. The developed method enabled the analysis of 288 CSF samples, providing valuable insights into endocannabinoid profiling in clinical studies while maintaining analytical robustness.

**Chapter 4** explores the application of micro-LC-MS for analyzing oxylipins, a class of bioactive lipids, in human plasma samples. Unlike endocannabinoids, oxylipins require negative ionization mode for optimal analysis, which is often affected by ionization discharge issues. These challenges were addressed using an OptiFlow ionization source, achieving superior sensitivity and robustness for oxylipin analysis in 5  $\mu\text{L}$  of plasma. The developed method was validated and compared with conventional UHPLC-MS, demonstrating significant sensitivity enhancements. The workflow was applied to 40 plasma samples from a healthy aging study, showcasing its applicability in clinical research and biomarker discovery.

Miniaturized analytical methods are not limited to hydrophobic compounds analyzed via LC-MS. **Chapter 5** presents the development of a sheathless CE-MS workflow for polar and charged compounds, specifically targeting creatinine quantification in residual pediatric plasma samples. CE-MS is particularly advantageous for volume-limited samples due to its zero dead volume and high ionization efficiency. The sheathless CE-MS method demonstrated high sensitivity and reliability, enabling creatinine quantification using only 5  $\mu\text{L}$  of plasma. A multi-segment injection strategy was implemented, allowing seven samples to be analyzed in a single electrophoretic run. The results correlated well with clinical measurements, validating the method's applicability in healthcare settings. Beyond creatinine, the method also identified a range of metabolites, highlighting its potential for metabolomics applications in neonatal healthcare.

The final chapter synthesizes the key findings of this thesis, emphasizing the promising future of miniaturized MS-based analytical methods for addressing complex biological and pharmaceutical questions in biomass-restricted samples. By integrating state-of-the-art microsampling devices, efficient sample processing techniques, and robust miniaturized

analytical instruments, significant biological insights can be obtained from minute sample volumes, paving the way for new advancements in clinical and metabolomics research.

## Samenvatting

Massaspectrometrie (MS)-gebaseerde analytische methoden worden veel gebruikt in zowel academisch als farmaceutisch onderzoek en bieden cruciale inzichten in biologische en ziekteprocessen. Ondanks hun hoge gevoeligheid en doorvoersnelheid ondervinden conventionele MS-methoden aanzienlijke uitdagingen bij de analyse van volume/materiaal-gelimiteerde biologische monsters. Het samenvoegen van dergelijke monsters om detectielimieten te bereiken gaat ten koste van de heterogeniteit van de steekproef, een essentiële factor in metabolomics en gepersonaliseerde geneeskunde. Bovendien leveren niet-invasieve bemonsteringstechnieken slechts picoliters tot microliters monstervolume op, wat leidt tot een mismatch tussen de beschikbare monstervolumes en de mogelijkheden van standaard analytische methoden.

Om deze uitdagingen aan te pakken, onderzoekt dit proefschrift geminiaturiseerde analytische technieken die de gevoeligheid en prestaties verbeteren zonder de robuustheid in gevaar te brengen. Door micro-flow vloeistofchromatografie-massaspectrometrie (micro-LC-MS) en sheathless capillaire elektroforese-massaspectrometrie (CE-MS) te optimaliseren, worden analytische workflows aangepast aan specifieke metabolietklassen op basis van hun fysisch-chemische eigenschappen. Micro-LC-MS wordt gebruikt voor de analyse van lipiden, terwijl sheathless CE-MS wordt toegepast op polaire en geladen metabolieten, zoals aminozuren. Deze methoden worden gevalideerd en toegepast op verschillende materiaal-gelimiteerde biologische monsters, waarmee hun bruikbaarheid voor biologisch en klinisch onderzoek wordt aangetoond.

Hoofdstuk 1 beschrijft de beperkingen van conventionele MS-methoden voor de analyse van materiaal-gelimiteerde monsters en introduceert geminiaturiseerde MS-workflows als oplossing. Daarnaast wordt ingegaan op de opzet en doelstellingen van het proefschrift.

Hoofdstuk 2 biedt een kritische bespreking van microschaal analytische technieken, met de nadruk op hun relevantie voor metabolomics en de analyse van kleine biologische monstervolumes. Recente ontwikkelingen op het gebied van micro-LC-MS, nano-LC-MS en CE-MS worden besproken, waarbij de nadruk ligt op hun gevoeligheid, robuustheid en toepasbaarheid. Hoewel deze geminiaturiseerde methoden veelbelovend zijn, is verdere optimalisatie van bemonstering en monstervoorbereiding noodzakelijk om hun volledige



potentieel te benutten. Ook wordt het belang van systeemcomponenten—zoals low-flow LC en geoptimaliseerde MS-ionisatiebronnen—benadrukt, die speciaal zijn ontworpen voor minimale monstervolumes.

Endocannabinoïden spelen een cruciale rol in hersenfunctie en pathologie, maar hun analyse in biomassa-beperkte monsters, zoals humaan hersenvocht (cerebrospinal fluid, CSF), blijft een uitdaging. Hoofdstuk 3 beschrijft de ontwikkeling van een micro-LC-MS workflow voor de selectieve en gevoelige bepaling van endocannabinoïden en hun analogen in CSF. Een aangepaste micro-elektrospray ionisatie (micro-ESI) spraynaald (Shimadzu Mikros) werd gebruikt om de gevoeligheid en duurzaamheid te verbeteren. De ontwikkelde methode maakte de analyse van 288 CSF-monsters mogelijk en bood waardevolle inzichten in de klinische studie van endocannabinoïde-profielen, terwijl de analytische robuustheid behouden bleef.

Hoofdstuk 4 onderzoekt de toepassing van micro-LC-MS voor de analyse van oxylipinen, een klasse bioactieve lipiden, in humaan plasma. In tegenstelling tot endocannabinoïden vereisen oxylipinen negatieve ionisatiemodus voor optimale analyse, wat vaak wordt beïnvloed door ontladingsproblemen bij de ionisatie. Deze uitdagingen werden aangepakt met behulp van een OptiFlow-ionisatiebron, wat resulteerde in een superieure gevoeligheid en robuustheid voor de analyse van oxylipinen in slechts 5  $\mu$ L plasma. De ontwikkelde methode werd gevalideerd en vergeleken met conventionele UHPLC-MS, waarbij aanzienlijke verbeteringen in gevoeligheid werden aangetoond. De workflow werd vervolgens toegepast op 40 plasma-monsters uit een studie over gezond ouder worden, waarmee de toepasbaarheid in biomarker en klinisch onderzoek werd aangetoond.

Geminiaturiseerde analytische methoden zijn niet beperkt tot hydrofobe verbindingen die via LC-MS worden geanalyseerd. Hoofdstuk 5 richt zich op de ontwikkeling van een sheathless CE-MS workflow voor polaire en geladen verbindingen, met een specifieke focus op de kwantificering van creatinine in resterende pediatrische plasma-monsters. CE-MS is bijzonder geschikt voor volume-gelimiteerde monsters vanwege het ontbreken van dode volumes en de hoge ionisatie-efficiëntie. De sheathless CE-MS methode toonde een hoge gevoeligheid en betrouwbaarheid aan, waardoor creatinine kon worden gekwantificeerd met slechts 5  $\mu$ L plasma. Een multi-segment injectiestrategie werd

toegepast, waardoor zeven monsters in één elektroforetische run konden worden geanalyseerd. De resultaten correleerden goed met klinische metingen, en naast creatinine werden ook andere endogene metabolieten geïdentificeerd, wat daarmee de potentie van deze methode aantoonde om bruikbare metabole profielen te genereren in volume-gelimiteerde klinische monsters.

Het laatste hoofdstuk vat de belangrijkste bevindingen van dit proefschrift samen en benadrukt de veelbelovende toekomst van geminiaturiseerde MS-gebaseerde analytische methoden voor het oplossen van complexe biologische en farmaceutische vraagstukken in biomassa-beperkte monsters. Door de integratie van geavanceerde microsamplingsapparaten, efficiënte monsterverwerkingstechnieken en robuuste geminiaturiseerde analytische instrumenten kunnen waardevolle biologische inzichten worden verkregen uit minimale monstervolumes, wat de weg vrijmaakt voor nieuwe vooruitgangen in klinisch en metabolomics onderzoek.

## **Curriculum vitae**

Bingshu He was born on October 3rd, 1993, in Chifeng, China. After graduating from Ningcheng High School in Inner Mongolia in 2011, she was admitted to the Biology program at Minzu University of China in Beijing. In 2016, she began her master's studies in the group of Prof. Dr. Zeper Abliz under the supervision of Dr. Zhonghua Wang. During these three years, she focused on diabetic nephropathy metabolomics and drug metabolomics in animal models using liquid chromatography–mass spectrometry and air-flow-assisted desorption electrospray ionization mass spectrometry imaging. This research led to her first scientific publication in 2018, titled “A rapid, sensitive, and selective liquid chromatography–mass spectrometry method for simultaneous quantification of astragaloside IV and cycloastragenol in mouse plasma and its application to a pharmacokinetic study”. In 2019, she obtained her master's degree and was awarded the Outstanding Graduate Award of Beijing.

In September 2019, she began her PhD project under the supervision of Prof. Dr. Thomas Hankemeier, Dr. Rawi Ramautar, and Dr. Amy Harms at Leiden University. Between 2019 and 2023, she dedicated her research to developing micro-flow LC-MS and CE-MS methods for metabolomics studies in biomass-restricted samples.

---

**List of publications**

1. He, B.; Zhang, W.; Guled, F.; Harms, A.; Ramautar, R.; Hankemeier, T. Analytical Techniques for Biomass-Restricted Metabolomics: An Overview of the State-of-the-Art. *Microchemical Journal* 2021, 171, 106794.
2. He, B.; Di, X.; Guled, F.; Harder, A. V. E.; van den Maagdenberg, A. M. J. M.; Terwindt, G. M.; Krekels, E. H. J.; Kohler, I.; Harms, A.; Ramautar, R.; Hankemeier, T. Quantification of Endocannabinoids in Human Cerebrospinal Fluid Using a Novel Micro-Flow Liquid Chromatography–Mass Spectrometry Method. *Analytica Chimica Acta* 2022, 1210, 339888.
3. He, B.; Ramautar, R.; Beekman, M.; Slagboom, P. E.; Harms, A.; Hankemeier, T. A Micro-Flow Liquid Chromatography–Mass Spectrometry Method for the Quantification of Oxylipins in Volume-Limited Human Plasma. *ELECTROPHORESIS* 2024.
4. van Mever, M.; He, B.; van Veen, M.; Slaats, J.; Buijs, M. M.; Wieringa, J. E.; Hankemeier, T.; de Winter, P.; Ramautar, R. Capillary Electrophoresis–Mass Spectrometry for Creatinine Analysis in Residual Clinical Plasma Samples and Comparison with Gold Standard Assay. *ELECTROPHORESIS* 2024, 45 (15–16), 1316–1324.

**Not part of this thesis**

1. He, B.; Wang, Z.; Chen, L.; Zhou, Z.; Abliz, Z. A Rapid, Sensitive, and Selective Liquid Chromatography–Mass Spectrometry Method for Simultaneous Quantification of Astragaloside IV and Cycloastragenol in Mouse Plasma and Its Application to a Pharmacokinetic Study. *International Journal of Mass Spectrometry* 2018, 434, 130–135.
2. Wang, Z.; He, B.; Liu, Y.; Huo, M.; Fu, W.; Yang, C.; Wei, J.; Abliz, Z. In Situ Metabolomics in Nephrotoxicity of Aristolochic Acids Based on Air Flow-Assisted Desorption Electrospray Ionization Mass Spectrometry Imaging. *Acta Pharmaceutica Sinica B* 2020, 10 (6), 1083–1093.
3. Wang, Z.; Fu, W.; Huo, M.; He, B.; Liu, Y.; Tian, L.; Li, W.; Zhou, Z.; Wang, B.; Xia, J.; Chen, Y.; Wei, J.; Abliz, Z. Spatial-Resolved Metabolomics Reveals Tissue-Specific Metabolic Reprogramming in Diabetic Nephropathy by Using Mass Spectrometry Imaging. *Acta Pharmaceutica Sinica B* 2021, 11 (11), 3665–3677.

## Acknowledgements

I would like to express my gratitude to everyone who has supported me in completing this thesis. This achievement would not have been possible without your guidance, encouragement, and assistance.

First and foremost, I extend my deepest appreciation to my supervisors for their invaluable mentorship, insightful discussions, constructive feedback, and unwavering motivation, all of which have been instrumental in shaping this research. Prof. Dr. Thomas Hankemeier, thank you for giving me the opportunity to learn and conduct research in a state-of-the-art lab and for encouraging me to explore new techniques. Dr. Rawi Ramautar, I am truly grateful for your continuous support, patience, and expert guidance throughout my PhD journey. Dr. Amy Harms, your encouragement and expertise have profoundly contributed to the success of this work.

I sincerely appreciate the support and camaraderie of my colleagues. Special thanks to Faisa for teaching me how to work with micro-flow from the very beginning. I could not have achieved this without your technical assistance and valuable advice. Xinyu and Wei Yang, thank you for sharing all the crucial information that helped me set up my miniaturization method. Wei Zhang, I deeply appreciate your guidance in CE; your thorough explanations allowed me to truly appreciate its intricacies. Marlien, collaborating with you has been a delightful experience, and I am grateful for the wonderful times we shared both in and outside the CE room. I also extend my thanks to everyone who contributed to the warm and supportive atmosphere in the lab, which made my research journey truly enjoyable.

Having one true friend is already a blessing, meeting a whole group of incredible friends is beyond words. Pingping, thank you for sharing countless moments of laughter and stress with me throughout these years. Wei Zhang, Zhengzheng, Wei Yang, Xinyu, Yupeng, LuoJiao, Congrou, Mengle, Lu, Yu, Xiaoyue, and Yiwei, your companionship and encouragement have brought so much joy to my life. The memories we have created together will be treasured for a lifetime.

Xiaotian, thank you for always being there for me. Your constant support has been my source of strength and motivation.

Last but not least, I am deeply thankful to my parents and family for their unwavering support and love throughout this journey.

我由衷地感激我的父母和家人，在这段旅程中给予我坚定不移的支持和深深的爱。